Univerzita Karlova v Praze

Přírodovědecká fakulta

Studijní program: Geologie

Studijní obor: Geochemie

Bc. Ladislav Polák

Geochemie silně siderofilních prvků a izotopů Re-Os karbonatitů a přidružených alkalických hornin vybraných lokalit Indie

Highly siderophile element and Re-Os isotopic geochemistry of carbonatites and associated alkaline rocks from selected occurrences in India

Diplomová práce

Vedoucí diplomové práce: doc. Mgr. Lukáš Ackerman, Ph.D.

Praha 2017

i

Prohlášení:

Prohlašuji, že jsem závěrečnou práci zpracoval samostatně a že jsem uvedl všechny použité informační zdroje a literaturu. Tato práce ani její podstatná část nebyla předložena k získání jiného nebo stejného akademického titulu.

V Praze, 11. 5. 2017   Podpis

ABSTRAKT

Karbonatity jsou horniny extruzivního a intruzivního typu, které obsahují minimálně 50 % karbonátových minerálů, pocházejících převážně ze svrchního pláště. Reprezentují potencionální ekonomický zdroj, jakožto zdroj prvků platinové skupiny, tak jako je tomu v Palawboře v Jižní Africe nebo v Ipanamě v Brazílii. Toto je první studie, která přináší informace o koncentracích silně siderofilních prvků (HSE) spolu s izotopickými poměry $^{187}Os/^{188}Os$ pro karbonatity, silikokarbonatity a přidružené alkalické horniny (pyroxenit, syenit, monzogabro a tonalit) z dvou neoproterozoických (~ 800 milionů let) oblastí ze Samalpatti a Sevatturu, regionu Tamil Nadu v jižní Indii. Data byla pořízena standartní metodou za pomoci rozložení vzorků v *Carius Tubes*. Separace Os probíhala pomocí chlorofrmu ($CHCl_3$), následovaná mikrodestilací a separací Ir, Ru, Pt a Pd za pomoci iontové chromatografie. Výsledky ukazují, že karbonatity ze Samalpatti a ze Sevatturu jsou charakteristické nízkými koncentracemi HSE, nižšími než ostatní mafické horniny derivované z pláště, jako jsou bazalty nebo komatiity. Suprachondritické poměry Os_N/Ir_N mohou napovídat, že karbonatity jsou schopny koncentrovat nezanedbatelné množství Os. Kvůli vysokým, nejednotným poměrům $^{187}Os/^{188}Os$ předpokládáme, že zdroj karbonatitové taveniny byl vysoce heterogenní s vysokým příspěvkem materiálu z kůry (například eklogit). Některé Sevatturské karbonatity jsou značně obohacené o Cu a vypadá to, že toto obohacení je spojeno s vysokým obsahem P_2O_5 a FeO_{tot} (mineralizace apatitu a magnetitu). Analyzované Mg-Cr-bohaté silikokarbonatity mají mnohem vyšší obsah HSE než ostatní vzorky. Plochý profil I-PGE je typický pro pyroxeny a konvexně kladný sklon profilu P-PGE-Re může indikovat, že Mg-Cr-bohaté silikokarbonatity prošly pozdními procesy jako metasomatóza nebo alterace. Kvůli vysokému obsahu Os, Ir, Ru a petrografii silikokarbonatitů, můžeme předpokládat, že tyto silikokarbonatity vznikaly v blízké asociaci s fenitizovaným pyroxenitem a reprezentují směs primárně derivované CO_2 bohaté alkalické plášťové taveniny a okolní horniny. Alkalické horniny ze Samalpatti, široce kolísají v obsahu HSE, který je převážně vázaný ke koncentracím síry. V některých pyroxenitech byla nalezena mineralizace pyritu, která způsobila porušení Re-Os izotopického systému. Pro vzorky, u kterých bylo možné spočítat iniciální poměry $^{187}Os/^{188}Os$ předpokládáme, že jejich původ je spjatý s derivací korového materiálu. Profil HSE a izotopický poměr $^{187}Os/^{188}Os$ monzogaber a syenitů odpovídá hodnotám kontinentální kůry. Alkalické horniny ze Sevatturu mají velmi nízké HSE koncentrace a jejich izotopické $^{187}Os/^{188}Os$ poměry, taktéž napovídají, že jejich původ je spjatý s kůrou.

SUMMARY

Carbonatites are intrusive and extrusive rocks with content of carbonate minerals > 50% predominantly derived from upper mantle. They represent a potential economical source for platinum-group elements as can be seen on actively mined sites like Phalaborwa in South Africa or Ipanema in Brazil. The first complete dataset for highly siderophile element (HSE) abundances along with their $^{187}Os/^{188}Os$ compositions for carbonatites, silicocarbonatites and associated alkaline rocks (pyroxenite, syenite, monzogabbro and tonalite) from two Neoproterozoic (~ 800 Ma) suites from Samalpatti and Sevattur, Tamil Nadu region in south India is presented. The data were obtained by a standard methods in involving decomposition of samples in *Carius Tubes*, Os separation by $CHCl_3$ following microdistillation and Ir, Ru, Pt, Pd isolation by anion exchange chromatography. The data show that carbonatites from Samalpatti and Sevattur are characterized by very low HSE contents, lower than other mantle-derived mafic melts such as basalts or komatiites. Suprachondritic Os_N/Ir_N ratios might suggest that carbonatites are able to concentrate not negligible amount of Os. Due to high, non-uniform $^{187}Os/^{188}Os$ ratios, we suggest that the source of carbonatitic melts was largely heterogeneous with high contribution of crustal material like eclogite. Some Sevattur carbonatites are considerably enriched in Cu and it seems that this feature is connected with high contents of P_2O_5 and FeO_{tot} associated with high proportions of apatite and magnetite. Analysed Mg-Cr-rich silicocarbonatites have much higher contents of HSE than other examined samples. Flat I-PGE patterns resemble that typical for pyroxenes and convex-upward distribution of P-PGE-Re may indicate that the Mg-Cr-rich silicocarbonatites undergone through some post-processes like metasomatism or late alteration. Due to their high contents of Os, Ir, Ru and their petrography, we believe that these silicocarbonatites originated in a close association with a fenitized pyroxenite and represent mixed primary mantle-derived alkali-CO_2-rich melts and the host rock. The alkaline rocks from Samalpatti widely vary in their HSE contents, which are predominantly related to their sulphur concentrations. Within this suite, late-stage pyrite mineralization found in some pyroxenites caused high perturbation of Re-Os isotopic system. For those samples, where it is possible to calculate initial $^{187}Os/^{188}Os$ ratios, we suggest that their origin is a result of derivation from crustal lithologies. Patterns for monzogabbros and syenites and their highly radiogenic $^{187}Os/^{188}Os$ compositions correspond to continental crust. Alkaline rocks from Sevattur are very low in HSE contents and their $^{187}Os/^{188}Os$ ratios also imply that these rocks have a crustal origin.

TABLE OF CONTENTS

Figures

Tables

PODĚKOVÁNÍ

Rád bych poděkoval svému školiteli doc. Mgr. Lukáši Ackermanovi, Ph.D. za odborné vedení diplomové práce, za pomoc při laboratorních pracích, za pomoc při vyhodnocování výsledků a zejména za důvěru. Další dík patří všem, kteří se podíleli na sběru vzorků a Geologickému ústavu AV ČR za poskytnutí zázemí a jeho zaměstnancům za pomoc a podporu.

x

1   INTRODUCTION

Carbonatites are effusive or intrusive magmatic rocks typically associated with alkaline silicate rocks such as syenite, pyroxenite, gabbro or dunite and preferentially emplaced through continental rifting. The carbonatitic melts are presumed to remain unaffected by a crustal contamination because of their low temperature (600–800 °C; Jones et al., 2013) and extremely low viscosity (<0.065 PaS) permitting their fast transport to the Earth`s surface. These characteristics making them as remarkable candidates for the investigation of the compositions of subcontinental upper mantle (e.g., Pandit et al., 2002; Schleicher et al., 1998). Carbonatites contain at least 50 % of carbonate minerals (Howie, 2002) and they are divided into three groups according to predominant carbonate mineral (calcite carbonatites, dolomite carbonatites and ankerite carbonatites) and their origin is attributed to three different processes and/or their combination. I. direct partial melting of metasomatized mantle source, which is primary CO_2-bearing peridotite, II. crystal fractionation of carbonated alkaline silicate melt (e.g., nephelinite or melilite-bearing melt) and III. derivation, separation and/or fractionation by immiscibility from silicate melts (for example: Brooker, 1998; Veksler et al., 1998; Wallace and Green, 1988).

Indian Peninsula hosts a several occurrences of carbonatite bodies, mostly in the Tamil Nadu region in the south and Deccan trap basalts-related occurrences in the Middle West. Age of these bodies vary from 66.6–68.5 Ma for Amba Dongar (Duncan and Pyle, 1988) within Deccan traps to 2.4 Ga for Hogenakal carbonatite (Kumar et al., 1998) in Tamil Nadu. The Tamil Nadu region hosts several carbonatite bodies, from which two of carbonatite-alkaline complexes have been selected for this study – Samalpatti and Sevattur. These bodies have been recently characterized in terms of their major/trace element and Sr–Nd–Pb–C–O systematics suggesting their contrasting petrogenesis (Ackerman et al., 2017). On Samalpatti locality, the carbonatites are commonly associated with silicocarbonatites, which differentiate by their higher SiO_2 contents at least 20 wt. %. Two groups of these rocks have been identified: calcite-rich silicocarbonatites and magnesium-chromium-rich silicocarbonatites. Associated alkaline rocks are represented by pyroxenite, monzogabbro, syenite (Samalpatti) and phosphate with phlogopite, monzogabbro and tonalite (Sevattur).

Analyses of highly siderophile elements (HSE – Os, Ir, Ru, Pt, Pd, Re) combined with Re–Os isotopic determinations can provide a unique insights into the sources of mantle-derived melts, evolution of such melts through their transport to the Earth`s surface (see review of Day et al. 2016 and references therein). While significant amount of studies exists for mafic mantle-derived melts such as basalts (MORB, OIB etc.) or komatiites, they are virtually no data for carbonatitic magmas in terms of their HSE contents/distributions except uncomplete datasets from China (Xu et al., 2003; Xu et al., 2008) without Re–Os isotopic measurements. Moreover, the studies focused on HSE contents of carbonatites can be also important for the exploration activities as preliminary data for phoscorite-carbonatite complexes from Brazil (e.g., Ipanema) and South Africa (Phalaborwa) have shown, that carbonatites could be economically significant as their HSE contents can reach up to 13.5 ppm of I-PGE and 3.2 ppm of P-PGE (Fontana, 2006).

This MSc. thesis reports the first high-precision data for all HSE paralleled by Re–Os isotopic compositions for a suite of samples consisting of carbonatite, silicocarbonatite and associated alkaline silicate rocks from Samalpatti and Sevattur, Tamil Nadu, South India. These data are combined with analyses of sulphur and other chalcophile/siderophile elements. Wide range of HSE contents for individual rock types have been shown and discussed in a frame of current knowledge coming from the studies of mafic mantle-derived melts and available petrogenetic models for Samalpatti and Sevattur complexes.

2   CARBONATITES

Carbonatites are igneous rocks, intrusive as well as extrusive, which contain more than 50% by volume of carbonate minerals (Howie, 2002). Those with predominance of calcite ($CaCO_3$) are called calcite carbonatites (also sövite and alvikite), while those containing dolomite ($MgCO_3$) as major carbonate phase are called dolomite carbonatites (also rauhaugite and/or beforsite). Ankerite carbonatites (might be seen also with prefix ferro) are rocks with predominant type of carbonate in the form of ankerite (Ca–Mg–Fe)(CO_3). Preferred names are calcite carbonatite, dolomite carbonatite and ankerite carbonatite. If the carbonate mineral, or minerals, have not been identified but whole-rock chemical analysis is available, carbonatites can be classified according to the weight proportions of CaO, MgO and $FeO + Fe_2O_3 + MnO$ (Fig. 1; Wooley and Kempe, 1989) if the SiO_2 contents do not exceed 10 wt. %. Calcite carbonatites are defined as containing (normalized by all above-mentioned oxides) > 80% CaO, dolomite carbonatites have $MgO > FeO + Fe_2O_3 + MnO$ while those with $FeO + Fe_2O_3 + MnO > MgO$ are called ankerite carbonatites. Carbonatites with more than 20 wt. % of SiO_2 are called silicocarbonatites (Woolley and Kempe, 1989).
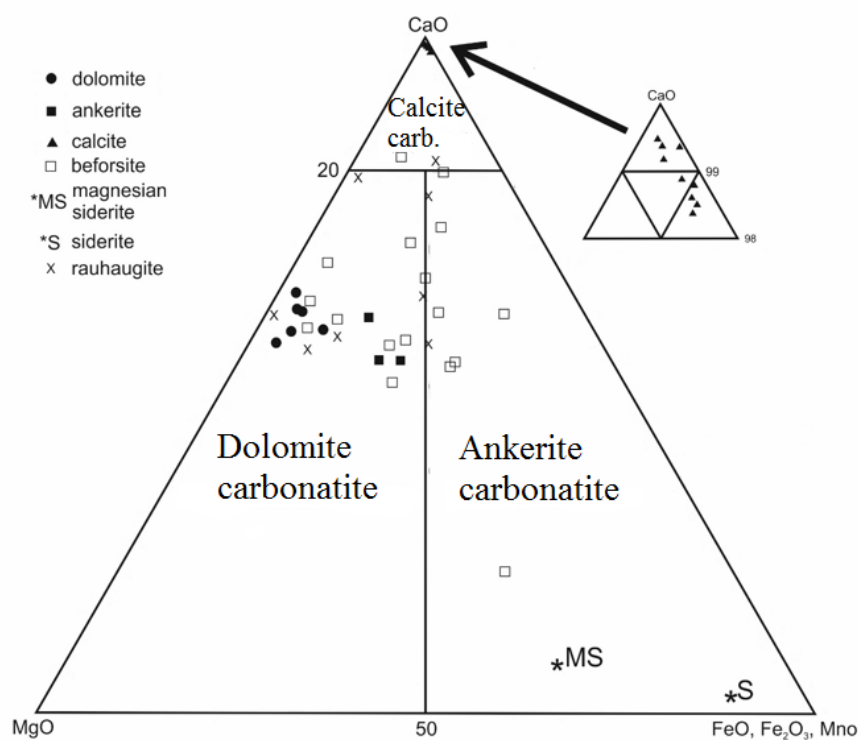
Fig. 1. Suggested classification of carbonatites in terms of CaO-MgO-(FeO, Fe$_2$O$_3$, Mno) (wt. %). Modified from Woolley (1982) and Woolley and Kempe (1989)

Carbonatites have characteristic chemical compositions distinguishing them from other types of igneous rocks. Except from main components such as CaO a CO_2, carbonatites have typically very high to sometimes extreme concentrations of P, K, Na, Ba, Sr, Nb, rare earth elements (REE) and other incompatible trace elements. Carbonates itself are clearly different from those of sedimentary origin by different $^{87}Sr/^{86}Sr$, $\delta^{18}O$ and $\delta^{13}C$ isotopic compositions as follows:

- Average values of $^{87}Sr/^{86}Sr$ in carbonatites vary from 0.7024 to 0.7075 (Guarino et al., 2012; Kumar et al., 1998), much lower than reported for sedimentary rocks (0.7194–0.7431 (Dasch, 1969).

- Average values of $\delta^{18}O_{SMOW}$ in carbonatites worldwide are in the range from 6.7 to 15.4 ‰ and $\delta^{13}C_{PDB}$ from –6.4 to –4 ‰ (Deines et al., 1989 and references therein). However, carbonatites from Samalpatti located in southern India are significantly enriched in $\delta^{13}C_{PDB}$ (+4.2 ‰) and $\delta^{18}O_{SMOW}$ (24–25.4 ‰) (Ray and Ramesh, 2006). In contrast (Fig. 2.A), average $\delta^{13}C$ values in inorganic sedimentary carbonates are about 0 ‰ and organic carbon has lighter value with $\delta^{13}C$ being typically below –20 ‰ (Deines, 2002). The $\delta^{18}O_{SMOW}$ values of igneous rocks such basalts ranging around 5–8 ‰, with the common sandstone, shale and arkose are only enriched by about 5–10 per mil over basalts and gabbros.

- Initial ratios of Nd isotopes are calculated towards Chondritic Uniform Reservoir (CHUR) and can produce model ages of segregation from the mantle. Average values of $\varepsilon_{Nd(i)}$ for carbonatites are low and fluctuate between 0.1 to –20.1 (Ackerman et al., 2017; Kramm et al., 1997; Schleicher et al., 1998). Sedimentary rocks values of ε_{Nd} are commonly around –10 ± 3 (Bockrath, 2004; Grousset et al., 1988; Jones et al., 1994). Fig. 2.C show fields of ε_{Nd} for mid-ocean ridge basalts, island arc volcanics and early Precambrian crust. Sediments from cratonic/passive margin settings commonly have lower ε_{Nd}, suggesting an older provenance. Active margin sediments commonly have higher ε_{Nd} values (McLennan and Hemming, 1992).
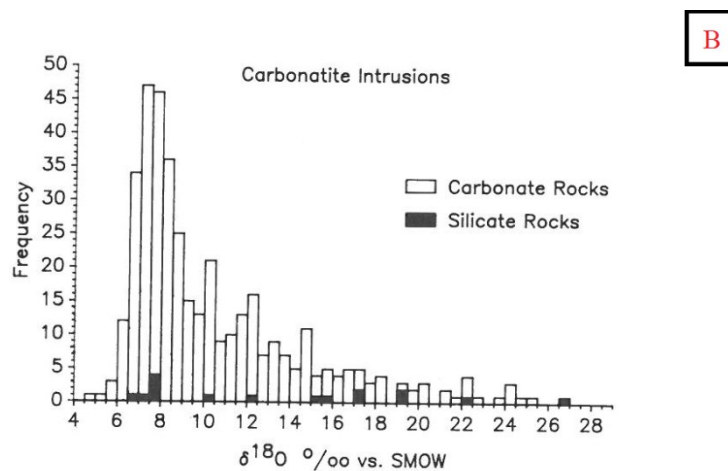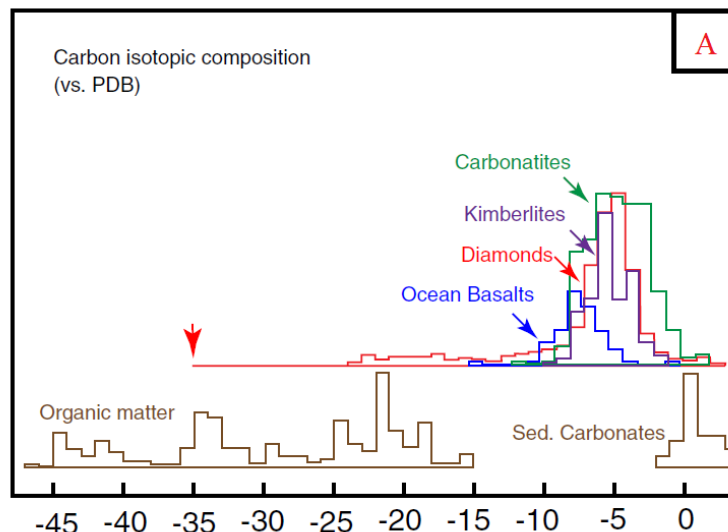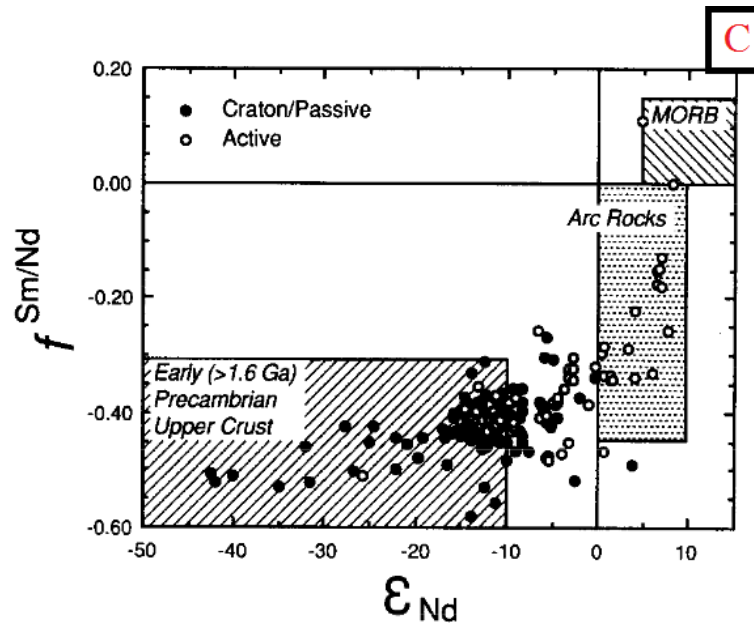
Fig. 2. A) Carbon isotopic composition of the main carbon-bearing samples (Hammouda and Keshav, 2015); B) Oxygen isotopic composition of carbonatite intrusions (Deines, 1989; C) Plot of $f^{Sm/Nd}$ versus ε_{Nd} for modern sediments (McLennan and Hemming, 1992).

Carbonatites are typically located within intraplate settings, over half of which are in Africa, often occurring in peripheral regions to orogenic belts showing an apparent link to orogenic events or plate separation. The occurrence of carbonatites in continental crust has perpetuated interpretation of their geochemistry in terms of a genetic connection and they have been variously related to mantle plums and large igneous provinces (LIPs) (Ernst and Bell, 2010). Carbonatites tend to not occur as single rock unit but rather as a suite in association with alkaline silicate rocks, including a wide variety of ultramafic to felsic silicate igneous rocks from dunites to syenites (Jones et al., 2013; Schleicher et al., 1998). Carbonatites concentrations are also associated with topographic swells up to 1000 km across (Srivastava and Hall, 1995).

Approximately half of the known carbonatite bodies occur in Africa, with the majority concentrated in or close to the East African Rift, in a broad zone trending southwards from Kenya through Mozambique into South Africa (Woolley, 1989). Other famous sites include Phalaborwa in South Africa (Groves and Vielreicher, 2001), Ipanema in South America in Brazil (Guarino et al., 2012), Mountain Pass in North America in USA (Rowan and Mars, 2003), Mount Weld in Australia (Lottermoser, 1990) and Bayan Obo in China (Xu et al., 2010).

Some of the carbonatite bodies have been mining for various products. Phalaborwa is famous body for its high amount of Cu and mined products as magnetite, vermiculite and gold (< 0.8 g/t). Minerals and elements are hosted in wide spectra of rocks and different variation, for example in skarn, breccia pipe, pluton-related gold veins, low-sulphidation epithermal gold veins and volcanogenic massive sulphide deposits associated with alkaline rocks (Sillitoe, 2002). This metal association is accompanied by light rare earth element (LREE), F and P variable enrichments and elevated contents of Ag, As, Ba, Co, Mo, Nb, Ni, Th and/or U (Groves and Vielreicher, 2001). Ipanema is known as medium deposit of nickel. Some of the rocks in Ipanema are enriched in Al and Fe hosted in glimmerite with subordinate shonkinite, diorite, syenite and mela-syenite (Guarino et al. 2012). The Mountain Pass calcite carbonatite intruded into gneiss and contain 8–12 % of rare earth element oxides, mostly contained in bastnaesite (Rowan and Mars, 2003). China is a dominant producer of rare earth elements (up to 95 %) and about half of this production comes from Bayan Obo. In 2001, China produced about 81 000 tons of rare earth elements and in 2006 120 000 tons (Huang et al., 2006).

Some other sites with important mineralization are located in Greenland (Sarfartôk), India (Amba Dongar), Russia, Mongolia, Pakistan or Afghanistan. Age of carbonatite bodies varies considerably with the oldest carbonatites found in Phalaborwa (~2047 Ma) and Greenland in Turpetalik (~2650 Ma) (Woolley, 1989). Eruptions of carbonatitic magmas on the surface are very rare and only one volcano, Ol Doinyo Lengai (Tanzania), is currently active producing Na-rich carbonatitic lavas (Gaillard et al., 2008).

Carbonatites are preferentially concentrated in Precambrian rocks. Approximately two-thirds of known carbonatites can be found in the Precambrian regions. However, 64% of dated carbonatites are post-Precambrian in age, i.e. younger than 542 Ma. Hence, carbonatites of Phanerozoic age tend to be emplaced into Precambrian rocks (Woolley and Bailey, 2012).

Activity of carbonatite intrusions increases with time (Fig. 3). A major period started ~200 Ma ago is perhaps associated with the breakup on Pangea continent. The gradual increase in the number of carbonatite occurrences with time is undoubtedly real, and implies that the condition necessary for the production of carbonatite magmas were not only established by Late Archean, but become increasingly widespread with time (Woolley, 1989). On the other hand, Veizer et al. (1992) argue that the half-life of carbonatites caused by crustal erosion and preferential recycling is ~445 Ma. However, according to (Jones et al., 2013), this argument is not valid because cratonic material in which carbonatites are concentrated, is not readily subducted.
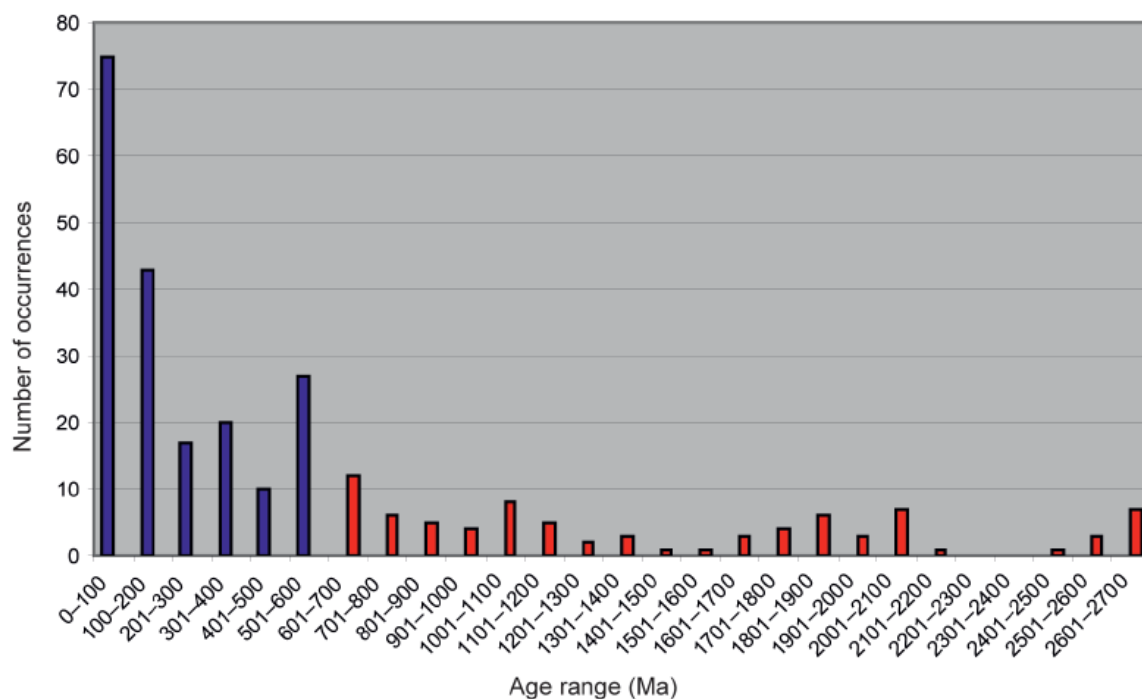
Fig. 3. A frequency of carbonatite ages plotted against time. There are 192 post-Precambrian dates (blue) and 82 Precambrian dates (Woolley and Bailey, 2012).

The repetition of alkaline and carbonatitic igneous activity at continental rift intersection, over periods of large-scale plate movement, must indicate that the structural fabric of the lithosphere determines the site of the magmatism (Bailey, 1977). Repetition cannot therefore be ascribed to plumes that have fixed sources below the lithosphere (Woolley and Bailey, 2012). Examples of such repetition could be found in the Monteregain Province in Canada, in the Rungwa-North Nyasa Province of Africa and in the southern part of Greenland, where are four or possibly five periods of carbonatite activity over a period of 2500 Ma (Bailey and Woolley, 2005). The existence of these repeated carbonatitic

activity is evidence for the control of carbon release through the lithosphere, because of movement of the plates during the extensive periods of time involved (Woolley and Bailey, 2012). The Fig. 4 shows repetition of carbonatites activity over the last 2750 Ma.
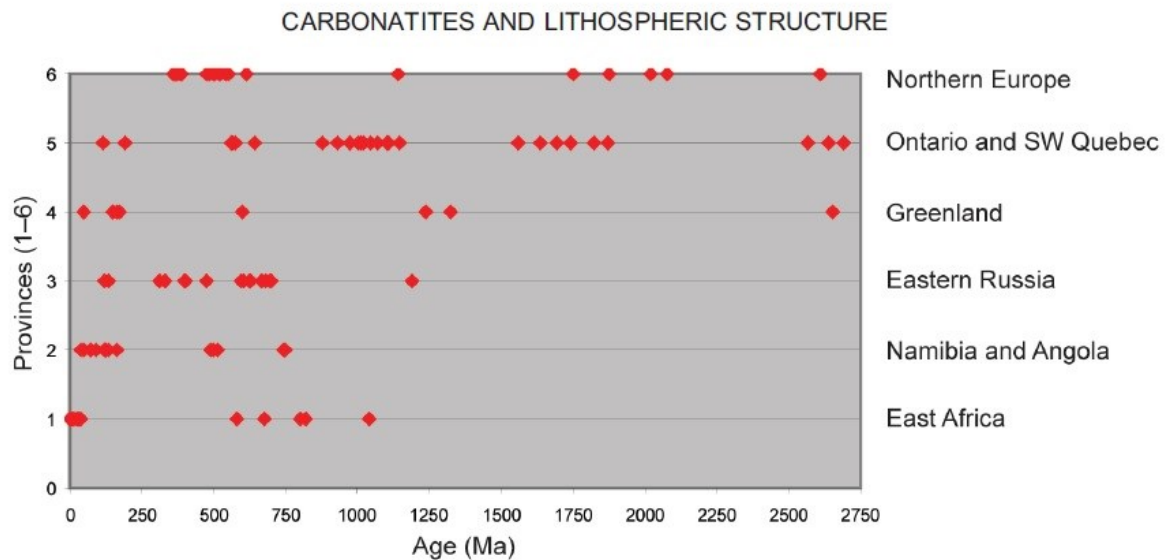
Fig. 4. Age of carbonatite bodies in six restricted areas showing the repetition of carbonatitic activity with time. These are follows: 1- East Africa (Kenya, Uganda, Tanzania and one occurrence in Zambia); 2- Namibia and Angola; 3- Eastern Russia (East Tuva, Enisei, East Sayan, Baikal, Aldan); 4- Greenland; 5- Ontario and southwest Quebec, 6- Northern Europe (Kola Peninsula, northern Norway, Sweeden, Finland) (Woolley and Bailey 2012).

Carbonatites predominantly occur within the continental crust. In the oceanic settings, they have been identified only in three areas – Canary Islands, the Cape Verde Islands and the Kerguelen Islands. The first two archipelagos are located close to the west coast of Africa and it seems probable that there are remnants of continental lithosphere beneath them. These remnants probably generated thermal and chemical conditions that are favourable to the formation of carbonatitic magmas. The carbonatites in Kerguelen Islands represent the only one known example with a pure oceanic petrogenesis (Woolley and Bailey, 2012). According to this paper, the reason why carbonatites are more common in continental areas than in oceanic settings, are not generally conductive to a large-scale production of carbonatite that can survive to the surface. This is probably because, unlike the continental plates, they are neither robust enough nor thick enough to absorb, conserve and accumulate the necessary CO_2, and the geothermal gradient is too steep.

Very low magmatic temperatures and viscosities are striking features of alkali-carbonatitic lavas at low pressure (Jones et al., 2013). The low carbonatitic melt viscosity was first measured accurately in experiments using in-situ synchrotron radiation to track rapidly falling spheres (Tab. 1). Fundamental understanding of carbonatites was largely achieved in the last century, when developments in technology enabled experimental petrology to unlock the secrets of how carbonatites actually form, including their important connections with water, enabling early formative predictions about the stability of carbonate minerals in the upper mantle; the significance of free CO_2 and H_2O in the mantle transition zone; the derivation of kimberlitic and carbonatitic melts; and mantle metasomatism (Wyllie and Huang, 1976; Wyllie and Lee, 1998). Self-diffusion coefficients qualitatively suggested, that $CaCO_3$ melts have very low viscosities at high-pressure up to 11 GPa. The low viscosity and chemical composition of carbonatitic melts make them as excellent metasomatic agents (Jones et al., 2013).

6

Composition	Pressure [GPa]	T [C°]	Density [g/cm3]	Comment	Viscosity [PaS]	Reference
$K_2Mg(CO_3)_2$	atm	500	2.262			[1]
$K_2Ca(CO_3)_2$	atm	859	2.058			[2]
$MgCO_3$ = Mc	atm		2.30			[1]
$K_2Mg(CoO_3)_2$	3.00	800			0.036	[1]
	3.00	900			0.022	[1]
	5.50	1200			0.006	[1]
$K_2Ca(CO_3)_2$ = Kc	2.50	950	2.75		0.032	[1]
	2.50	1150	2.58		0.018	[1]
	4.00	1050	2.80		0.023	[1]
$Mc_{25}Kc_{75}$	2.00	1250			0.065	[1]
K_2CO_3	4.00	1500	3.10		0.023	[1]
RE-carbonatite	3.00	530	4.10		0.155	[1]
$CaCo_3$				Thermal expansivity		[2]
Ca-Carbonatite	atm	800		calculated	0.080	[3]
Natrocarbonatite	atm	800		calculated	0.008	[3]

Tab. 1. Carbonate melt physical data measured *in situ* using synchrotron X-ray falling sphere method and calculation for pressures up to 5,5 GPa. Source [1] Dobson et al., 1996; [2] Genge et al., 1995; [3] Wolff, 1994 from (Jones et al., 2013 and references therein).

Simulations predict that the stable $MgCO_3$ and $CaCO_3$ phases at pressure > 82 GPa and > 19 GPa, respectively are dominated by corner-shearing CO_4 tetrahedral networks, with those of $CaCO_3$ adopting a β-cristobalite structure, and $CaCO_3$ adopting a pyroxene-like structure at pressures > 110 GPa (Jones et al., 2013).

Carbonatitic melts are ionic liquids consisting of carbonate CO_3^{2-} molecular anions. According to Mysen (1983), CO_2 dissolves primary to form CO_3^{2-} complexes. If the rare earth elements partitioning between carbonate-rich melts and host lamprophyres is representative for all coexisting carbonate-silicate liquids, then REE can be used to evaluate a co-magmatic/immiscibility origin for other carbonatite-alkaline rock association (example from Callander Bay, Ontario, Canada). The REE are clearly favoured by carbonate liquids, and a mechanism of liquid immiscibility is preferred to explain the REE data rather than fractional crystallization. The discrepancy between La/Lu ratios at some carbonatites can be explained by greater mobility of the heavy REE relative to the light REE due to volatile transport as CO_3^{2-} or F-complexes out of carbonatite melts compared to the separated silicate melts (Cullers and Medaris, 1977). This is resulting in increase of La/Lu ratio in the carbonatite melt compare to silicate melt.

Young carbonatites share significant isotopic similarities with young oceanic island basalts (OIB). Thus, alkaline silicate magmas and carbonatites in the East African Rift, including the active carbonatite volcano Oldoinyo Lengai, lie close to the mixing line HIMU-EM1 (two mantle end-member components, HIMU stands for reservoir with high ratio U/Pb, EM1 stands for metasomatized subcontinental lithosphere) which were first identified in OIB (Fig. 5.). This mixing may represent either a lithospheric or a deeper mantle sub-lithospheric signature related to a mantle plume. In general, carbonatites contain very low concentrations of Pb, far below crust levels, offering their clear distinction from crustal carbonates.
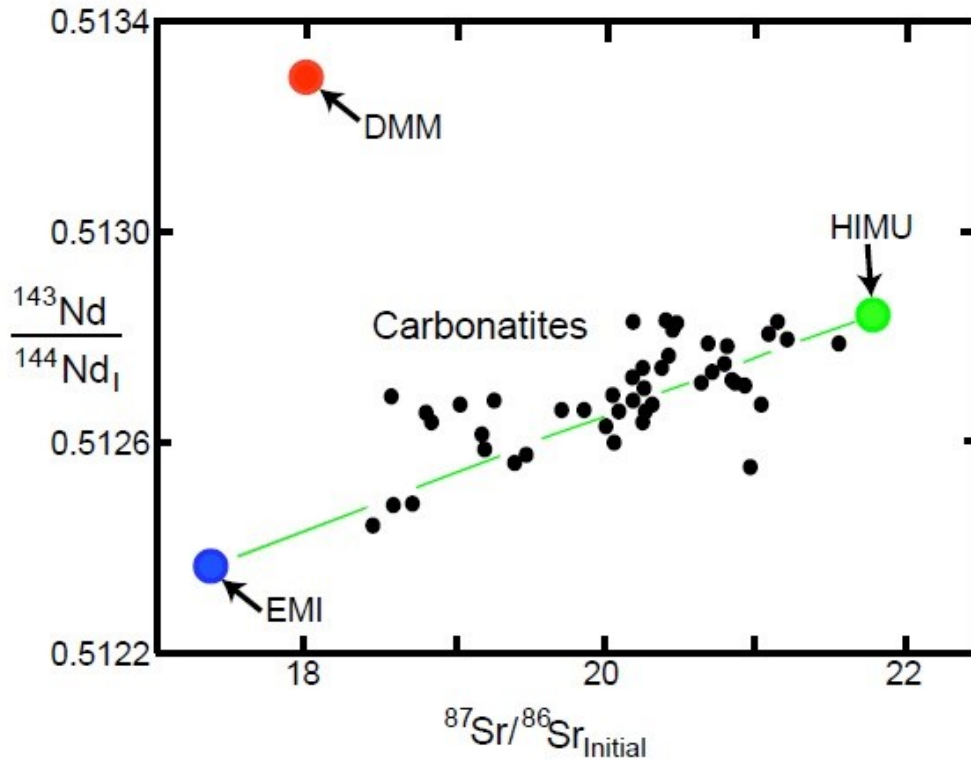
Fig. 5. Isotopic covariation of Nd and Sr isotopes for geologically young carbonatites, plotted as $^{143}Nd/^{144}Nd$ initial versus $^{87}Sr/^{86}Sr$ initial, including positions of end member isotope reservoirs known as HIMU, DMM and EMI (Jones, 2013 from Bell and Tilton, 2001)

Carbonatitic melts have been invoked to explain deep regions of the mantle asthenosphere characterized by anomalous conductivity (Jones et al., 2013). Experiments of Gaillard et al. (2008) showed that, the conductivity of carbonatites melt increases from 50 to 200 $S.m^{-1}$ for temperature from 400 to 1000 ° C. The experiment was performed on Li-free and Ca-rich system in 1 atm of CO_2 pressure.

2.1 Genesis of carbonatite magmas

Carbonatitic magmas can be produced in three different ways or combination by these processes:

1. Direct partial melting of metasomatized mantle source, which is primary a CO_2-bearing peridotite (Wallace and Green, 1988; Ying et al., 2003; Wyllie and Lee, 1998)
2. Crystal fractionation of carbonated alkaline silicate melt (e.g., nephelinite or melilite-bearing melt; Veksler et al., 1998)
3. Derivation, separation and/or fractionation by immiscibility from silicate melts (Kjarsgaard and Hamilton, 1988; Brooker, 1998; Lee and Wyllie, 1997)

Combinations of these three processes are common. For example, carbonatite liquids generated by deep melting of carbonated eclogite in the upper mantle infiltrate overlying peridotite and evolve to produce silica-undersaturated carbonate-bearing melts, which then intruded the crust (Yaxley and Brey, 2004). Carbonatites have also been considered to be generated in the lithospheric mantle as partial melts rising rapidly above a hot ascending mantle plume. As the much hotter centre of the plume approaches, melting is induced in the metasomatic horizon and results in generation of the carbonatite melts that are observed on the surface (Bizimis et al., 2003). Although the plume model is quite attractive, recent recognition of strong and repeated lithospheric controls in the compilation of global carbonatites ages are thought to argue against a direct connection to mantle plumes (Woolley and Bailey, 2012).

Infiltrating experiments demonstrate that such melt can percolate very quickly in polycrystalline olivine-rich matrix. Carbonatites can travel over several millimetres in one hour and the infiltration rate is kinetically controlled by cation diffusion in the melt (Hammouda and Laporte, 2000). The observed rates are several orders of magnitude higher that those previously found for basalt infiltration in mantle lithologies. Infiltration proceeds by a dissolution-precipitation mechanism where porosity is created in the dunite by dissolution of olivine at grain boundaries. This reaction is accompanied by secondary olivine precipitation in carbonatite reservoir. Such a mechanism would likely favour chemical exchange between melt and matrix during percolation (Hammouda and Laporte, 2000).

2.2   Effect of age on composition of carbonatites

It appears the Proterozoic carbonatites are more enriched in PGE, REE or Cu than younger carbonatites. The temperature of the carbonate-mica-peridotite solidus is significantly lower than the geotherm during episodic intervals of mantle overturn, which were caused by subduction of slab through the mantle phase barrier in the Proterozoic. The implication is that underplating would either induce metasomatism in established Sub-Continental Lithospheric Mantle (SCLM) or destroy products of metasomatism by large fraction melting in new SCLM with higher heat flow. Between the intervals of mantle overturn in the Proterozoic, the carbonate-mica-peridotite solidus is largely coincident with the Proterozoic geotherm at pressures greater than approximately 4 GPa. Melts produced would have compositions intermediate between carbonatite and kimberlite and would have the potential to generate metasomatism in the SCLM, or to transport incompatible mantle components including critical metals to the crust. Apatite is recognised as an important host for REE in the mantle but phlogopite also has the potential to host a variety of critical metals, most significantly Ba, in mantle metasomatic peridotites, and to transport and concentrate critical metals in carbonate-rich magmas. Zoning in phlogopite macrocrysts in near-primary kimberlite and carbonatite compositions shows a rapid increase in critical metal concentration from high to intermediate pressures. Mechanisms that are considered to be of importance in concentrating critical metals in phlogopite in near-primary Proterozoic magmas are (1) enhanced metasomatic formation in established Proterozoic SCLM due to mantle overturns and (2) volume loss (OH- and K+) from magma and replacement of phlogopite, such that secondary phlogopite becomes enriched (Kavecsanski et al., 2016).

3 GEOLOGICAL SETTING

3.1 Regional Geology of Tamil Nadu region

Age of the rocks located at south India vary from 2.6–2.5 Ga to 800–750 Ma. There are roughly 8 carbonatite occurrences related to the major northeast – southwest fault zone (Nilgiri rift) in Tamil Nadu, and together form the largest carbonatite-alkalic sub-province in South India (Pandit et al. 2002; Schleicher et al. 1997; Viladkar and Subramanian 1995; Viladkar and Bismayer 2014). In Tamil Nadu region, more than 40 alkaline complexes belong to Precambrian alkaline magmatism ~1600–600 Ma whereas the carbonatites in north-west India are closely associated with Deccan trap basalts (Mesozoic; Schleicher et al., 1998). Most of these alkaline complexes are located near the western margin of the Eastern Ghats Mobil Belt (EGMB) and seem to be confined to the junction between cratonic non-charnockitic (amphibolite facies) and the mobile belt charnockitic (granulite facies) regions (Schleicher et al. 1998). Many granulite facies, including charnockites, have a number of significant features in common, including CO_2-rich, H_2O-poor fluid inclusion, depletion of some large-ion trace element, such as Rb, U, Th and heavy rare earth elements. At several localities in southern India, both tonalitic and granitic gneisses are cross-cutted with irregular patches and stringers of charnockite which appear to have developed from the penetration of CO_2-rich fluids along shear zone in the gneiss (Condie et al., 1982; Pichamuthu, 1975). These granulite facies reach up Archean ages. Age of charnockites in Tamil Nadu region vary from 2.5 to 2.7 Ga (Janardhan et al., 1982). Studies of contacts between gneisses and charnockites indicate that charnockites are formed by metamorphic and metasomatic processes from the gneiss and supracrustal rocks. Pegmatitic phases of all gneissic varieties has been also found (Pichamuthu, 1975). Carbonatites in this region are associated mostly with pyroxenites and nepheline-free syenites (usually with small amount of modal quartz) and with dunites which form small plugs in some area (Condie et al., 1982; Miyazaki et al., 2000; Pandit et al., 2002). An extensive mafic crust is produced from partial melting of enriched ultramafic rocks in upper mantle. Burial and metamorphism of this crust under conditions with variable water content results in mineral assemblages ranging from dominantly clinopyroxene-plagioclase to dominantly hornblende-plagioclase (Condie et al., 1982). More detailed mineralogical data are given in next capture.

3.2 Carbonatite-alkaline rocks complexes in Tamil Nadu

The Tamil Nadu hosts several carbonatite-alkaline and/or alkaline silicate rock complexes such as Hogenakal, Pakkanadu, Yelagiri, Sevattur and Samalpatti.

Hogenakal carbonatites occur as a series of discontinuous bodies within two sub-parallel pyroxenites dykes that intrude the gneissic charnockite (with xenoliths of amphibolite and quartzite) country rocks. Each carbonatite body consist of discrete veins and lenses and show strong fenitization of the pyroxenite host. Pyroxenite and syenite xenoliths are also presented in the carbonatite bodies. The Hogenakal carbonatites appear to be un-deformed with well-preserved pristine magmatic texture and exhibit only stress banding in calcite twin lamellae (Pandit et al., 2002). Combined whole-rock data give age of 2.40 ± 0.03 Ga for Sm–Nd method and 2.42 ± 0.01 Ga for Rb–Sr method. The oxygen and carbon isotopic composition of calcites from four silicocarbonatites and single calcite carbonatite from Hogenakal have average values of $\delta^{18}O_{SMOW} = +7.8$ and $\delta^{13}C_{PDB} = -6.1‰$, this range seems belong to the group of mantle-derived carbonatite magma (Kumar et al., 1998). As Fig. 6 shows, the values of $\delta^{18}O$ and $\delta^{13}C$ correspond to mantle-derived material defined for example by Deines (2002). According to this paper, the primary material is generated within the mantle with isotopic composition in equilibrium, uncontaminated carbonate magmas crystalize to produce clusters or trends in the $\delta^{18}O$ versus $\delta^{13}C$ plot. Post-crystallization alteration can disperse values in various directions. Primary magma differs by secondary especially higher sparsity. This ability enables primary magma rise to the surface and form volcanic rock whereas secondary magma remains in depth where there is transformed to pluton. That is reason why primary mantle-derived magma is important carrier of information about mantle.
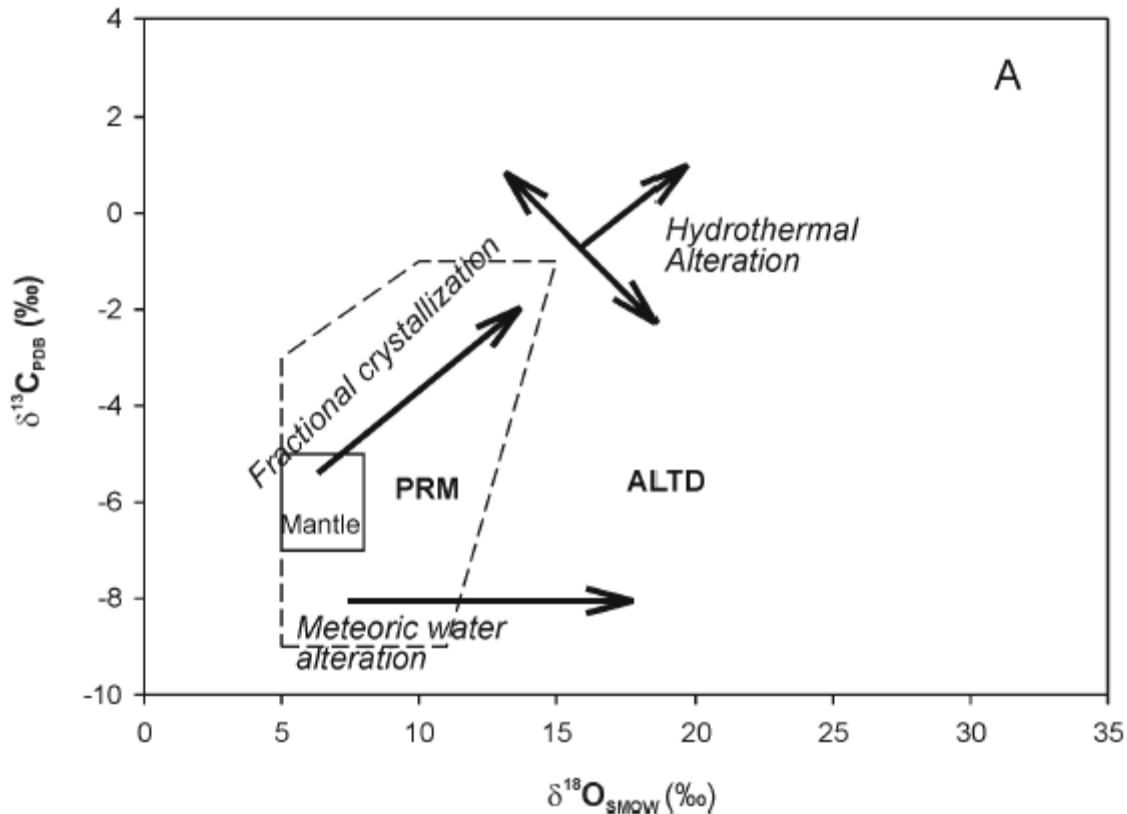
Fig. 6. Carbon and oxygen isotope composition field for primary and altered carbonatites (Ray and Ramesh, 2006). PRM stands for primary, ALTD stands for altered.

Pakkanadu carbonatites occur as small dimension, concordant fracture-fills and diatremes within the pyroxenites and as concordant lenses and dykes within syenite. Ribbon-like bodies of xenolithic feldspathic breccia are present within the carbonatites (possibly represent the vent rock that were later disrupted, blown and flushed out by carbonatitic melt). The Pakkanadu carbonatites are significantly metamorphosed, as indicated by development of secondary monazite and macro-scale deformation (Pandit et al., 2002). Suggested age of Pakkanadu region is between 600 and 845 Ma (Schleicher et al. 1998). Pakkanadu values for $\delta^{18}O_{SMOW}$ is + 8.61 and for $\delta^{13}C_{PDB}$ is −5.3‰ (Pandit et al., 2002).

The Yelagiri pluton intruded into the epidote-hornblende gneisses, which constitute the country rocks of the region. The Yelagiri complex is almost entirely composed of syenite with pyroxenite and biotite pyroxenite forming elongated masses measuring up to 50 m. Pyroxenite also occurs as xenolithic blocks with a sharp contacts with the syenite. Although geological information on the Yelagiri pluton is not sufficient, almost all the constituent rocks of this pluton do not show strong deformation and metamorphism shown by the country rock. Hence, this pluton is consider to keep the initial intrusive character. Nine syenite samples from Yelagiri pluton define and isochron corresponding to an age of 757 ± 32 Ma (Rb–Sr; Miyazaki et al. 2000).

In the Tamil Nadu region, two groups of silicocarbonatites can be distinguished based on their SiO_2–CaO–MgO contents and concentrations of compatible elements (Cr, Co and Ni). These two groups are Mg-rich silicocarbonatites (high amount of Na_2O, K_2O, Cr, Co and Ni) and carbonate-rich silicocarbonatites (low amount of Na_2O, K_2O, Cr, Co and Ni; Ackerman et al. 2017).

3.3 The Sevattur and Samalpatti complexes

First discovery of carbonatites in south India was in 1966 at Sevattur (Viladkar and Bismayer, 2014). The main mass of Sevattur complex, consisting entirely of coarse-grained dolomitic carbonatite, forms a crescent-shaped intrusive body, which is in contact with pyroxenite in the west and northwest, gneiss in the southwest, and trachytic syenite in the east. The carbonatites incorporates a number of xenoliths of basement gneiss, syenite and pyroxenite (Schleicher et al. 1998). The Sevattur carbonatite occurs as an inwardly dipping, arcuate body sandwiched between a large syenitic stock and pyroxenite (Pandit et al., 2002). The main part of carbonatites is exposed in the form of an elongated crescent-shaped body intrusive in granite gneiss. A few small arcuate collars of carbonatite dykes rarely exceeding 30 cm in thickness are they are arranged concentrically with respect of the main mass. A thin fringe of ankeritic carbonatite intervenes between the calcite carbonatite and dolomite carbonatite. The evidence that carbonatite have acted as intrusive rock is provided by a network of fine stringed and dykes cutting through fenites and breccias. The outcrops exposed by excavation give an explicit view of the dykes of carbonatites bordered by fenites (Udas and Krishnamurthy, 1970). The Sevattur and Samalpatti carbonatites show the effect of tectonic stress as reflected in development of bounding aged structures, elongated and shared xenoliths and deformed calcite twins lamellae (Pandit et al., 2002).
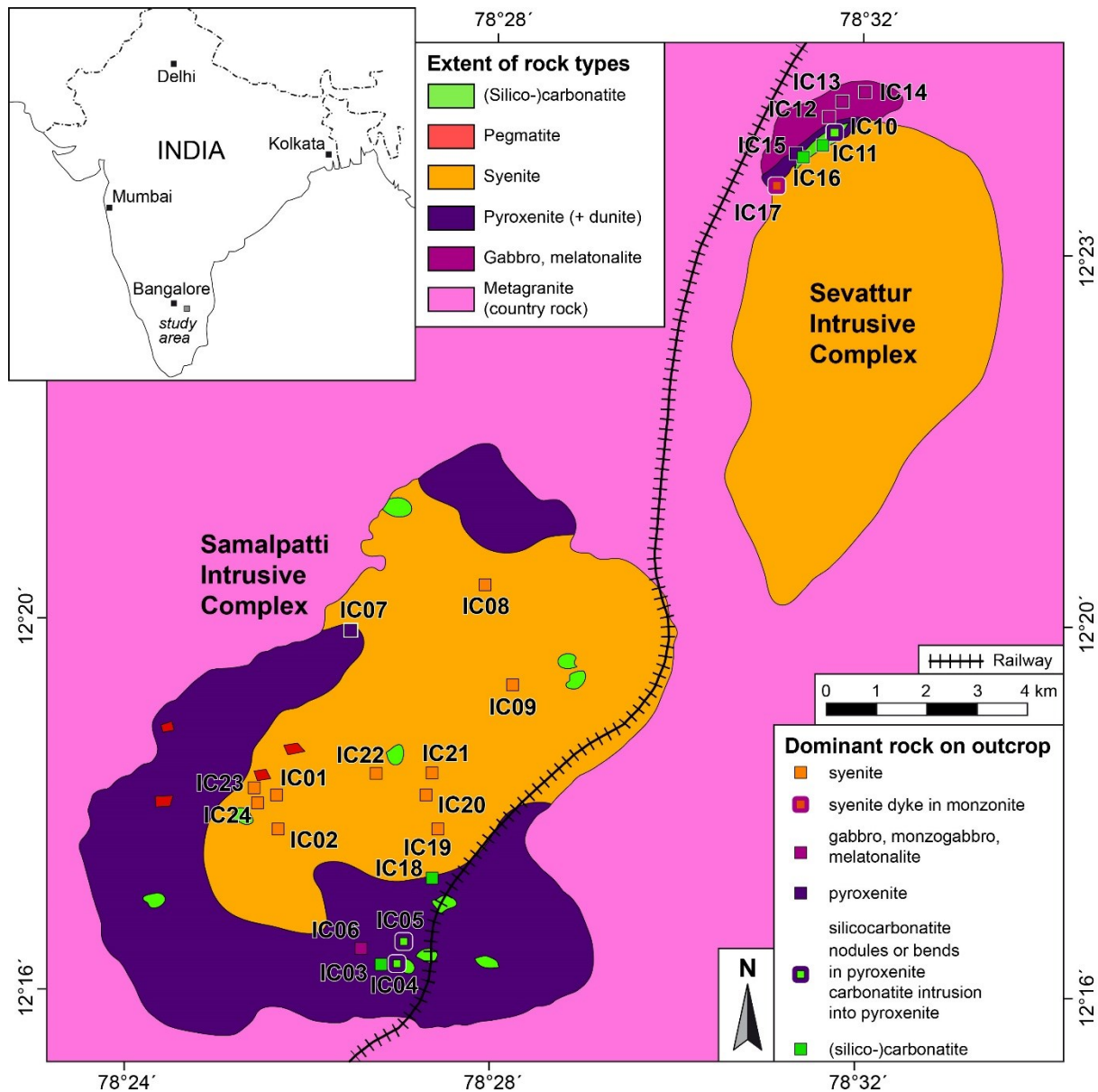
Fig. 7. Geological map of northern Tamil Nadu area (Ackerman et al. 2017).

The Sevattur-Samalpatti carbonatites with age of 730±30 Ma (Moralev et al., 1975) intruded into 2.55–2.53 Ga old (Peucat et al., 1993) granite gneiss terrain.

The Sevattur has the most varied mineral assemblage of all the Indian carbonatites (Suskhenswala and Viladkar, 1978). Magnetite and apatite are very common minerals, but there are minor occurrences of monazite, zircon, amphiboles, baddeleyite, urano-pyrochlore and allanite in various proportions (Schleicher et al. 1998). Monazite is presented in the Sevattur rauhaugite (hereinafter called the dolomitic carbonatite). Uranium-rich pyrochlore is frequent in the dolomitic carbonate of Sevattur. The carbonatite show rhythmic banding between medium and fine-grained types. Banding is accentuated by the presence of silicate minerals (olivine, phlogopite, aegirine and Na-amphibole) along with magnetite, apatite, pyrochlore, monazite and zircon. Pyrochlore is usually coarse-grained and occurs both as disseminated grains and in bands (Viladkar and Bismayer 2014). Detailed informations are given in table 2.

Colour of Sevattur carbonatites varies from white to pink. Rocks are coarse-grained and rarely associated with silicates. The apatite rich carbonatites contain frequently, randomly oriented up to 1.2 mm long grains of apatite accompanied by up to 3 mm pyroxene and magnetite grains enclosed in equigranular carbonate groundmass. The Sevattur carbonatites are uniformly enriched in REE ($\sum$ REE= 1126–2200 ppm) with steep patterns ($La_N/Sm_N = 2.5$–4.7 and $La_N/Yb_N = 22$–59). These carbonatites are enriched in Sr and Ba (~9000 ppm for Sr and ~4280 ppm for Ba). Rb/Sr ratios are extremely low (< 0.0006) as a result of the absence of silicate mineral phases (Ackerman et al., 2017) Pyroxenites are mostly medium-grained rocks with preferentially-oriented 6–8 mm long pyroxene prisms that have been replaced by phlogopite. Associated alkaline pyroxenites have highly variable major element composition as a result of variable carbonate and phlogopite contents, but typically are Mg-rich (MgO up to 19.6 wt. %; Ackerman et al., 2017). Major element concentrations of tonalite, granodiorite, monzogabbro and monzodiorite are predominantly controlled by variable proportions of plagioclase, K-feldspar and quart (Ackerman et al., 2017). Gabbroic rocks of the Sevattur complex (monzogabbro and melatonalite) exhibit variable grain-size with some varieties containing 1–2 cm crystals of plagioclase surround by fine-grained pyroxene, amphibole and biotite matrix with accessory apatite, pyrite and garnet. Tonalite and granodiorite represent the felsic members of Sevattur complex. Typically, these rocks contain plagioclase, quartz and small amount of K-feldspar (Ackerman et al. 2017).

In highly altered pyrochlore, the maximum loss is seen in Na followed by Ca and maximum gain in Ba and Sr. Therefore, the alteration of pyrochlore leads to enrichment in Ba, Sr and K and such alteration occurs at low temperature hydrothermal conditions. All pyrochlore grains, irrespective of intensity of alteration, show high concentration of uranium (11.31 wt. % to 18.32 wt. %). Uranium in Sevattur can be incorporated in minerals structures showing alpha and beta radiation. This may initiate a process of metamictization. It is reasonable to assume that these pyrochlore grains are metamictic (Viladkar and Bismayer, 2014).

Carbonatites in Sevattur are predominantly composed from CaO and CO_2 (together 45–90 wt. %), MgO (0.5–16 wt. %) and Fe_2O_3 (up to 11 wt. %). The SiO_2 values reaches 3.5 wt. % at maximum (in silicocarbonatites, this value 25 wt. % and lower) and volume of P_2O_5 is up to 6 wt. %. Contents of TiO_2, Al_2O_3, MnO, K_2O and Na_2O are usually equal or below 1 wt. %. Rubidium is ranging from 0.5 to 3.3 ppm and Sr from 7600 to 11300 ppm. Noteworthy is concentration of Ba (800–3800 ppm). Rare earth elements (REE) show Eu negative anomaly (18 ppm) and La varies from 15 to 870 ppm, Ce up to 1200 ppm to Dy (30 ppm) and Lu 0.1 to 1.1 ppm (Schleicher et al. 1998; Ackerman et al., 2017).

Stable isotopic compositions of $\delta^{18}O_{SMOW}$ in Sevattur varies from + 6.7 to +10.5 ‰ and $\delta^{13}C_{PDB}$ varies from −4.8 to −6.2 ‰ (Kumar et al. 1998; Ackerman et al. 2017). Therefore, the origin of Sevattur carbonatites is attributed to from primary, mantle-derived type.

The Samalpatti carbonatite complex is more than 125 km^2 in extent and comprises of dunite, pyroxenite, syenite and carbonatite. Whole complex intrudes in a discordant fashion the country rock which is a hornblende epidote gneiss. The pyroxenite has a circular shape with inwards dips suggesting a cone. Primary foliation is prevalent in porphyritic syenites and in some spots in carbonatite (Subramanian et al., 1978). The average width of pyroxenite outcrops is about 2 km with length of about

16 km. Its contact with syenite is uniformly coarse-grained. Syenites appear to have been emplaced in several phases. In addition to the centre core, it also forms satellite bodies of small dimensions with pyroxenite. It carries xenoliths of both gneiss and pyroxenite. The texture of calcite carbonatites varies from coarse- to fine-grained, sometimes becoming equigranular. (Viladkar and Subramanian, 1995). Dunites exposures are seen at several places in the pyroxenite body. Small mounds and boulders of carbonatite, probably representing stocks or plugs, are spread throughout pyroxenitic and syenitic bodies. Carbonatites also occurs as small dykes varying in width 20 and 40 cm, veins (fracture filling that are 5–20 cm in width), and lenses up to 10 m long (Srivastava et al., 2005). The complex shows an overall enrichment of LREE, Nb, Ba, P and Zr, the distribution of Th is in excess to that U and both features are reflected by the presence of monazite, cherkinite, allanite, ilmenorutile, thorite and zircon (Subramanian et al., 1978).

Colour of Samalpatti carbonatites is also white to light-pink. Carbonatite rocks contain 0.8–1.66 mm large crystals of calcite and 0.1–1 mm long pyroxene crystals (locally associated with accessory apatite). Carbonatites in Samalpatti show overall low content of REE ($\sum$REE = 14–216 ppm) with negative Eu anomaly (Eu/Eu* = 0.6-0.8). The Rb/Sr ratios vary from 0.002 to 0.27. Contents of Sr are lower than 1000 ppm and contents of Ba are lower than 1030 ppm (Ackerman et al., 2017). Contents of SiO_2 in calciocarbonatites are variable and reach up to 9.5 wt. %. This fact with low MgO and FeO_t contents correlating with Na_2O, K_2O and FeO_t abundances reflect modal proportions of K-feldspar, plagioclase, phlogopite and clinopyroxene. Pyroxenites contain >12 wt. % MgO and high amount of compatible trace elements and vice versa low amounts of Al_2O_3, <10.6 wt. % and alkalis K_2O+Na_2O < 4 wt.%. Monzogranites and monzonites have low MgO and high Al_2O_3 contents and very high content of alkalis, $Na_2O + K_2O$ is ranging from 9.6 to 12.6 wt. % (Ackerman et al., 2017). In Samalpatti region has been found several rocks that can be classified as silicocarbonatites. Silicocarbonatites form xenoliths with size up to 30 cm in pyroxenites and gabbros. Most of the silicocarbonatites are greenish in colour and they are predominantly composed of randomly oriented needle-like to subautomorphic grains. Few Cr-rich silicocarbonatites show slightly sinusoidal REE patterns depleted in light REE (La_N/Sm_N < 0.8 and La_N/Yb_N from 3.1 to 5.7) while all other silicocarbonatites and calciocarbonatites have La_N/Sm_N > 0.8 and La_N/Yb_N from 7.6 to 16.5. (Ackerman et al. 2017).

As was mentioned above, the Samalpatti suite is dominated by silicocarbonatites. CaO and CO_2 together ranging from 20 wt. % to 87 wt.%. In our case, SiO_2 reaches up to 40 wt. % and more (SiO_2 in Schleicher et al., 1998 has only 4 wt. % maximum) and MgO span around 15 wt. %. Other oxides like Fe_2O_3, Al_2O_3, TiO_2 and MnO have low values, only up to 3 wt. %. In contrast to Sevattur region, Ba is ranging from 340–900 ppm, but Schleicher et al. (1998) recorded in Samalpatti carbonatites 4150 and 34030 ppm of Ba. Lanthanium varies from 2 to 12 ppm and Lu around 0.1 ppm. Europeum negative anomaly has been observed. Again, Schleicher et al. (1998) presented different results with one sample reaching La up to 32400 ppm and Ce, Nd, Sm and Eu also show very high contents: 21800, 24700, 2700, 403 ppm.

Values of stable isotopes in Samalpatti measured by Ackerman et al. (2017) ranging from –4.0 to + 4.1 ‰ for $\delta^{13}C$ and $\delta^{18}O$ largely varies from 10.1 to 25.5 ‰. Carbonatites in Samalpatti are more or less altered as by hydrothermal processes by meteoric water and only a part of the source is primary.

	Carbonatite type		
Minerals	Calcitic	Dolomitic	Ankeritic
1. Carbonates			
Calcite	✔	✔	X
Dolomite	✔	✔	X
Ankerite	✔	✔	✔
2. Oxides			
Bastnaesite	X	✔	X
Magnetite	✔	✔	✔
Ilmeno-rutile	✔	✔	✔
Nb-rutile	✔	✔	✔
Ilmenite	✔	✔	✔
Pyrochlore	X	✔	X
Perovskite	✔	✔	X
Calzirtite	X	✔	X
3. Phosphates			
Apatite	✔	✔	✔
Monazite	X	✔	✔
4. Sulphates			
Baryte	✔	X	✔
5. Sulphides			
Pyrite	X	✔	✔
Chalcopyrite	X	✔	✔
Pyrrhotite	X	✔	X
6. Silicates			
Thorite	X	X	✔
Zircon	X	✔	✔
Allanite	X	X	✔
Mica	✔	✔	✔
Olivine	✔	✔	X
Amphibole	✔	✔	✔
Na-pyroxene	✔	✔	X
Wollastonite	✔	X	✔
Orthoclase	✔	X	X
Albite	✔	X	X

Tab. 2. Mineralogy of carbonatites from the Sevattur and Samalpatti (Viladkar et al., 1995)

Alkaline silicate rocks from Samalpatti and Sevattur have a similar content of REE ($\sum$REE 5–823 and 41–715) and both are enriched in volume of Ba (up to 61500 ppm). Depletion in Nb–Ta is more common in Samalpatti but Nb/Tb and Zr/Hf ratios largely overlap for silicate rocks from the two complexes, and no difference in the extent of Zr/Hf fractionation is observed. Pyroxenites in Sevattur compared to Samalpatti pyroxenites are enriched in Nb. Sevattur carbonatites are more depleted in Zr relative to Hf (< 0.37 for Sevattur, > 0.73 for Samalpatti). Sevattur have also higher LREE/HREE ratios for non-carbonate fraction over carbonate fraction (La_N/Yb_N) non-carbonate$/(La_N/Yb_N)$ carbonate >5 for Sevattur and <2.3 for Samalpatti. Compatible lithophile elements like Sc, V, Cr, Ni or Co are dominated by non-carbonate fractions (Ackerman et al., 2017).

Study of Ackerman et al. (2017) have shown, that the Samalpatti calciocarbonatites ranging in $^{87}Sr/^{86}Sr_{(i)}$ ratio values from 0.7067 to 0.7075 and $\varepsilon_{Nd(i)}$ from –9.0 to –14.4. Schleicher et al. (1998) reported the values of $^{87}Sr/^{86}Sr_{(i)}$ ratios from 0.7045 to 0.7054 and ε_{Nd} were lower (–8.8 to –20.1). The Mg-Cr-rich silicocarbonatites from Samalpatti have $^{87}Sr/^{86}Sr_{(i)}$ ratio 0.7052–0.7063, $\varepsilon_{Nd(i)}$ have wide range from –5.3 to –42.4. The Ca-rich silicocarbonatites have $^{87}Sr/^{86}Sr_{(i)}$ from 0.7069 to 0.7083 and uniform $\varepsilon_{Nd(i)}$ values, -6.9. $^{87}Sr/^{86}Sr_{(i)}$ ratio of alkaline silicate rocks from Samalpatti is 0.703–0.7092 and $\varepsilon_{Nd(i)}$ is –3.3. Regional metadiorite from both complexes yields $^{87}Sr/^{86}Sr_{(i)}$ and $\varepsilon_{Nd(i)}$ 0.7059 and –21.5, respectively (Ackerman et al., 2017).

Samalpatti carbonatites show a large variability in $\delta^{13}C$ (–5 to +4.1 ‰) and $\delta^{18}O$ (+6.5 to +25.5 ‰; Ackerman et al., 2017; Ray and Ramesh, 2006 and references therein). Cr-rich silicocarbonatites tend to have lower values of this stable isotopic compositions. Calciocarbonatites have $\delta^{13}C$ around –2.6 ‰ and high values of $\delta^{18}O$ = 19.2 ‰. Sevattur carbonatites tend to have more uniform values of stable isotopes with the $\delta^{13}C$ ranging from –6 to –4.8 ‰ and $\delta^{18}O$ ranging from +7.6 to +10.5 ‰ (Ackerman et al., 2017).

3.4   Fenitization in carbonatites in Tamil Nadu

The carbonatites have fenitized surrounding Archean gneisses and pyroxenites extensively, however, the zone of fenitization are not well defined. Adjacent to the carbonatite zone, contact fenitization is pronounced and the effects gradually diminish farther from the contact. In the initial stage of fenitization of granite-gneiss, feldspar become clouded while quartz is replaced by either Na-amphibole or Na-pyroxene. The latter also form ramifying veins in some fenites. With progressive fenitization feldspar becomes clear and small amount of micro-perthite develops. Quartz gradually diminishes in amount. The mineralogy of high-grade fenite is similar to syenitic rock consisting of large crystals of Na-amphibole, Na-pyroxene, microperthite, orthoclase, albite, carbonate, apatite and magnetite. At greater distance from the carbonatite contact, the effect of K-fenitization is prominent resulting in the formation of orthoclase-rich rocks. Pyroxenites have also been fenitized at the carbonatite contacts to mica-rich rock. The process of phlogopitization is also accompanied by aegiritisation of some original pyroxenes. Calcite and apatite are found to be abundant in such rock. Chemical changes during fenitization of granite-gneiss involve addition of K, Na, Mg and Fe in large amounts accompanied by dilution of Si (Viladkar and Subramanian, 1995).

Highly siderophile elements (HSE) consist of platinum-group elements (PGE – Os, Ir, Ru, Rh, Pd and Pt), Au and Re. The HSE are key tracers of planetary accretion and differentiation processes due to their high affinity for metal and sulphur relative to silicate. There are light platinum group metals (Ru, Rh and Pd) with density roughly 12 g.cm^{-3} and heavy platinum group metals (Os, Ir and Pt) with density roughly 22 g.cm^{-3}. Palladium is great dissolvent of gas. On the basis of association, the PGE´s may be divided into two other groups: the iridium-group PGE (I-PGE) consisting of Ru, Os and Ir, and the platinum-group PGE (P-PGE) consisting of Rh, Pt and Pd. The refractory metal´s hypothesis suggest that the I-PGE might be thought of as being present in the mantle as refractory metals such as Os-Ir alloys while the P-PGE are present in sulphides. Thus, during partial melting the sulphide dissolve and release the accompanying P-PGE, which may enter the melt. The Os-Ir alloys dissolves at much higher temperatures and therefore, a very little of I-PGE enters the melt (Barnes et al., 1985). The HSE are geochemically distinct in that, with the exception of Au, they have elevated melting points relative to iron (Re and Os are even higher), low vapour pressures, and they are resistant to corrosion or oxidation. Ruthenium, Rh, Os, Ir and Pt belongs to refractory elements, Pd is transitional element and Au among to moderately element. 50% condensation temperature (Tc) of Au is 1060 K, Pd 1324 K, Fe 1334 K, Rh 1392, Pt 1408 K, Ru 1551 K, Ir 1603 K, Os 1812 K and Re 1821 K (measured at 10^{-4} atm; Lodders, 2003; McDonough and Sun, 1995 and references therein). Assuming abundances of the HSE in materials that made up the bulk Earth were broadly similar to modern chondrite meteorites, mass balance calculation suggests that > 98% of these elements reside in the metallic core (O´Neill and Palme, 1998). In practical terms, the resulted low HSE abundances inventories in differentiated silicate crust and mantle enable the use of these elements to track metallic core formations and the subsequent additions of HSE-rich impactors to planets and asteroids. In absence of metal, the HSE are chalcophile, so these elements are also affected by processes involving growth and breakdown of sulphides (Day et al., 2015). The siderophile behaviour of some of the HSE may be greatly reduced at high P-T conditions, and on this basis it has been suggested that high-pressure equilibration at the base of the deep molten silicate layer or „magma ocean" on the early Earth, may account for their abundances in the upper mantle (Gannoun et al., 2016; Murthy, 1991). High-pressure experiments that simulate the conditions of core formation do indeed indicate that the HSE are less siderophile under these conditions (Mann et al., 2012). However, the range of HSE partition coefficients, even at elevated P-T conditions, cannot account for either the absolute or relative abundances in terrestrial mantle, suggesting that the high-pressure equilibration was not the dominant process controlling their present distribution. Therefore, mantle HSE abundances have long been taken to suggest that between 0.5 and 0.8% by mass of „late-accreted" broadly chondritic material was added to Earth after the core formation was completed. Differing absolute abundances, but similar chondrite-relative HSE abundances have also been inferred for the Moon, Mars and other meteorite parent-bodies (see next chapter), suggesting that late accretion was common phenomenon to terrestrial planets, setting HSE abundances in planetary mantles. In this way, core formation and late addition of meteorite material are thought to have established the HSE abundance in Earth´s silicate mantle, providing a framework for understanding the long-term effect of mantle melting (Gannoun et al., 2016).

Under low-pressure conditions, the HSE are defined by having metal-silicate partition coefficients in excess of 10^4 (Day et al., 2015). Some works suggest that the HSE might become much less siderophile at high pressures and temperatures (Righter and Drake, 1997), other suggest that the metal-silicate distribution coefficients for at least some of these elements are > 10^6 at both low and high pressures (Ertel et al., 2001).

The main control on HSE fractionation during partial melting in the Earth`s mantle provide base-metal sulphides (e.g., MSS, pentlandite, pyrrhotite), platinum-group element minerals and the presence or absence of residual metal (Day et al., 2015). For example, the distribution of the HSE between a liquid metal phase and solid metal restite during partial melting in the Fe–Ni–S system is dependent on the S contents of extracted melts, and on C and P that enter the metallic phase (Day et al., 2015; Chabot

and Jones, 2003). Osmium isotopic studies and distribution of PGE in sulphides have revealed significant compositional and isotopic heterogeneity of sulphides in mantle peridotites. It has been observed that Cu–Pd–Pt-rich sulphides tend to occur preferentially along silicate grain boundaries in peridotites, while presumably primary Ni-rich sulphides are predominantly hosted by silicates (Becker et al., 2006; Luguet et al., 2003). Such bimodal characteristic of sulphides in peridotites may be a common feature in oceanic and continental environments (Becker et al., 2006) and have been interpreted as metasomatic addition of Pd- and Pt- enriched sulphides along grain boundaries by percolating sulphide or silicate melts, fluids, or incomplete extraction of silicate melt (Becker et al., 2006; Luguet et al., 2003). Good correlations between incompatible HSE with lithophile fertility indicator such as Al_2O_3 suggest that the bulk HSE budget in peridotites has been little affected by sulphide melt or fluid mobility while positive correlation between Pd/Ir with Al_2O_3 and S might show effect of percolation of sulphide melts (Becker et al., 2006). Concentrations of Ir, Ru and Os tend to increase with increasing degree of partial melting (Becker et al., 2006). Osmium behaves as a highly compatible element during partial melting and therefore, it is preferentially retained in the residual mantle. In contrast, Re is moderately incompatible and preferentially enters into the melt. Re is removed into both silicate and sulphide phases during fractional crystallization (Gannoun et al., 2016).
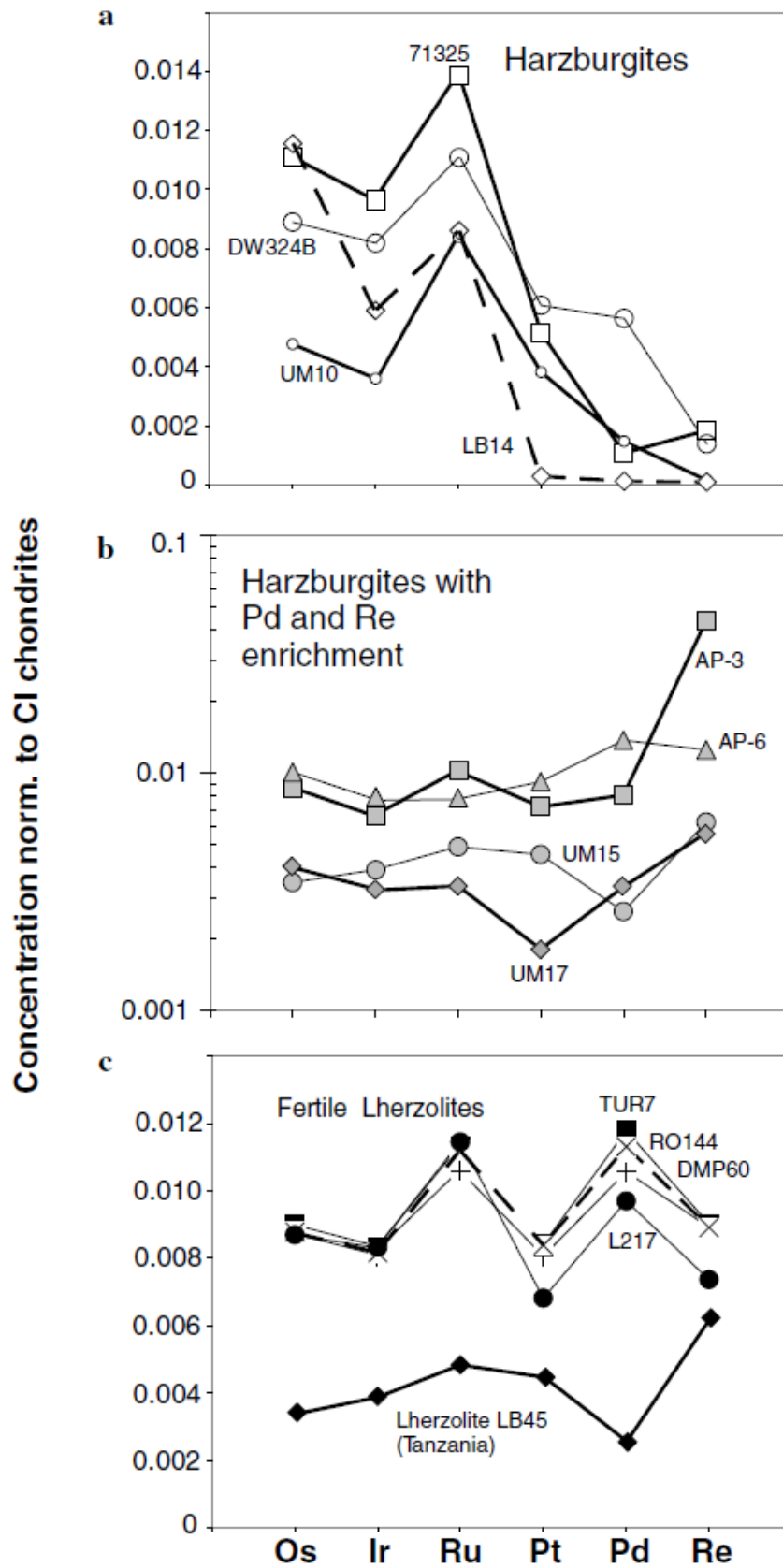
Fig. 8. Example of concentrations of HSE in a) normal harzburgite; b) harzburgite enriched by Pd ad Re; c) fertile harzburgite (Becker et al., 2006).

Compositional models of the Earth in respect to HSE are critically dependent on three main sources of information: the seismic profile of the Earth and its interpretation, comparison between primitive meteorite and the solar nebula composition, and chemical and petrological models of peridotite-basalt melting relationship (McDonough and Sun, 1995). They are two major models describing bulk Earth`s mantle composition. First one is pyrolite model (Ringwood, 1966) using the complementary melt-residuum relationship between basalts and peridotites as a basis for estimating the major and minor element composition of Earth´s upper mantle. The second model can generally be referred to as the CI chondrite type, where the Earth is assumed to have a bulk major-element composition equal to that of CI chondrites. This model assumes that the Earth has a major-element composition of CI chondrites, but is depleted in volatile trace elements relative to CI chondrites (McDonough and Sun, 1995). These models in terms of HSE are compared in Tab. 3.

Element	CI model*	Pyrolite model*	Continental crust**
Os	490	3.4	0.05
Ir	455	3.2	0.05
Ru	710	5.0	0.1
Pt	1010	7.1	0.4
Pd	550	3.9	0.4
Re	40	0.28	0.4
Rh	130	0.9	0.06
Au	140	1.0	2.5

Tab. 3. HSE composition of the Earth`s mantle and continental crust; *McDonough and Sun 1995; **Wedepohl 1995. Given values are in ppb.

Because their siderophile nature and considering the fact that Pt is moderately compatible, Pd is moderately incompatible and Os is compatible during melt generation, the Re–Os and Pt–Os isotopic systems differ significantly from other useful long-lived radiometric systems (e.g., Rb–Sr, Sm–Nd, Lu–Hf, U–Th–Pb), where both parent and daughter elements are preferentially concentred into the melt (Gannoun et al., 2016) and elements are predominantly lithophile. The [187]Re–[187]Os isotopic system is based on the long-lived β[-] decay, where [187]Re is a major isotope (62.6%) of Re, and has a half-life of ~42 Ga (Day et al., 2015). The Re–Os system is fairly resistant to some alteration processes on the seafloor, and therefore the [187]Os/[188]Os of dredged seafloor peridotites can be used to obtain information on primary mantle characteristic (Martin, 1991). Radiogenic [187]Os/[188]Os composition for MORB from the south Atlantic were attributed to metasomatism of the asthenospheric mantle, and local effects from plum-ridge interaction (Escrig et al., 2005). Moreover, the osmium isotopic composition can potentially provide an exceptional tracer of recycled lithosphere in Earth´s mantle because both oceanic and continental crust possess exceptionally high Re/Os (parent/daughter ratios), and develop radiogenic Os isotope over time (Gannoun et al., 2016) relative to PUM (Pearson et al., 1995). The example of use of Os ratios as [187]Os/[188]Os variations can be nicely seen through the study of HIMU mantle-component (part of mantle with high proportion of recycled or metasomatically enriched oceanic crust enriched in U/Pb ratio and depleted in [87]Sr/[86]Sr ratios) within ocean island basalts. These studies indicate the presence of material that has evolved over a long-time period with a high Re/Os, consistent with model indicating recycled oceanic lithosphere in the source of these volcanic rocks (Day, 2013). The systematic nature of such fractionations, suggest either that they are dominantly controlled by a single process, such as mantle melting or fractional crystallization, or several processes act to have the same effect, for example, fractionation by refractory mantle sulphide and also by sulphide segregation during fractional crystallization (Gannoun et al., 2016). Rhenium shows a broadly positive co-variation with Al_2O_3 and sulphur, which is consistent with the incompatibility of other elements during mantle melting. Extreme Os composition of continental intra-plate alkali volcanic rocks could reflect low degrees of partial

melting and preferential sampling of more fusible mafic components, such as pyroxenite, in the asthenospheric mantle. Alternatively, melting of metasomatized lithosphere during rifting events may also be responsible for the HSE abundances (Gannoun et al., 2016).

HSE linear correlations of elements over Ir provide estimated abundances for these elements in the Earth`s mantle. Using these estimates, the overall evidence from peridotites suites is that the Earth´s mantle has a generally uniform distribution of the HSE, albeit with some inter-element ratios (e.g. Ru/Ir, Pd/Ir) that may be supra-chondritic (Day et al., 2015).

Previous studies of peridotites have shown that Os, Ir and Ru behave compatibly up to moderately high degrees of melting of the Earth´s mantle, whereas Au and Re are incompatible elements. The PGE compatibility seems to be firmly established for mantle melting:

$D^{Os}_{solid/melt} \sim D^{Ir}_{solid/melt} \sim D^{Ru}_{solid/melt} > D^{Pt}_{solid/melt} > D^{Pd}_{solid/melt}$ (Becker et al., 2006; Pearson et al., 2004)

The absence of correlations of Pt and Pd with indices of melt extraction of fertile and moderately depleted peridotites was interpreted in terms of compatible behaviour of these elements during low to moderate degrees of partial melting (Handler and Bennett, 1999). Contrary to these results are data from Becker et al. (2006) and Pearson et al. (2004) which suggest that the Pt and Pd behave during peridotite-silicate melt partitioning as incompatible elements.

The effects of surface processes on composition of HSE are poorly described. It seems that during serpentinization, the $^{187}Os/^{188}Os$ systematics is not affected. In other words, there is no addition of radiogenic crustal Os because there is a good correlations of $^{187}Os/^{188}Os$ with Al_2O_3 for suites of highly serpentinized peridotites (Reisberg and Lorand, 1995). Osmium and aluminium are chemically so different that they should behave in contrasting way during alteration. Hence, secondary mobilization of Al or significant addition of radiogenic Os should result in degradation or obliteration of $^{187}Os/^{187}Os$-Al_2O_3 correlations of igneous origin (Becker et al., 2006).

Xenoliths derived from the mantle and brought to the surface via volcanism are among the few types of materials that permit direct study of the chemical composition of the Earth´s upper mantle. The best estimate for the $^{187}Os/^{188}Os$ composition of primitive upper mantle, that is a theoretical mantle composition with high Al_2O_3 that is consider to have experienced no depletion through melting, is 0.1296 ± 0.0008 (2σ; n=117) and $^{187}Re/^{188}Os$ value around 0.487 (Meisel et al., 2001).

Mid-ocean ridge basalts (MORB) form by partial melting of the depleted Earth mantle, and variations in their radiogenic isotope compositions or elemental ratios of incompatible elements are consider to reflect compositional heterogeneity of their mantle source. The fractionation of Re–Os accompanying the generation of MORB is one of the key processes controlling the distribution of these elements between Earth´s mantle and crust (Tatsumoto, 1966; Gannoun et al., 2016). Following data for MORB, OIB and komatiites are taken from (Barnes et al., 1985; Day, 2013; Day et al., 2013, 2010; Escrig et al., 2005; Gannoun et al., 2016, 2007, 2004 and references therein; Puchtel et al., 2005; Schiano et al., 1997). Osmium in MORB range from 0.002 to 0.17 ppb (abyssal peridotite from 0.003 to 13 ppb). The fact that Re is moderately incompatible results its higher concentrations in MORB (0.044–3 ppb) comparing to mantle peridotite with 0.010–0.450 ppb. Low Os concentrations are likely result, in part, from preferential partitioning into residual mantle sulphide and/or platinum group minerals (PGM) and, in part, to the low solubility Os in silicate melts. In contrast, the relative high Re concentrations result, in part, from that fact that Re is rather incorporated to low-melting point mantle sulphide and PGM phases and, in part, having a much higher solubility in silicate melts. $^{187}Os/^{188}Os$ ratios for MORB are in range of 0.126–0.148. $^{187}Re/^{188}Os$ in MORB have a large scale of variations (30–8000) due to silicate phases and glass.

Oceanic intra-plate volcanism is often assumed immune to lithospheric contamination. Compared to continental intra-plate eruptions, ocean islands basalts (OIB) do not interact with

thermo-chemically complex Sub-continental lithospheric mantle. The low Os content in OIB (typically < 1 ppb; alkali basalts reach lower values) make the Re-Os isotope system a particularly sensitive indicator of lithospheric contamination and/or recycled crust incorporation. Rhenium in OIB achieves concentration in the hundreds of ppt and lower. The relatively low Re concentrations is result of volatile behaviour during sub-aerial eruption. Relatively un-radiogenic $^{187}Os/^{188}Os$ composition (< 0.18) of OIB relative to local oceanic crustal reservoirs (>0.4) make the tracing of assimilation of crustal or lithospheric mantle materials in OIB a straightforward process.

Fig. 9. and its description shows the schematic formation of OIB and MORB.
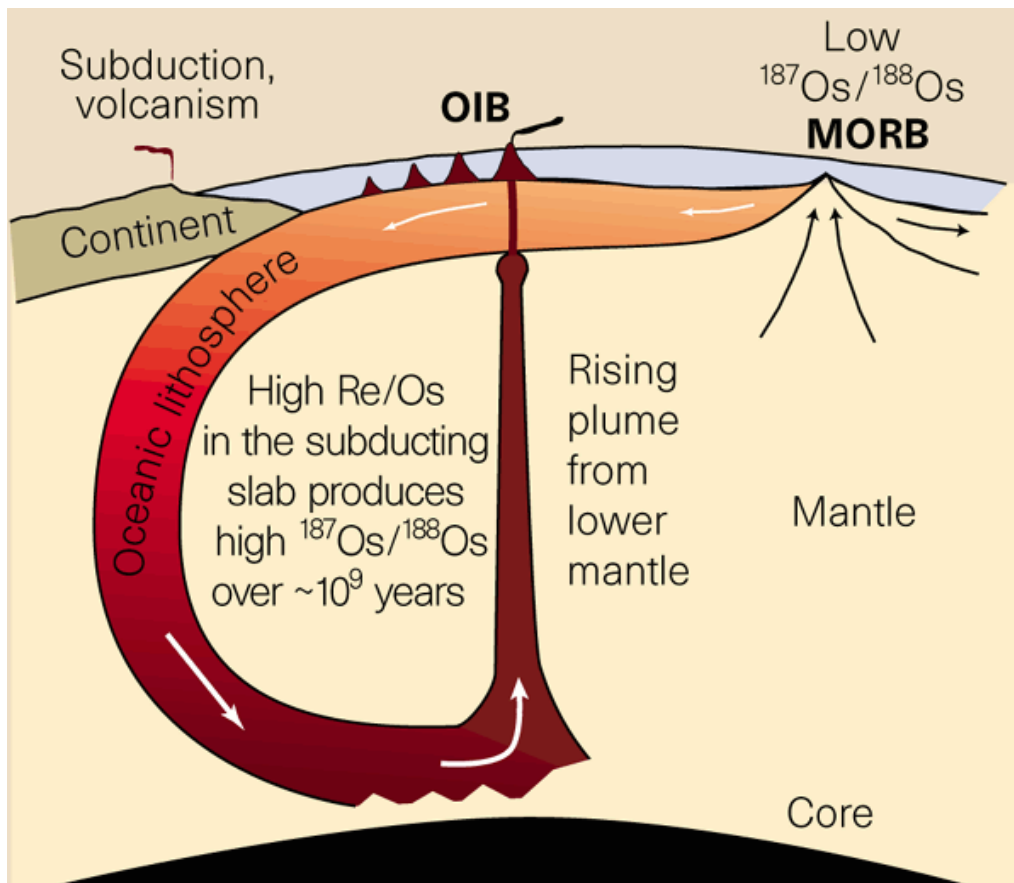
Fig. 9. Production of MORB and OIB such as that which form Hawaii, as seen in the slab recycling model. Subduction of oceanic lithosphere continuously transports rocks that are produced near the Earth´s surface, in particular MORB and associated sediments, back into deep mantle. These introduced heterogeneities are stirred and distorted by convection in the hot mantle. Eventually they can be become buoyant and rise melt to produce OIB. The time taken for this recycling process is thought to be typically about a billion years. By the time the plume melts to produce OIB has aged isotopically and has higher $^{187}Os/^{188}Os$ than surrounding mantle (Halliday, 1999).
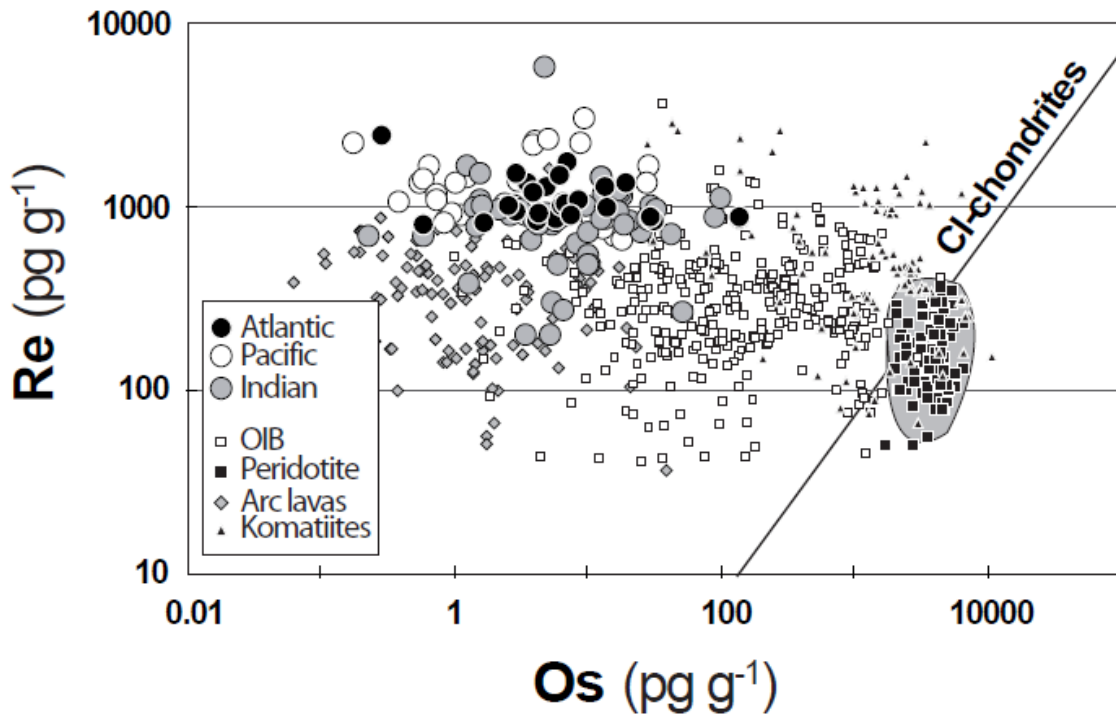
Fig. 10. Rhenium against osmium (ppt) plot for terrestrial basalts (Gannoun et al., 2016 and refferences therein).

Komatiites erupted billions of years ago (there are a few findings from Proterozoic and Phanerozoic) as pulsating stream of white-hot lava. Their unusual chemical composition and exceptionally high formation temperatures produced highly fluid lava that crystallized as a spectacular layered flow. Investigation of these extreme conditions in which komatiites forms provides important evidence about the thermal and chemical evolution of the planet, and the nature of the Precambrian mantle (Arndt et al., 2008). Komatiites have generally much higher Os concentrations, up to 10000 ppt with similar range of Re (40–920 ppt) concentrations as MORB. Re/Os and $^{187}Re/^{188}Os$ ratios widely vary from 0.006 to 0.5 and 0.3 to 2.41, respectively. Ratio of $^{187}Os/^{188}Os$ in komatiites has been determined to 0.11015–0.21678. Such combined values most likely reflect high-degrees of partial melting (>40 %) of mantle during the formation of these melts.
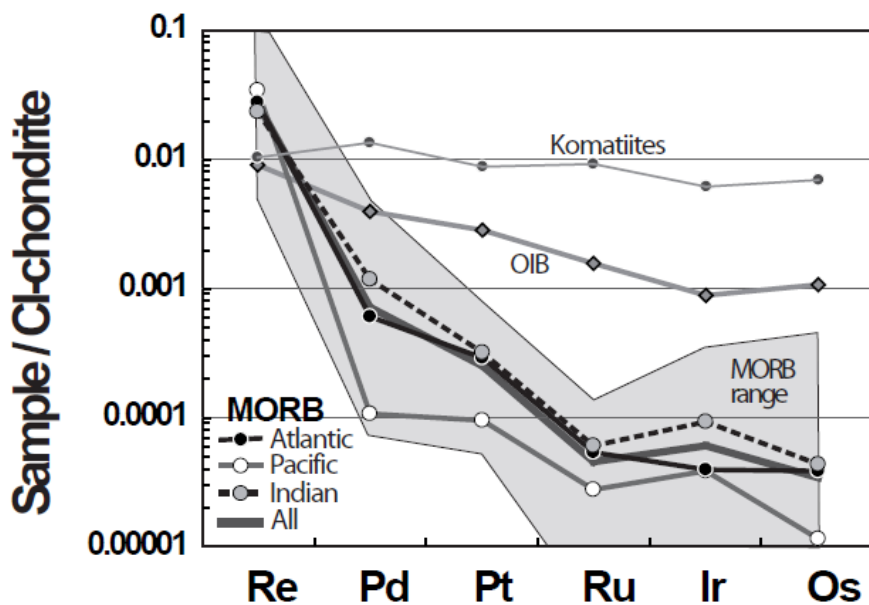
Fig. 11. MORB, OIB and komatiites plot of HSE contents normalized to CI-chondrites (Gannoun et al., 2016).

Reservoir/element	Re	Os	Ir	Ru	Pt	Pd
Primitive mantle	0.35	3.9	3.5	7	7.6	7.1
Ocean crust	0.7	0.05	0.13	0.7	2.1	2.1
Continental crust	0.2	0.03	0.02	0.21	0.51	0.52
MORB	0.86	0.03	0.055	0.061	0.053	1.19
OIB tholeiite + alkali	0.38	0.07-0.64	0.17-0.45	0.34-1.11	2.27-2.6	1.4-2.2
Komatiite	0.34	1.35	1.41	6.56	9.07	7.05
Carbonatite	0.03-0.378**	0.008-0.35**	<0.78	<6.75	0.1-38.0	<3.65

Reservoir/element	Rh	Au	$^{187}Re/^{188}Os$	$^{187}Os/^{188}Os$
Primitive mantle	1.2	1.7	0.4353	0.1296
Ocean crust	-	-	-	0.15
Continental crust	0.38	-	-	1.1
MORB	-	-	30-8000*	0.126-0.148
OIB tholeiite + alkali	-	-	>0.5	0.145-0.310
Komatiite	-	-	0.3-2.41	0.110-0.216
Carbonatite	0.08-0.14	1.24-8.61	-	-

Reservoir/ratio	$^{187}Os/^{188}Os$
Fertile convecting mantle	
Chondritic reference	0.127
Primitive upper mantle	0.129
Subcontinental lithospheric mantle	
Average	0.113
Range	0.105-0.129
Depleted mantle	
Average	0.125
Range	0.123-0.126
Enriched plume	0.130-0.135
HIMU	0.15
Enriched mantle 1	0.152
Enriched mantle 2	0.136

Table. 4. Estimates of HSE abundances (ppb), $^{187}Re/^{188}Os$ and $^{187}Os/^{188}Os$ ratios in selected terrestrial reservoirs (Day, 2013; Honda et al., 2002; Shirey and Walker, 1998; Walker et al., 1999 and references therein). *MORB glass included, ** our measurement

4.1 HSE in planetary objects

As HSE preferentially partition into metallic phases, the HSE concentrations in planetary objects depend on the percentage of metal in parent body, which is also reflects its oxidation state (Day et al., 2015). The compiled datasets of mantle-derived melts from planetary bodies reveals that fractional crystallization led to progressive fractionation of more compatible HSE from les compatible HSE in the order of Ir ≥ Os > Ru > Pt > Pd ≥ Re (Day et al., 2015).

Reservoir/element	Re (± 1 σ)	Os (± 1 σ)	Ir (± 1 σ)	Ru (± 1 σ)
Terrestrial mantle[1]	0.35 ± 0.06	3.9 ± 0.5	3.5 ± 0.4	7 ± 0.9
Terrestrial mantle (MgO)[2]	0.23 ± 0.05	3.1 ± 0.5	3 ± 0.5	6 ± 1
Lunar crust[3]	0.0029 ± 0.0001	0.0014 ± 0.0003	0.0015 ± 0.0006	0.0068 ± 0.027
Lunar mantle(MgO)[2]	0.01	0.1	0.1	0.1
Lunar mantle(MgO)[4]	0.009 ± 0.006	0.097 ± 0.03	0.087 ± 0.04	0.162 ± 0.05
Lunar mantle (I-HSE)[5]	0.004	0.07	0.07	0.1
Martian mantle[6]	0.3 ± 0.3	3.7 ± 2.9	3.3 ± 3	5.3 ± 4.9
Martian mantle(I-HSE)[5]	0.1	2.4	2.4	3
Martian mantle (Exp.)[7]	0.05	1.8	2.2	1.8
Ultramafic Shergottite[8]	0.08	3.26	2.25	3.44
Mafic Shergottite[8]	0.06	0.58	0.37	0.7

Reservoir/element	Pt (± 1 σ)	Pd (± 1 σ)	Rh (± 1 σ)	Au (± 1 σ)
Terrestrial mantle[1]	7.6 ± 1.3	7.1 ± 1.3	1.2 ± 0.2	1.7 ± 0.5
Terrestrial mantle (MgO)[2]	10 ± 2	9 ± 1.5		
Lunar crust[3]	0.016 ± 0.015	0.033 ± 0.03		0.028 ± 0.03
Lunar mantle(MgO)[2]	0.2	0.1		
Lunar mantle(MgO)[4]	0.211 ± 0.013	0.151 ± 0.1		
Lunar mantle (I-HSE)[5]	0.1	0.03		
Martian mantle[6]	3.7 ± 3.6	2.3 ± 2.1		
Martian mantle(I-HSE)[5]	4	3		
Martian mantle (Exp.)[7]	4.98	4.22		0.63
Ultramafic Shergottite[8]	2.81	1.62		
Mafic Shergottite[8]	5.7	3.32		

Reservoir/element	$^{187}Re/^{188}Os$ (± 1 σ)	$^{187}Os/^{188}Os$ (± 1 σ)	$^{187}Os/^{188}Os_c$[8]	DPUM
Terrestrial mantle[1]	0.4253	0.1296 ± 0.008	0.1296	-0.3
Terrestrial mantle (MgO)[2]	0.3516		0.1233	-4.8
Lunar crust[3]		0.1547		
Lunar mantle(MgO)[2]	0.4739	0.129 ± 0.002	0.1331	2.7
Lunar mantle(MgO)[4]	0.4319	0.13 ± 0.006	0.1293	-0.2
Lunar mantle (I-HSE)[5]	0.2708		0.1169	-10
Martian mantle[6]	0.3843	0.1284 ± 0.0003	0.126	-2.8
Martian mantle(I-HSE)[5]	0.1975		0.111	-14
Martian mantle (Exp.)[7]	0.1333		0.1057	-18

Tab. 5. Estimates of HSE abundances (in ng/g) and $^{187}Os/^{188}Os$ in various reservoirs. Table overwritten from Day, Brandon, and Walker 2015 and references therein. 1 Re, Os, Ir, Ru, Pt, Pd from Becker et al. 2006, and Au and Rh from Fischer-Gődde et al. 2011 assuming primitive mantle Al_2O_3 of 4.25 ± 0.25 wt.% $^{187}Os/^{188}Os$ from Meisel et al. 2001; 2 Estimates from Day et al. 2007; 3 Lunar crustal composition from Day et al. 2010; 4 Estimate of lunar mantle using data from Day et al. 2007 and Day and Walker; 5 Estimate using inter-element method of Dale et al. 2012; 6 Estimate of Martian mantle given in Day 2013 and derived from MgO regression method using data in Brandon et al. 2012; 7 Experimental constraints applying 14 GPa, 2100 °C partitioning from Righter et al. 2015; 8 Values of $^{187}Os/^{188}Os_c$ calculated assuming in-growth of 187Os as a function of Re/Os over 4,568 Ga of evolution from a Solar System initial $^{187}Os/^{188}Os$ = 0.0952. DPUM is difference in % from PUM estimate of $^{187}Os/^{188}Os_c$. 8 (Day, 2013)
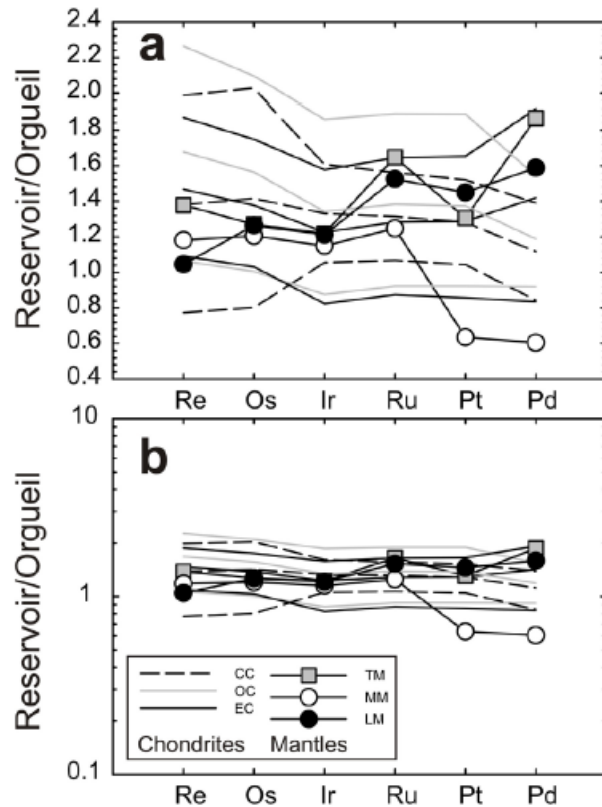
Fig. 12. Plot of average, minimum and maximum HSE abundance for carbonaceous (CC), ordinary (OC) and enstatite (EC) chondrites and mantle estimates for Earth ($\times$ 150; TM), Mars ($\times$ 150, MM) and the Moon ($\times$ 6000, LM). In a) Y-axis is linear; b) Y-axis is logarithmic (Day et al., 2015).

Studies of lunar crustal samples have recognized the importance of identifying samples that experienced impactor contamination on the lunar surface. These studies have used Ir contents, petrography and other geochemical arguments to establish a "pristinity" filter (Day et al., 2015). The Ir abundance filter for "pristinity" (< 130 pg/g Ir Waren and Wasson 1977) was based on observation that most chondrites and iron meteorites have much higher HSE concentrations than lunar crustal rocks (typically $> 10^5$ enrichment), so even limited meteoric addition will dominate the HSE inventory of impact-contaminated rocks. The HSE in particular, are sensitive tracers of impactor contamination in rocks with initially low HSE abundances. Osmium isotopic composition is especially diagnostic of meteoritic contamination because the limited range in Re/Os among chondrites and some iron meteorites leads to a restricted, well-defined range in present-day $^{187}Os/^{188}Os$ (Day et al., 2015).

4.2   HSE analyses and measurements

Several problems arising from the measurement of HSE in peridotites and other terrestrial samples has been discussed by Becker et al. (2006). First of all, it is difficult to digest large amount of samples (more than 1 gram in weight) of ultramafic rocks (e.g. Puchtel and Humayun 2005). Complete digestion is a prerequisite for most precise concentration measurements involving solution chemistry and external or internal calibration techniques such as standard addition and isotope dilution. In particular, refractory phases such as spinel and platinum group element alloys are notoriously difficult to dissolve. This may result in poor yields and incomplete sample-spike equilibration. In high precision measurements, they are high requirements for purity and accuracy of spikes. The second issue concerns the possibility of addition or mobilization of HSE as a result of chemical reaction of melt or fluid percolation through the mantle (Becker et al., 2006). Studies indicated that dissolution and precipitation processes in zone of focused melt flow (high melt/ rock ratios) may lead to substantial HSE

27

redistribution and fractionation of HSE ratios (e.g. Os/Ir and Pt/Ir) and increase ^{187}Os/^{188}Os in reacted rocks (Becker et al., 2006; Büchl et al., 2002).

One of the technique used for HSE measurement is dissolution of samples in reverse *aqua regia* in high pressure Carius tube at temperatures from 230 °C to as high as 330 °C (using quartz glass). Other method use microwave oven. High-pressure PTFE (polytetrafluoroethylene) bombs and High-Pressure Asher (HPA-S) are used to decompose a variety of matrices e.g. road dust, soil, airborne particulate, and biological materials (Skoog et al., 2005). Some other method is based on dokimastic separation into NiS. Sample is mixed with Ni, S, quartz sand and $Na_2B_4O_6$ and heated to 1100° C. Created NiS button undergoes additional treatment (e.g. Mihaljevič et al. 2013). One of the method how to obtain more accurate results of Os is microdistillation (Birck et al., 1997). Becker et al. (2006) also mentioned that the techniques based on open beaker attack in HF-HNO$_3$, NiS fire assay or reverse *aqua regia* in Carius tube at 220–240°C may not always result in complete digestion. Improved digestion techniques may lead to better analytical resolution, which in turn may provide new constrains of the origin of the HSE in the Earth´s upper mantle (Becker et al., 2006).

While most of the HSE are pretty easy to measure via ICP-MS techniques, osmium have high ionization potential (9eV) and therefore for its accurate measurements, the best choice is a negative thermal ionization mass spectrometry (N-TIMS), where Os is measured as osmium trioxide (OsO$_3^-$) via heating on platinum filaments with an electron donor (Gannoun et al., 2016).

In this study was used method of reverse *aqua regia* at high temperature treatment with modified analytical protocol (more in chapter 5).

5   METHODS

5.1   Decarbonisation and dissolution

Amounts of samples (usually 0.5–2g) were weighted into 60 ml teflon beakers and decarbonized by overall 10 ml of concentrated hydrochloric acid (HCl), added one millilitre by one. After subsides all visible reactions, teflon beakers were closed and put on a hot plate at 60 °C for 24 hours. Beakers were opened and samples were dried down at the same temperature. After that, samples were transferred into Carius tubes (high pressure and high temperature Pyrex tubes) cooled down by a crushed ice or mixture of ethanol-liquid CO_2. Appropriate quantities of ^{185}Re-^{190}Os and ^{191}Ir-^{99}Ru-^{194}Pt-^{105}Pd spikes, 4 ml HCl and 5 ml nitric acid (HNO_3) have been added to create reverse *aqua regia*. High pressure tubes were sealed, shaked, packed into the Al-foil and put into oven. For first 24 hours temperature, the oven was set to temperature of 160° C. After this time, temperature was increased by 10 °C every half hour to total 240° C and at the tubes was left in this temperature for ~72 hours. Before opening, the Carius tubes were again cooled by crushed ice.

5.2   Separation and microdestilation of osmium

Dissolved samples in aqua regia were transferred into 15 ml centrifuge tubes and centrifuged for 10 minutes at 4000 rpm. Then the sample was transferred to 50 ml centrifuge tubes and 2 ml of chloroform ($CHCl_3$) was added. The tubes were shaken and again centrifuged for 3 minutes. After that, $CHCl_3$ now contains Os that was separated from the remaining aqua regia. $CHCl_3$ was carefully removed ($CHCl_3$ is lighter than aqua regia) by pipette (pipette tips were changed with every sample) and putted into 15 ml teflon beaker containing 4 ml of hydrobromic acid (HBr). This procedure was repeated three times for higher Os gain. The throat of beakers was wrapped in teflon tape due to prevention of Os leak. Beakers with samples with HBr and $CHCl_3$ were put on heating block for 12 hours at 70 °C. Meanwhile rest of aqua regia was put under the stand with lamps and evaporated to dryness. After 12 hours heating block were turned off and waited until teflon beakers were cooled. In this stage Os was in HBr. Substance was transferred into clean 50 ml centrifuge tube and centrifuged for 2 minutes. After this procedure $CHCl_3$ was separated ($CHCl_3$ is heavier than HBr) and put into waste container. HBr was putted under the stand with lamps and dried. Residue in 15 ml beakers were dissolved by 50 microliters HBr. These substances were transferred on opened cover from 5 ml beakers and dried under the lamps (Fig. 13). The throat of rest beakers were wrapped by teflon tape. On dried samples were pipetted 37 µl of chromium oxide (Cr_2O_3) and in top of the conus were pipetted 19 µl HBr. Caps were carefully covered by conus, pack into the Al-foil and putted to heating block for 3-4 hours at 75 °C. After this time, beakers were removed out of the heating block, unpacked from foil and opened. If after added few drops of water was residue red or yellow, separation was successful. If residue was green, procedure was repeated. The beakers were left for 12 hours and after that time, samples were dried under lamps. On the bottom left small dark residue (smaller the 1 mm). Samples were analysed on N-TIMS.
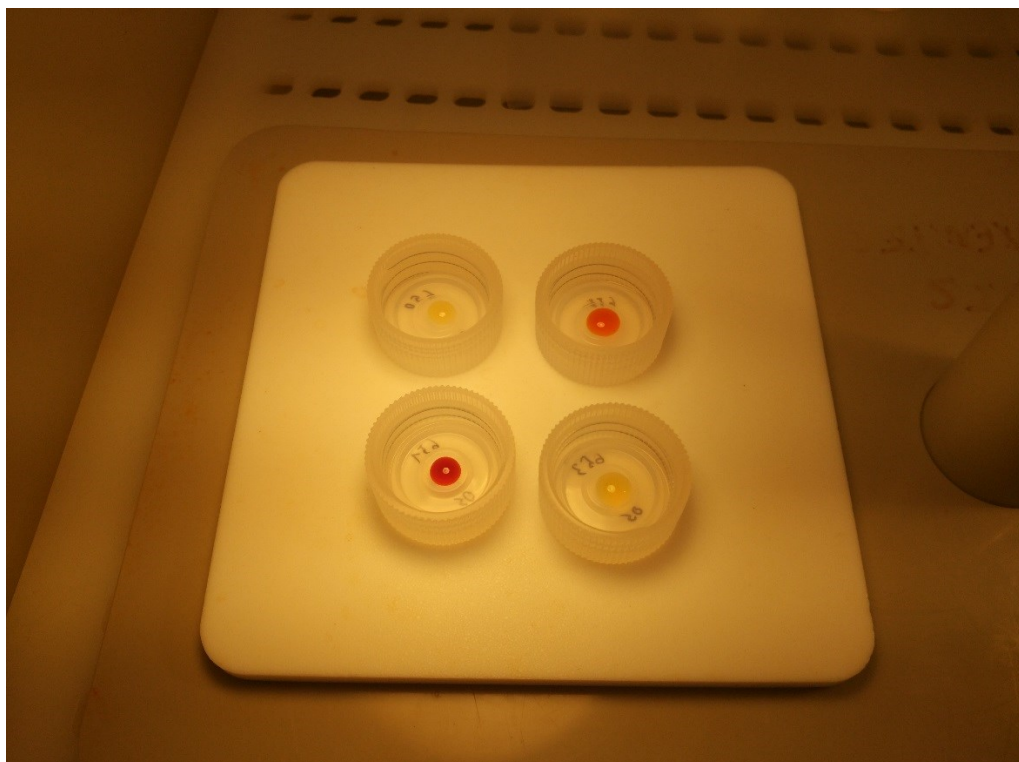
Fig. 13. Drying residues on top of the teflon beakers cups dissolved by 50 µl HBr.

5.3   Separation of Re and PGE

The remaining aqua regia containing Re and PGE has been dried under heating lamps (Fig. 14). After that, 10 ml of 6 M HCl was added and the beakers were putted on the hot plate at 75° C until most of residue was dissolved. Solutions were dried again under heating lamps. Then, 5 ml of 1 M HCl was added to teflon beakers and left on a hot plate until most of residue was dissolved. This solution was transferred into 15 ml centrifuge tubes and centrifuged for 10 minutes on 4000 rpm.
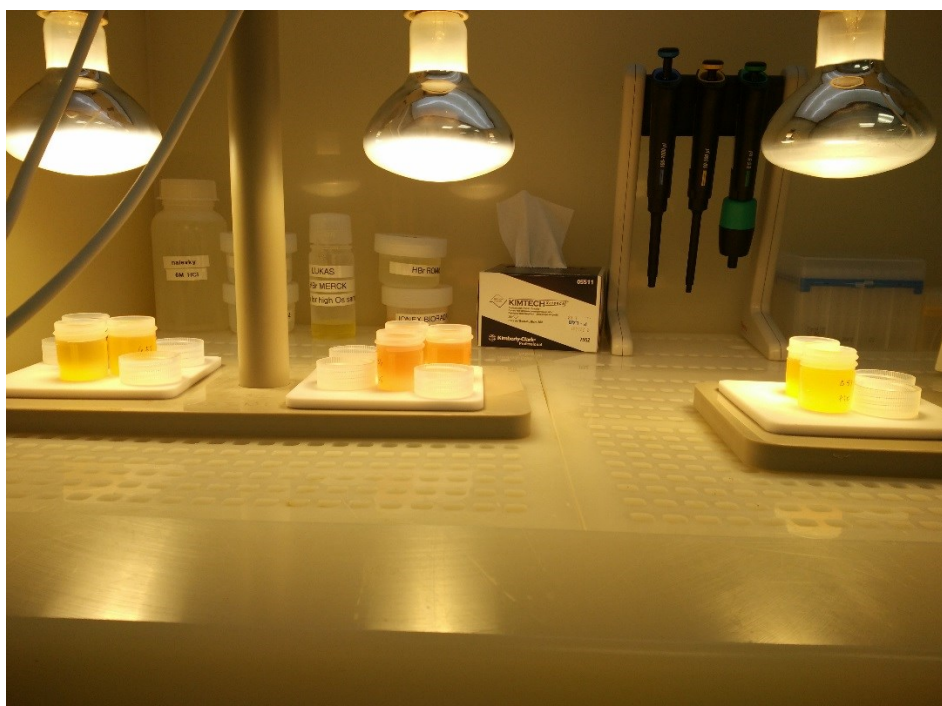
Fig. 14. Drying samples dissolved in aqua regia under lamp stands.

Teflon beakers used for Os analysis and for PGE dissolutions, were filled by 5 ml 14 M HNO₃ and warmed at 90 °C. After one-hour, acid was poured down the sink, beakers were cleaned by Milli-Q water and thoroughly rubbed by KIMTECH napkins. Into 16 ml anion exchange column, 1.6 ml of anion exchange resin (Eichrom AG 1x8 100-200 mesh) was pipetted and the separation of Ir, Ru, Pd, Pt and Re have been performed using the scheme described in Tab. 6. and shown on Fig. 15.

Step	Procedure	Used solution
1	Cleaning resin	5 ml MQ H_2O
2	Cleaning resin	10 ml 8M HNO_3
3	Cleaning resin	10 ml 14M HNO_3
4	Cleaning resin	2 ml MQ H_2O
5	Cleaning resin	10 ml 12M HCl
6	Cleaning resin	2 ml MQ H_2O
7	Equilibration of the column	2 ml 1M HCl (2 X)
8	Sample loading	Sample in 5 ml 1M HCl
9	Matrix elution	2 ml 1M HCl (2 X)
10	Matrix elution	2 ml 0.8M HNO_3
11	Matrix elution	1 ml 1M HCl-1M HF (2 X)
12	Matrix elution	2 ml 0.8M HNO_3
13	Elution of Re+Ru fraction	12 ml 6M HNO_3
14	Elution of Pt+Ir fraction	15 ml 14M HNO_3
15	Elution of Pd fraction	15 ml 12M HCl

Tab 6. Summary of anion exchange chemistry protocol used for the obtaining of HSE fractions.
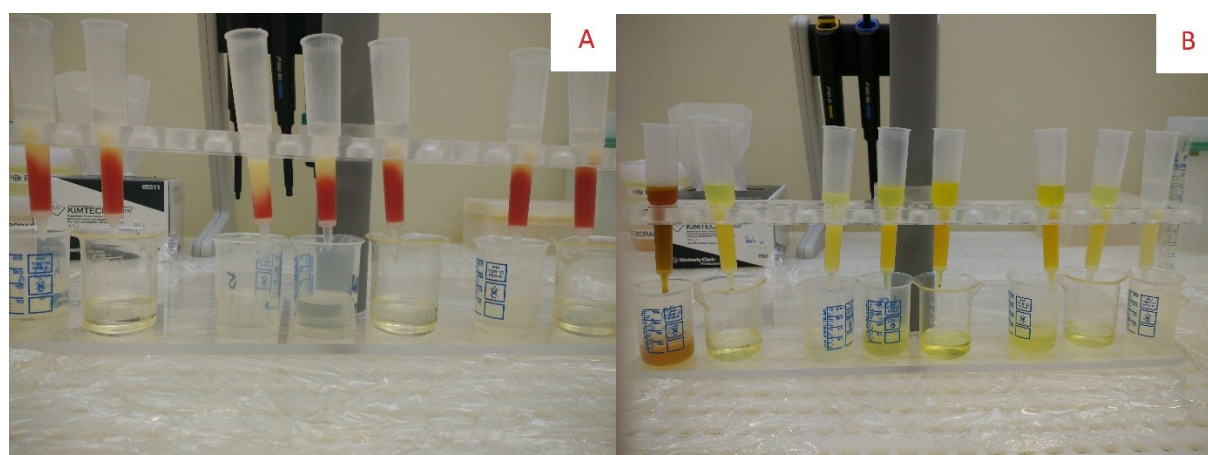
Fig 15. A) Purifying ion-exchanger. Red part is ion-exchanger cleaned by HNO₃ and yellow part is now cleaning by H2O. B) Transferred samples to column. Tint depends on content of Fe in sample.

After eluting all PGE+Re fractions, beakers were dried under lamps. Into dried beakers with Pd, 1 ml of 0.8M HNO₃ was added and to the blank 0.5 ml 0.8M HNO₃ was added. Into dried beakers with Re + Ru fraction and Pt + Ir fraction, 1 ml of 1M HCl was added and 0.5 ml of the same acid was added to the blanks. These solutions were transferred to 1.5 ml microtubes.

Concentration of Ir, Ru, Pt, Pd and Re were calculated using the isotopic dilution through the analyses of respective isotopic ration on high-resolution sector field ICP-MS *Thermo ELEMENT 2* (Germany) at the Institute of Geology, The Czech Academy of Sciences. Sample injection was performed by *Aridus II* (CETAC) desolvating nebuliser and mass bias was corrected using the analyses of natural Ir, Ru, Pt, Pd and Re solutions. Osmium concentrations and isotopic compositions were determined using N-TIMS technique (Creaser et al., 1991; Völkening et al., 1991) mostly on *Finnigan MAT 262* (Germany) housed at the Czech Geological Survey, Prague and partly on Thermo Triton housed at the Scripps Institution of Oceanography, San Diego. Osmium was loaded onto Pt filaments in concentrated HBr. Production of negative ions was maintained by the addition of 0.3 µl of $Ba(OH)_2$ activator continuous bleeding of O_2 during measurements. The samples and all blanks were run on an electron multiplier in a peak hopping mode (Jonasova et al., 2016).

Total sulphur and CO_2 content were analysed by an *Electra CS 500* C-S analyser. Major element compositions of the whole suite were determined by AAS, flame photometry and titration. The precision of major element determinations ranges between 5 and 10%. Trace elements were determined using an *Agilent 7900x* ICP-MS. Cr and Ni content in carbonatites, and V in whole suite were determined by XRF. All these measurements were performed at the Czech Geological Survey and details on the analytical protocols used are given in Ackerman et al. (2017).

6   RESULTS

6.1   Highly siderophile (HSE), siderophile and chalcophile element systematics

6.1.1   Carbonatites

Carbonatites from both suites (Samalpatti and Sevattur) show mostly overlapping HSE contents (Tab. 7), which are very low comparing to other mantle-derived melts (Day et al., 2016 and references therein), but also mostly lower than estimates made for continental crust (e.g., Peucker-Ehrenbrink and Jahn, 2001). Two analysed carbonatites from Samalpatti contain very low I-PGE contents: 0.013 and 0.084 ppb Os, 0.005 and 0.012 ppb Ir, 0.027 ppb Ru. Incompatible Pt and Pd span in the range from 0.091 to 0.290 ppb while Re is extremely variable between these two samples: 0.006 and 0.179 ppb. Duplicate analysis of sample IC05A assume rather homogeneous distribution of HSE within the sample powder. Osmium and Ir in Sevattur carbonatites range from 0.016 to 0.20 ppb and 0.004 to 0.013 ppb, respectively, while Ru contents are very low, mostly below detection limits. Platinum and Pd contents are rather uniform (0.10–0.50 ppb) in comparison to Re, which again largely vary from 0.003 to 0.974 ppb. Total HSE concentration in both complexes overlap in the range of 0.29 and 1.25 ppb. Volume of sulphur in carbonatites in Samalpatti is ranging from 0.024 to 0.120 wt. % with 0.26% content of pyrite in IC05F1 sample. Contents of S in Sevattur carbonatites are slightly decreased, it is ranging from <0.010 to 0.017 wt. %.

Primitive mantle-normalized HSE patterns of Samalpatti and Sevattur carbonatites are plotted in Fig. 16. In overall, the patterns show enrichment from I-PGE to P-PGE-Re similar to most mantle-derived melts, however with some important striking differences. For example, all analysed carbonatites are systematically enriched in Os over Ir resulting in Os_N/Ir_N (N – primitive mantle) normalized ratios between 2.3 to 6.3 for Samalpatti and 2.7–15.1 for Sevattur carbonatites. In comparison, the Ir_N/Ru_N ratio of one Samalpatti sample (IC05F1) yields a value of 0.4 while two Sevattur samples show enrichment in Ir over Ru (~1 and 6). P-PGE (Pt, Pd) and Re are enriched over I-PGE resulting in very low Ru_N/Pt_N ratios of 0.03–0.10. The same trend can be observed at Pt_N/Pd_N ratios (0.09–0.60) except two samples (IC10A and IC05F1) yielding values of 1.4 and 0.9, respectively.

The γ Os value for Samalpatti carbonatites are +102 and +988. For Sevattur carbonatites, the γ Os were calculated only for two samples and the values are +237 and +5247.

Fig. 16. Distributions of highly siderophile elements of carbonatites in Sevattur and Samalpatti normalized to primitive mantle (Becker et al., 2006).

Cobalt contents in two Samalpatti carbonatites have values of 2.16 and 3.85 ppm, while two samples of Sevattur carbonatites are more enriched (15.7–16.9 ppm) and two (IC10A and IC6A) have such contents as carbonatites in Samalpatti (1.3–1.4 ppm). Copper seems to have similar trend and both elements show a negative correlation with Pd and Pt (Fig. 17B). Samalpatti carbonatites contain 4.42–6.21 ppm of Cu whereas carbonatites from Sevattur contain from 17.6 to 77.4 ppm of Cu and two samples (IC10A and IC16A) have a content of Cu 0.87 and 8.46 ppm. Nickel concentrations tend to be higher in Sevattur carbonatites (14–26 ppm) than in Samalpatti carbonatites (<2–4 ppm). Interestingly, except one sample, Ni positively correlates with Os for a Sevattur carbonatites (Fig. 17A). Samalpatti carbonatites exhibit variable FeO contents from 0.46 to 0.78 wt. % and it seems that Sevattur carbonatites are slightly enriched in FeO (0.61–1.42 wt.%). A negative correlation between Pt and Nb was observed for Sevattur carbonatites (Fig. 17E). None of the following elements does not correlate with HSE in Samalpatti or Sevattur. Contents of W and Cd are rather uniform at both regions (0.09–0.42 ppm). Pb is more enriched in Sevattur (19.4 – 68.8 ppm) more than in Samalpatti (5.1 – 6.8 ppm). Same patter can be seen on Ga. The Sevattur carbonatites are ranging in Ga from 9.77 to 12.30 ppm and Samalpatti carbonatites yield 2.62 and 4.26 ppm. Zinc is not uniform in Sevattur (0.23–27.0 ppm) and in Samalpatti concentrations is 13.9 and 17.7 ppm. Content of V is bellow detection limit on three samples. Samalpatti carbonatites contain 18 ppm of V and Sevattur 78 and 90 ppm.
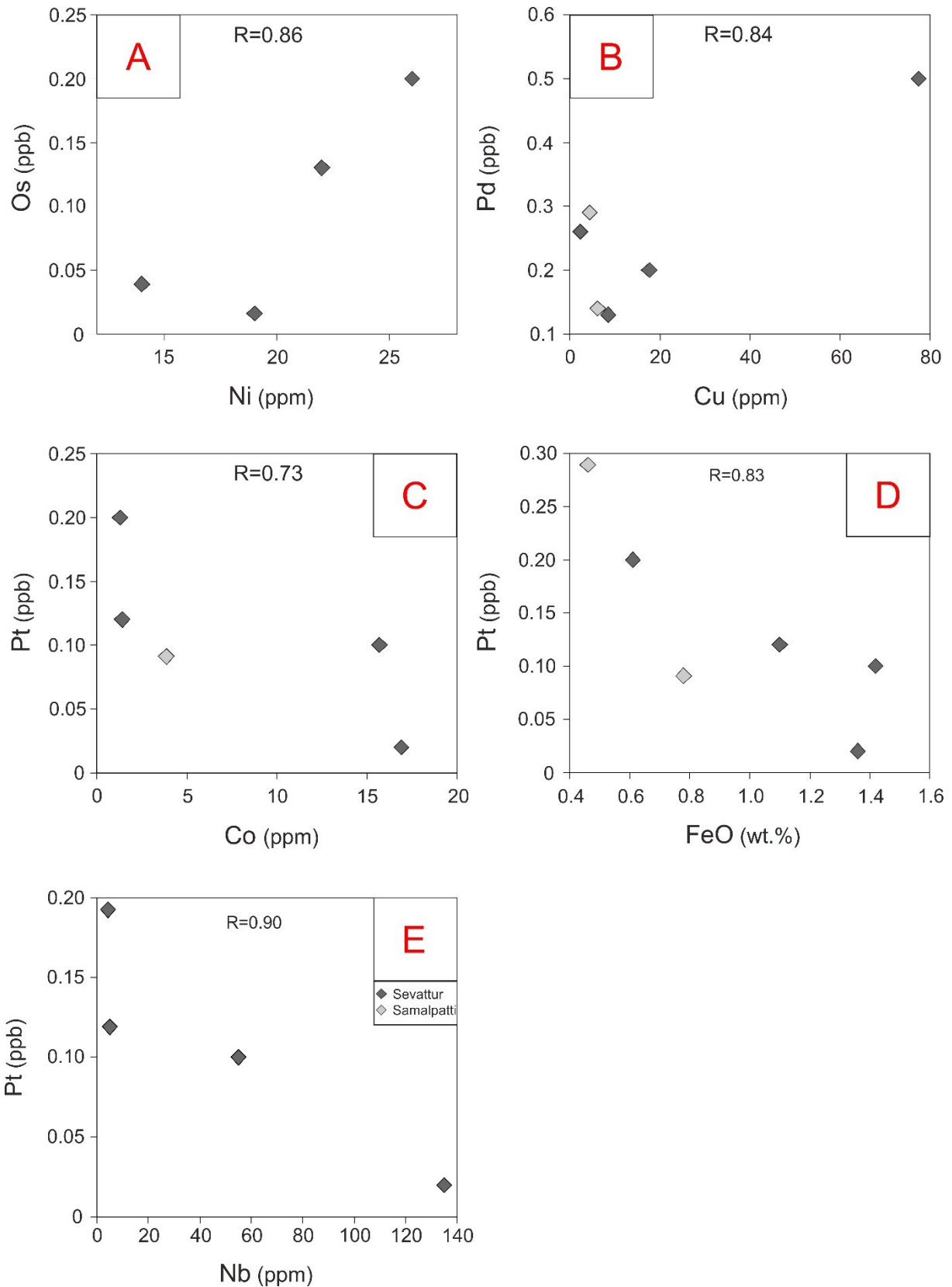
Fig. 17. Correlation diagrams with correlations indexes. A) Os/Ni ratio for carbonatites from Sevattur, B) Pd/Cu ratio for carbonatites from Samalpatti and Sevattur, C) Pt/Co ratio carbonatites from Samalpatti and Sevattur (IC05F1 excluded), D) Pt/FeO ratio for Samalpatti and Sevattur carbonatites, E) Pt/Nb ratio of Sevattur carbonatites

6.1.2   Silicocarbonatites from Samalpatti

The HSE concentrations in two types of silicocarbonatites (Ca-rich vs. Mg-Cr-rich) are highly variable (Tab. 7).

The Ca-rich silicocarbonatites have Os contents of 0.028 and 0.041 ppb, Ir of 0.011 and 0.021 ppb and Ru is the same for both samples (0.008 ppb). Platinum and Pd reach up to 0.36 ppb and 2.6 ppb, respectively. One sample (IC18C) is highly depleted in Re (0.005 ppb) whereas the second one (IC18C) is slightly enriched comparing to the primitive mantle (0.378 ppb). Total HSE contents in Ca-rich silicocarbonatites are 1.35 and 2.82 ppb.

The Mg-Cr-rich silicocarbonatites show much higher HSE values with Os concentrations ranging from 0.10 to 0.35 ppb, with the exception of one sample (IC03D; 0.008 ppb). Iridium values show large variation from 0.049 to 0.46 ppb while Ru is rather uniform with average value of 0.25 ppb. Platinum is highly enriched with values of up to 12.5–38.0 ppb with only one depleted sample IC06E (0.63 ppb). In comparison, Pd contents are lower with a variation from 0.12 to 3.41 ppb and Re is extremely depleted (0.003–0.029 ppb). The Mg-Cr-rich silicocarbonatites have the highest total HSE among the collected dataset (1.23–41.1 ppb) and show negative correlations with S (Fig. 27B). Conversely, the sample IC18A (calc-silicate marble) exhibits the lowest values in all HSE except Re (0.158 ppb). Samalpatti Ca-rich silicocarbonatites are against Mg-Cr-rich silicocarbonatites more enriched in sulphur 0.012 – 0.271 wt. % and <0.010 – 0.026 wt. %, respectively and content of pyrite in Ca-rich silicocarbonatite (IC18B) is 0.38%. One sample of calc-silicate marble has 0.010 wt. % of S.

Distributions of HSE in silicocarbonatites against primitive mantle are shown in Fig. 18. The Ca-rich silicocarbonatites are enriched in Os over Ir resulting in Os_N/Ir_N ratios of 1.8 and 2.3, but the Mg-Cr-rich silicocarbonatites show non-systematic behaviour (three samples have Os_N/Ir_N between 0.10 and 0.79 and three from 2.6 to 3.8). The Ca-rich silicocarbonatites have the lowest Ru contents among I-PGE and consequently high Ir_N/Ru_N ratios of 2.7 and 5.3. In contrast, for the Mg-Cr-rich silicocarbonatites, this ratio is mostly < 0.65 with only two samples reaching higher values, namely IC06E (0.90) and IC04A (2.62). Overall, the Mg-Cr-rich silicocarbonatites do not show significant I-PGE fractionations, but Ru_N/Pt_N ratios show large decrease due to positive Pt anomalies – all samples have a Ru_N/Pt_N ratio < 0.013 except sample IC06E (0.44). The Mg-Cr-rich silicocarbonatites show a decreasing trend from Pt to Re.
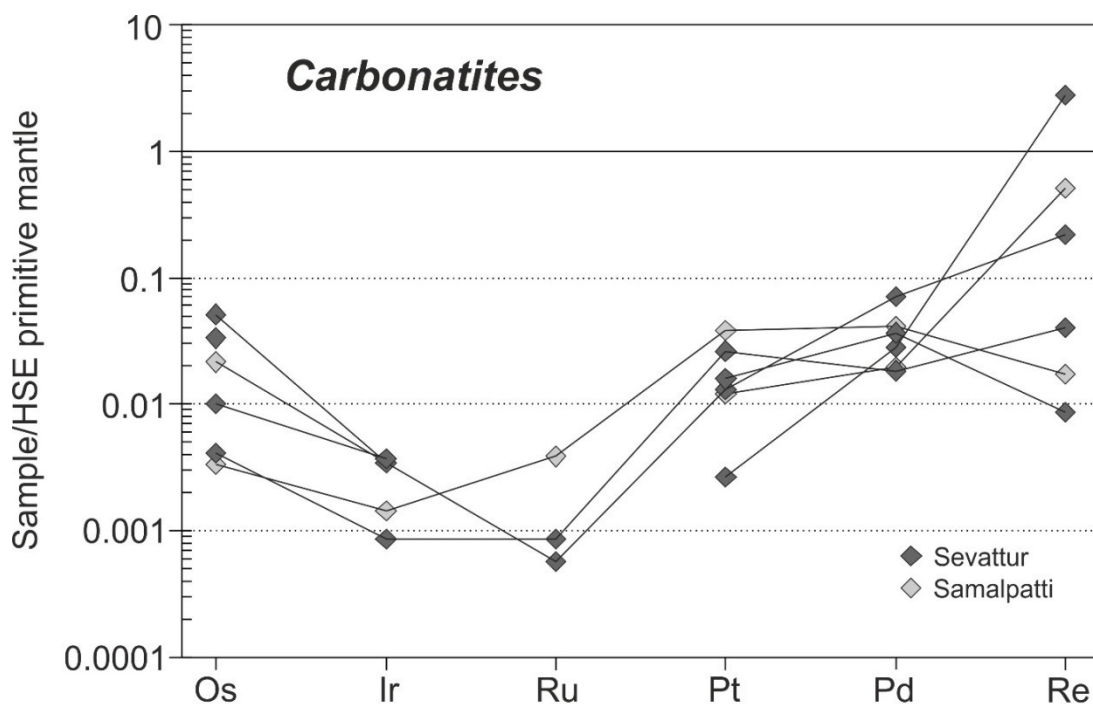
Fig. 18. Distributions of highly siderophile elements in the silicocarbonatites from Samalpatti normalized to primitive mantle (Becker et al., 2006).

Contents of V in two samples of Ca-rich silicocarbonatites are 13 and 28 ppm, in the calc-silicate marble 41 ppm and the Mg-Cr-rich silicocarbonatites contain 38 to 84 ppm of V. Positive correlation between HSE (e.g., Ir) and V can be seen across all silicocarbonatites (Fig. 19B) and the same trend can be also recognized with FeO (Fig. 19E). The Mg-Cr-rich silicocarbonatites also seem to be more enriched in Co and Ni (30–36 ppm and 165–176 ppm, respectively) comparing to the Ca-rich type and and marble (3.5–6.6 ppm and 8.1–15.8 ppm, respectively), Ni contents positively correlates with Os and negatively with Ir (Fig. 19A, C). Content of Cu rise from Mg-Cr-rich silicocarbonatites to Ca-rich silicocarbonatites from 1.95 to 15.40 ppm. Opposite pattern can be seen on Zn (13.6–150 ppm). Cd and W are ranging from 0.04 to 0.78 ppm on both localities. Neither Samalpatti nor Sevattur does not report significant different in content of Pb (5.9–26.5 ppm).
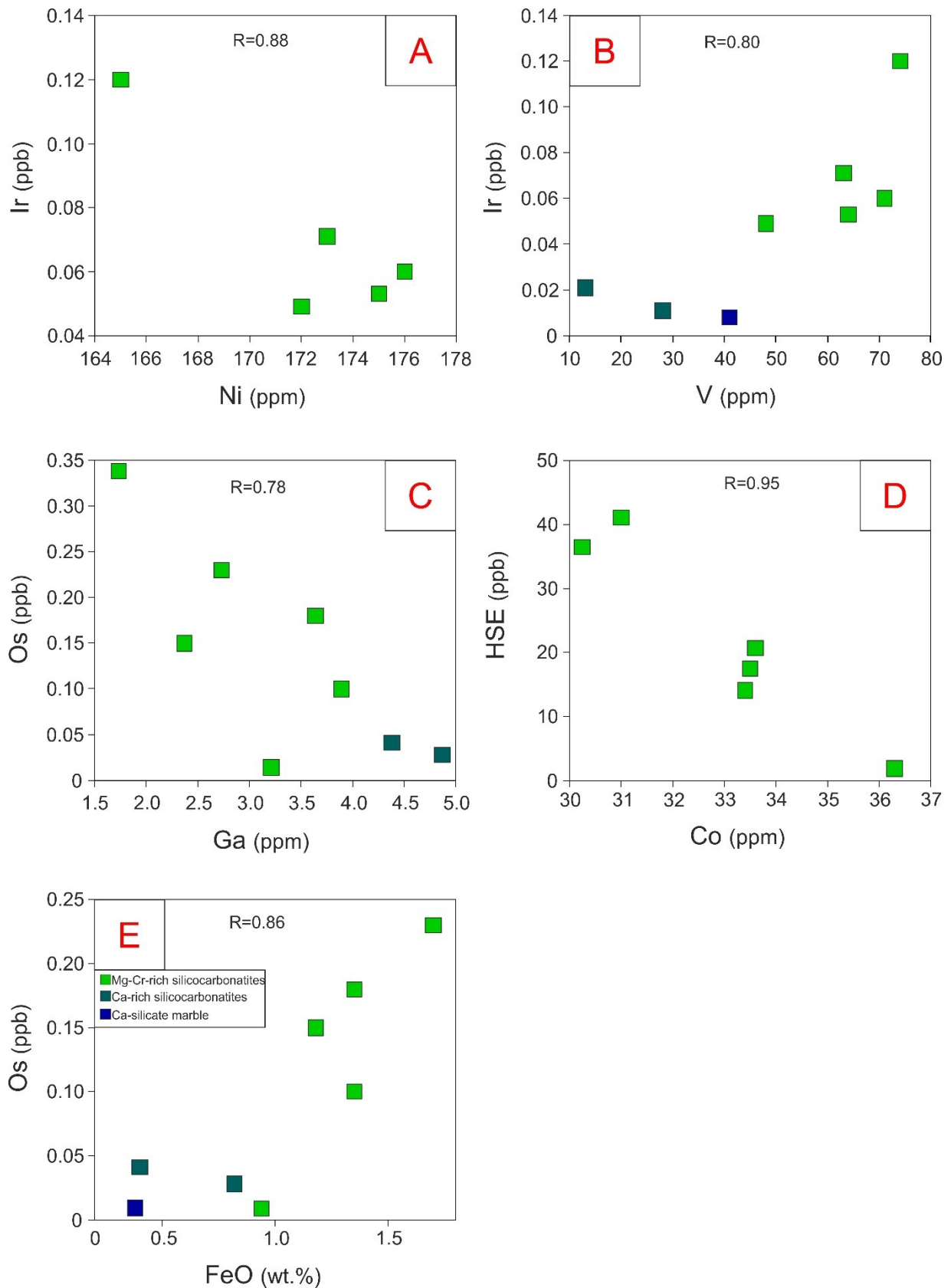
Fig. 19. A) Ir/Ni ratios of Mg-Cr-rich silicocarbonatites (IC04A excluded), B) Ir/V ratio of all silicocarbonatites in Samalpatti (IC04A excluded), C) Os/Ga ratio of Mg-Cr rich and Ca-rich silicocarbonatites, D) HSE/Co ratio of Mg-Cr-rich silicocarbonatites, E) Os/FeO ratio of all Samalpatti silicocarbonatites (IC04A excluded).

6.1.3   Alkaline rocks from Samalpatti

Samalpatti silicate rocks analysed within this study consist of monzogabbro, pyroxenite and syenite. All samples except two (IC23B and IC07D) yield very low concentrations of Os from 0.002 to 0.011 ppb. In comparison, the syenite IC23B contains 0.158 ppb Os and the pyroxenite IC07D 0.32 ppb Os. The latter sample also contains one of the highest values of other HSE, especially Pt reaching almost 11 ppb (Tab. 7). Ruthenium concentrations are typically very low, mostly below detection limit. Overall, the syenites show the lowest Ir, Ru, Pt and Pd contents among all analysed rocks, significantly lower than those reported for continental crust, but one sample (IC23B) is strongly enriched in Re (0.699 ppb). Three analysed pyroxenites exhibit highly variable HSE contents and it seems that the values are connected with the S contents. The sample IC05C containing the highest S contents (0.95 wt. %) yield the highest Re and Pd values (1.13 ppb and 20.4 ppb, respectively) paralleled also by elevated Pt (7.47 ppb). Total HSE contents in pyroxenites vary from 0.105 ppb to 29.08 ppb, and therefore, the pyroxenites seems to be enriched in most of the HSE (Fig. 21A, B, D). Pyroxenites in Samalpatti a sulphur content is from <0.010 to 0.945 wt. %; pyroxenite IC05C contains 0.34 vol. % of pyrite. In the other alkaline rocks in this region, like monzogabbro (<0.011–0.127 wt. % of S) and syenite (0.073–0.121 wt. % of S), no sulphides were detected.

The primitive mantle normalized HSE patterns of alkaline silicate rocks from Samalpatti are given in Fig. 20 showing generally increasing contents from Os to Re. One from each rock type have Os_N/Ir_N ratio higher than 1 (9.1, 3.3, 8.9; pyroxenite, monzogabbro, syenite), whereas the others have lower ratios from 0.04 to 0.52. Ir_N/Ru_N ratios are available only for 2 pyroxenites (0.29 and 4.15) and for one monzogabbro (0.82). The same applies for Ru_N/Pt_N (0.001 and 0.02 for pyroxenites and 0.011 for monzogabbro). The Pt_N/Pd_N ratios are generally around 1–2, except pyroxenites (0.34; 4.5) and one sample of monzogabbro (0.19).
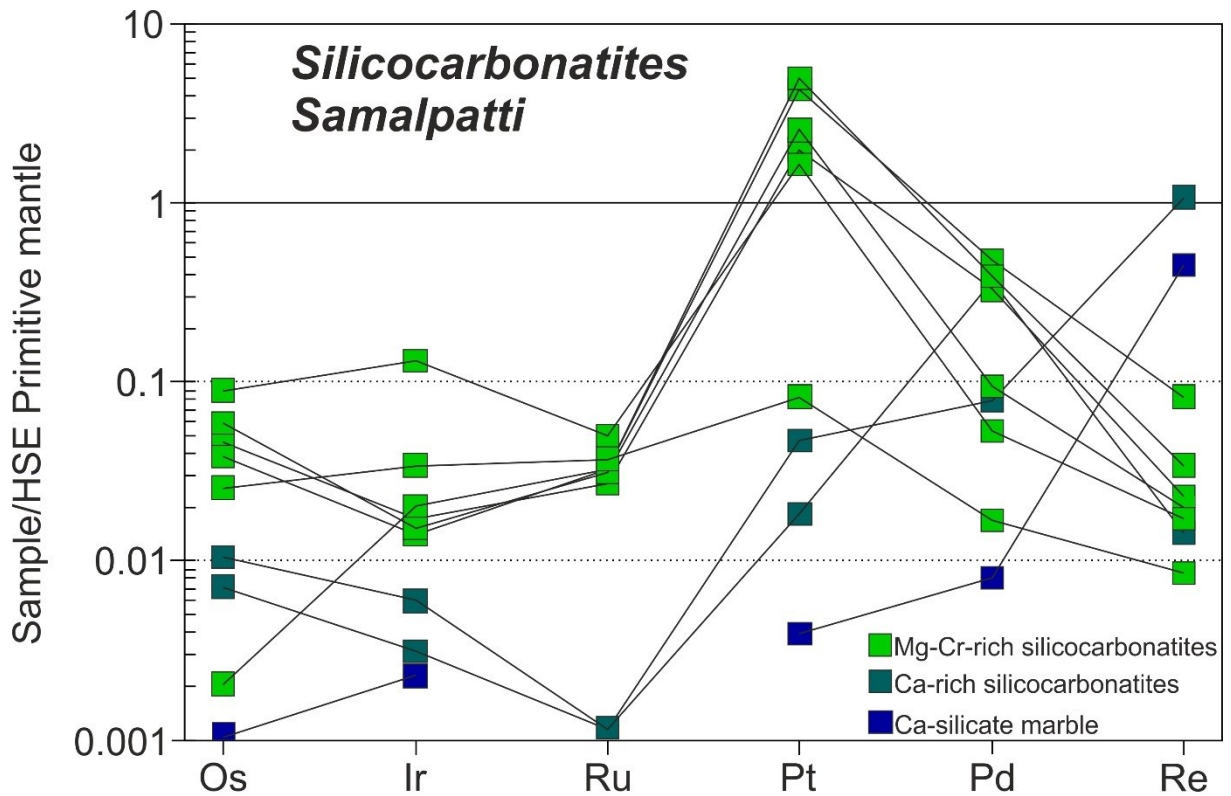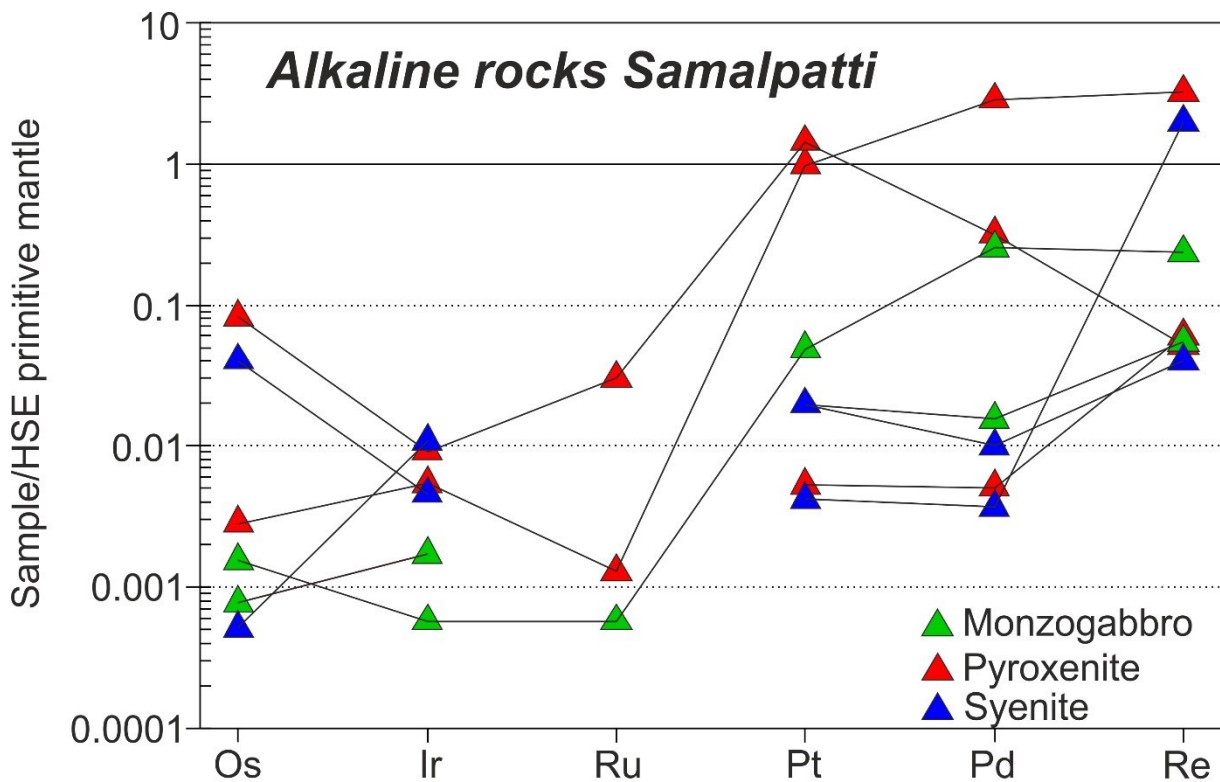

Fig. 20. Distributions of highly siderophile elements in alkaline rocks from Samalpatti normalized to primitive mantle (Becker et al., 2006).

Concentrations of Ga in Samalpatti alkaline rocks are higher in monzogabbros and syenites (about 15 ppm) and in one sample of pyroxenite (IC06D with 19.5 ppm). Two samples of pyroxenite contain 1.48 and 3.74 ppm of Ga. Contents of V are not uniform. For example, pyroxenites contains from 75 to 429 ppm, monzogabbros <2 to more than 1000 ppm and syenites from 73 to 102 ppm. Contents of FeO_{tot} are generally lowest in syenites (1.5–3.02 wt. %). Among monzogabbros, one sample is enriched (15.53 wt. % of FeO_{tot}) and one sample is largely depleted (0.33 wt. %). Volume of FeO_{tot} in pyroxenites vary from 4.76 to 15.53 wt. %. Positive correlation can be seen between SiO_2 and Ir (Fig. 28). On the other hand, Ir show a negative correlation with FeO_{tot} (FeO and Fe_2O_3 have a same pattern, Fig. 21E). Only one sample is enriched in Cu (IC06A; 1535 ppm), other reach values around 3 - 10ppm. Same sample is enriched also by Zn (126 ppm) as well as IC06D (146 ppm), other samples contain 3.8–32.4 ppm. Cd and W vary from 0.07 to 0.46 pm. Amount of Pb is divided into two groups. One contain 1.3–6.0 ppm of Pb and the second is enriched to 12.6–23.5 ppm.
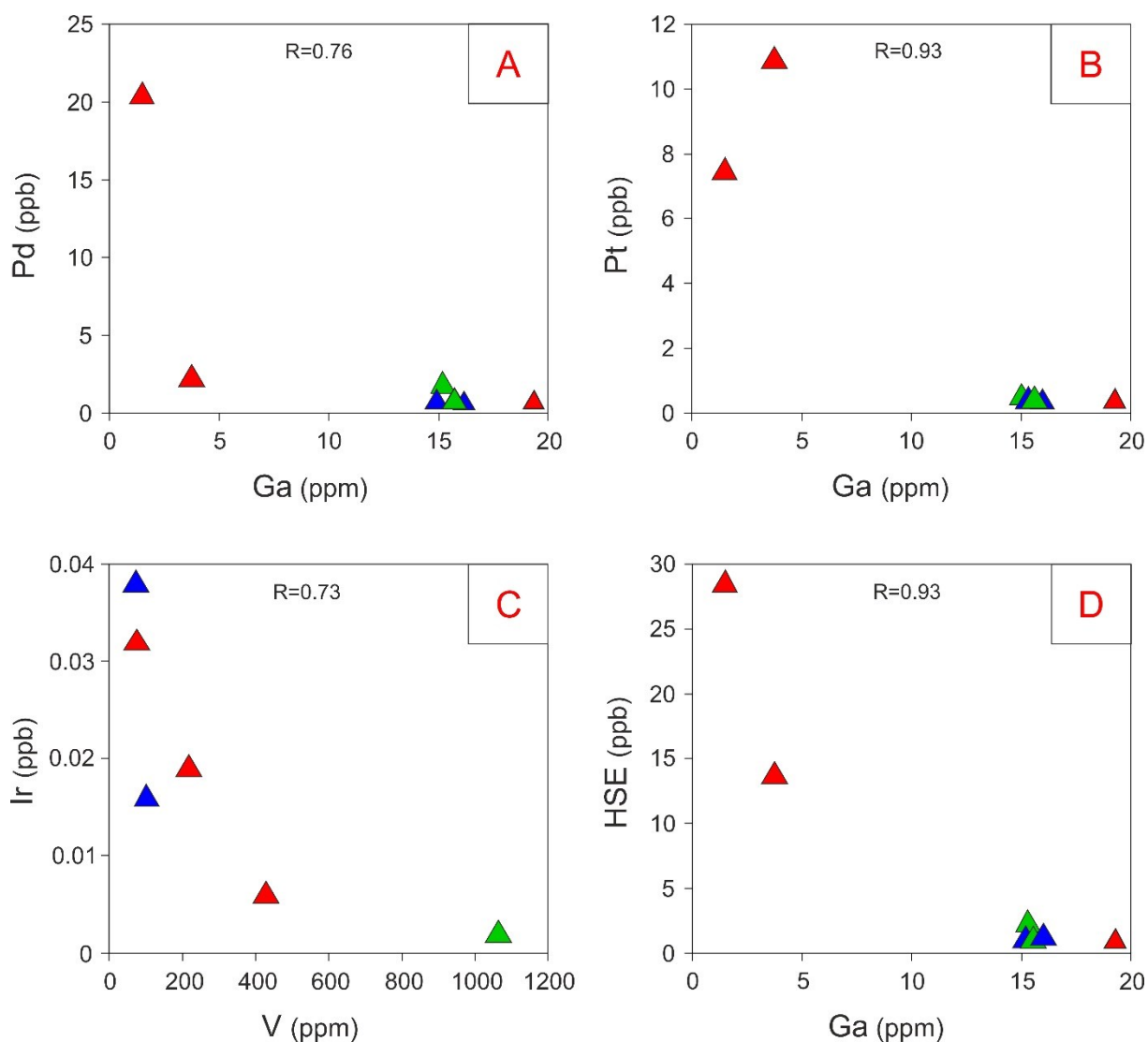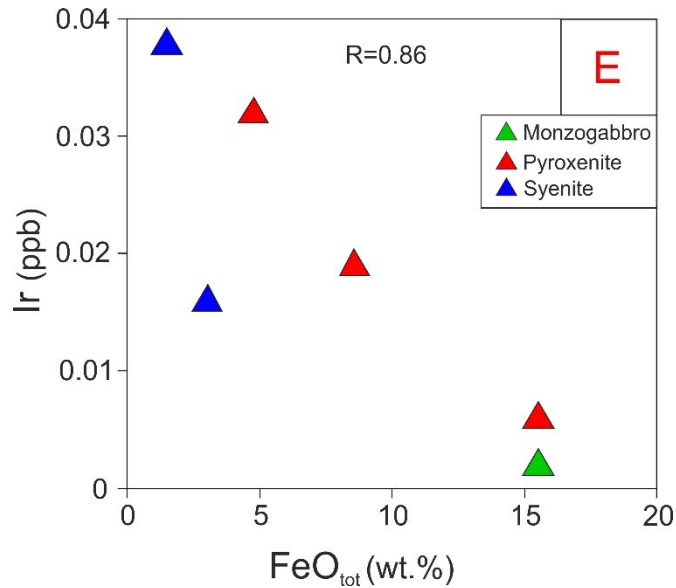
Fig. 21. A) Pd vs. Ga of alkaline rocks from Samalpatti, B) Pt/Ga of alkaline rocks from Samalpatti, C) Ir/V of alkaline rocks from Samalpatti (IC07E bdl.), D) Total HSE/Ga of alkaline rocks from Samalpatti, E) Ir/FeO$_{tot}$ ratio of alkaline rocks from Samalpatti (IC07E bdl).

6.1.4   Alkaline rocks and associated minerals from Sevattur

Analysed alkaline rocks/minerals from Sevattur include monzogabbro, tonalite, magnetite and phlogopite + phosphate. Most of the samples are extremely low in I-PGE contents: Os (0.002–0.018 ppb), Ir (0.002–0.030 ppb) and Ru (0.003–0.013 ppb). However, two samples have significantly higher Ru contents (IC12B2 tonalite and IC13A monzogabbro; 0.055 and 0.063 ppb). With the exception of two samples (IC11B, IC14), concentrations of Pt and Pd vary from 0.25 to 0.92. The magnetite (IC11B) separated from magnetite-rich carbonatite yield very low Pd (0.069 ppb). The highest content of Re shows tonalite (0.631 ppb) and this is most likely connected with the highest S contents among Sevattur rocks. Concentration of Re decreases in the order monzogabbro > magnetite > phosphate + phlogopite (0.28 > 0.009 ppb). Total HSE contents range from 0.47 ppb to 2.5 ppb. In alkaline rocks is volume of S 0.009, 0.017, 0.031, 0.135 in following orders for phosphate + phlogopite, monzogabbro, quartz monzogabbro and tonalite. In these rocks has been found minor contents of pyrite; syenite (IC12B2) 0.03 vol. %, monzogabbro (IC13A) 0.02 vol. % and quartz monzogabbro (IC14) 0.02 vol. %.

Primitive-mantle normalized concentrations are shown in Fig. 22. All analysed rocks have profiles similar to continental crust with generally increasing contents from Os to Re. The Os$_N$/Ir$_N$ ratios range from 0.25 and 0.70 (for phosphate and magnetite) to 3.5 and 5.4 for monzogabbro and tonalite whereas Ir$_N$/Ru$_N$ are mostly > 1, except monzogabbro which have Ir$_N$/Ru$_N$ ratio 0.09. With the exception of phosphate and tonalite, the samples exhibit enrichments of Pt over Pd

41
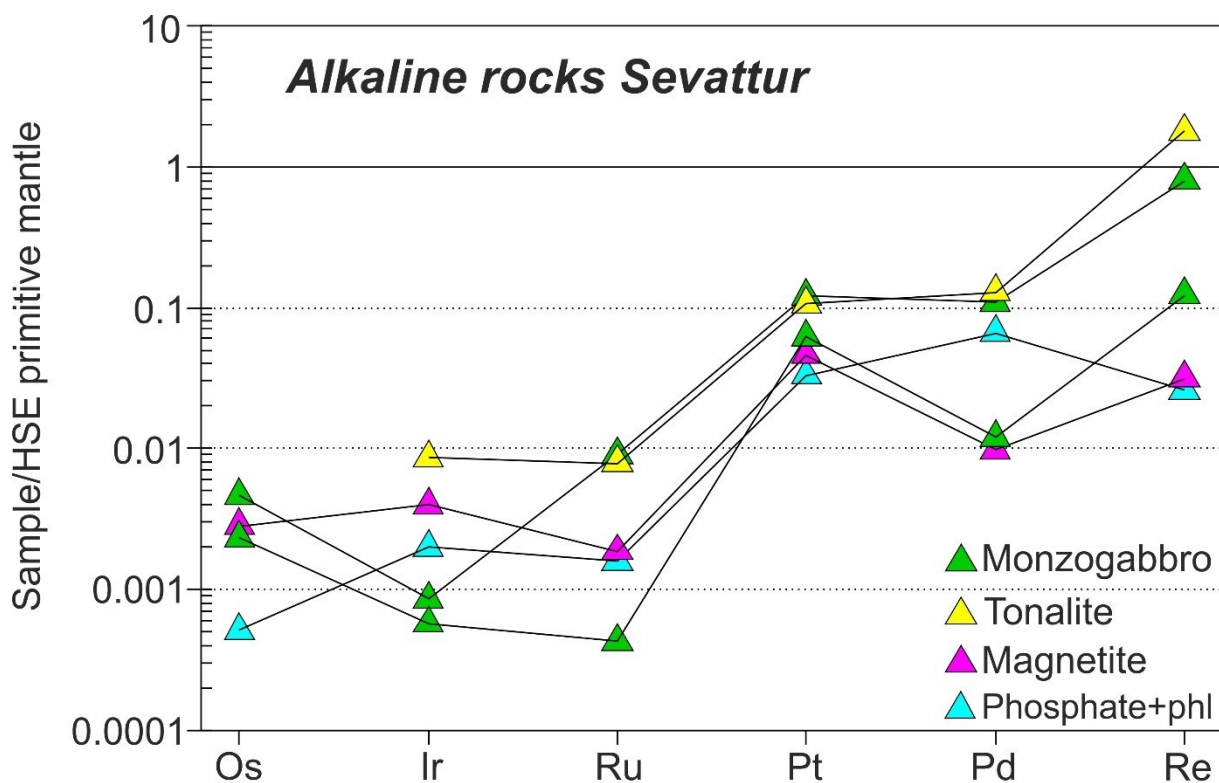
Fig. 22. Distributions of highly siderophile elements in alkaline rocks from the Sevattur normalized to primitive mantle (Becker et al., 2006).

Copper contents increase from monzogabbro, through magnetite to phosphate with phlogopite from 20.9 to 51.6 ppm, with the lowest value found in tonalite (8 ppm). Monzogabbros and phosphate with phlogopite contain about 23–28 ppm of Pb, magnetite and tonalite are ranging concentration of Pb from 2.3 to 5.4 ppm and negative correlation exists between Pb and Ir (Fig. 23C). Tungsten contents are low (<1.4 ppm), but positive correlation exists between W and Ru (Fig. 23B). Concentration of FeO in all samples except (IC11B; magnetite; 24.84 wt. %) vary from 0.38 to 2.17 wt. % and FeO is positively correlated with Pd and Re (Fig. 23D, E). Magnetite (IC11B) is enriched in V (3483 ppm) and Zn (269 ppm), other samples vary from 14 to 144 ppm. Concentration of Ga reach 3.4–22.7 ppm. Cd and W are uniform in all samples (0.05–1.39 ppm).
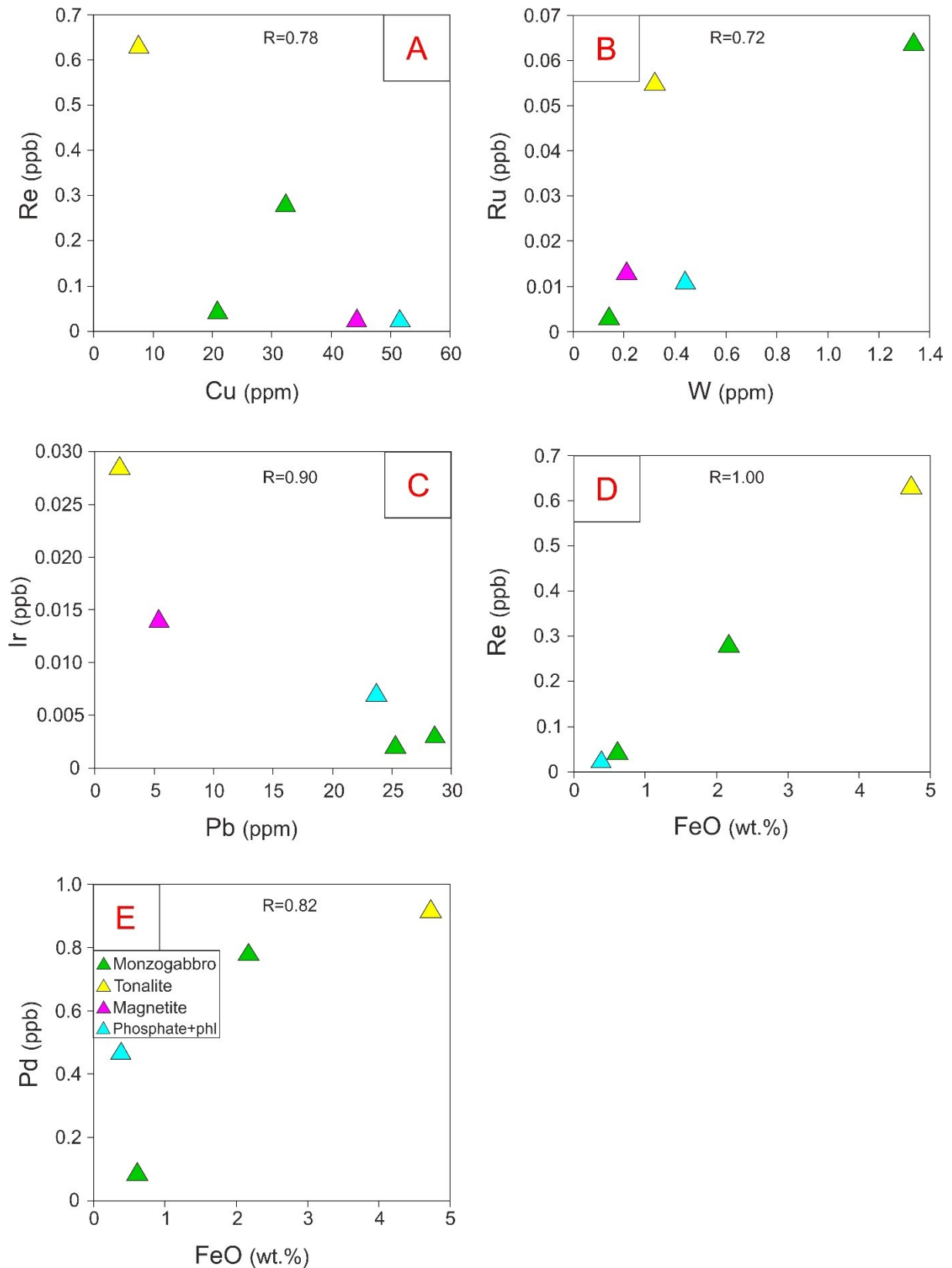
Fig. 23. A) Re vs. Cu of alkaline rocks from Sevattur, B) Ru vs. W of alkaline rocks from Sevattur, C) Ir vs. Pb of alkaline rocks from Sevattur, D) Re vs. FeO of alkaline rocks from Sevattur (IC11B excluded), E) Pd vs. FeO of alkaline rocks from Sevattur (IC11B excluded).

Sample	Locality	Rock	S wt.%	Re (ppb)	Os (ppb)	Ir (ppb)	Ru (ppb)	Pt (ppb)	Pd (ppb)	$^{187}Re/^{188}Os$	$^{187}Os/^{188}Os$	HSE (ppb)
IC05A	Samalpatti	carbonatite	0.024	0.179	0.084	0.012	bdl	0.091	0.140	10.6	0.387	0.506
IC05F1	Samalpatti	carbonatite	0.120	0.006	0.013	0.005	0.027	0.290	0.290	2.7	1.36	0.631
IC18B	Samalpatti	Ca-rich silicocarbonatite	0.271	0.378	0.028	0.011	0.008	0.36	0.56	67.000	0.420	1.349
IC18C	Samalpatti	Ca-rich silicocarbonatite	0.012	0.005	0.041	0.021	0.008	0.14	2.60	1.1	5.9	2.818
IC03A	Samalpatti	Mg-Cr-rich silicocarbonatite	<0.010	0.008	0.18	0.060	0.19	15.2	2.34	0.21	0.1834	17.987
IC03B	Samalpatti	Mg-Cr-rich silicocarbonatite	0.010	0.029	0.15	0.049	0.23	32.7	3.41	0.91	0.1634	36.527
IC03D	Samalpatti	Mg-Cr-rich silicocarbonatite	<0.010	0.012	0.008	0.071	0.23	38.0	2.79	7.7	0.460	41.078
IC03E	Samalpatti	Mg-Cr-rich silicocarbonatite	<0.010	0.007	0.23	0.053	0.22	19.5	0.67	0.15	0.1534	20.666
IC04A	Samalpatti	Mg-Cr-rich silicocarbonatite	0.020	0.006	0.35	0.46	0.35	12.5	0.38	0.076	0.1453	14.053
IC06E	Samalpatti	Mg-Cr-rich silicocarbonatite	0.026	0.003	0.10	0.12	0.26	0.63	0.12	0.17	0.5735	1.230
IC18A	Samalpatti	calc-silicate marble	0.010	0.158	0.004	0.008	bdl	0.030	0.057	201	0.590	0.257
IC05C	Samalpatti	pyroxenite	0.945	1.13	0.011	0.019	0.009	7.470	20.440	736	3.820	29.083
IC06D	Samalpatti	pyroxenite	0.016	0.021	0.003	0.006	bdl	0.040	0.036	46	2.900	0.105
IC07D	Samalpatti	pyroxenite	<0.010	0.018	0.32	0.032	0.21	10.9	2.25	0.27	0.1746	13.712
IC06A	Samalpatti	monzogabro	0.127	0.082	0.006	0.002	0.004	0.37	1.81	77	1.400	2.276
IC07E	Samalpatti	monzogabro	<0.011	0.019	0.003	0.006	bdl	0.15	0.11	34	1.000	0.297
IC09	Samalpatti	syenite	0.073	0.014	0.002	0.038	bdl	0.15	0.071	42	1.700	0.278
IC23B	Samalpatti	syenite	0.121	0.699	0.158	0.016	bdl	0.032	0.026	22	0.2700	0.931
IC10A	Sevattur	carbonatite	0.015	0.014	0.016	0.003	0.006	0.20	0.13	4.4	0.1873	0.370
IC10J	Sevattur	carbonatite	0.017	0.077	0.20	0.012	0.004	0.10	0.50	1.39	0.4500	0.893
IC11A	Sevattur	mt-carbonatite	0.017	0.974	0.039	0.013	bdl	0.020	0.20	282	10.3000	1.250
IC16A	Sevattur	carbonatite	<0.010	0.003	0.13	bdl	bdl	0.12	0.26	0.12	0.4100	0.509
IC10D	Sevattur	phosphate+phl	0.009	0.009	0.002	0.007	0.011	0.25	0.47	n.d.	n.d.	0.747
IC11B	Sevattur	magnetite	bdl	0.011	0.011	0.014	0.013	0.35	0.069	5.5	1.3000	0.469
IC13A	Sevattur	monzogabro	0.017	0.28	0.018	0.003	0.063	0.92	0.78	105	2.9600	2.073
IC14	Sevattur	qtz monzogabro	0.031	0.043	0.009	0.002	0.003	0.47	0.085	36	4.5000	0.613
IC12B2	Sevattur	tonalite with sulf	0.135	0.631	n.d.	0.030	0.055	0.811	0.918	n.d.	n.d.	2.445

Tab. 7. Concentrations, $^{187}Re/^{188}Os$ and $^{187}Os/^{188}Os$ ratios for carbonatites and associated alkaline rocks from Samalpatti and Sevattur

Sample	Locality	Rock	Os_N/Ir_N	Ir_N/Ru_N	Ru_N/Pt_N	Pt_N/Pd_N	Pd_N/Re_N
IC05A	Samalpatti	carbonatite	6.282	bdl	bdl	0.607	0.039
IC05F1	Samalpatti	carbonatite	2.333	0.370	0.101	0.934	2.247
IC18B	Samalpatti	Ca-rich silicocarbonatite	2.292	2.741	0.024	0.598	0.073
IC18C	Samalpatti	Ca-rich silicocarbonatite	1.752	5.250	0.060	0.052	24.859
IC03A	Samalpatti	Mg-Cr-rich silicocarbonatite	2.606	0.651	0.013	6.088	15.326
IC03B	Samalpatti	Mg-Cr-rich silicocarbonatite	2.826	0.422	0.008	8.935	5.835
IC03D	Samalpatti	Mg-Cr-rich silicocarbonatite	0.102	0.614	0.007	12.698	11.294
IC03E	Samalpatti	Mg-Cr-rich silicocarbonatite	3.790	0.480	0.012	27.386	4.644
IC04A	Samalpatti	Mg-Cr-rich silicocarbonatite	0.686	2.624	0.030	31.076	3.326
IC06E	Samalpatti	Mg-Cr-rich silicocarbonatite	0.793	0.901	0.447	4.985	1.707
IC18A	Samalpatti	calc-silicate marble	0.429	bdl	bdl	0.487	0.018
IC05C	Samalpatti	pyroxenite	0.528	4.155	0.001	0.341	0.888
IC06D	Samalpatti	pyroxenite	0.464	bdl	bdl	1.021	0.086
IC07D	Samalpatti	pyroxenite	9.147	0.295	0.021	4.516	6.167
IC06A	Samalpatti	monzogabro	3.266	0.824	0.012	0.190	1.092
IC07E	Samalpatti	monzogabro	0.429	bdl	bdl	1.269	0.298
IC09	Samalpatti	syenite	0.047	bdl	bdl	2.013	0.245
IC23B	Samalpatti	syenite	8.862	bdl	bdl	1.150	0.002
IC10A	Sevattur	carbonatite	4.821	0.993	0.033	1.373	0.459
IC10J	Sevattur	carbonatite	15.107	6.000	0.042	0.194	0.317
IC11A	Sevattur	mt-carbonatite	2.692	bdl	bdl	0.092	0.010
IC16A	Sevattur	carbonatite	bdl	bdl	bdl	0.442	4.239
IC10D	Sevattur	phosphate+phl	0.256	1.273	0.048	0.500	2.572
IC11B	Sevattur	magnetite	0.705	2.154	0.040	4.759	0.315
IC13A	Sevattur	monzogabro	5.423	0.095	0.074	1.102	0.138
IC14	Sevattur	qtz monzogabro	3.507	1.410	0.008	5.187	0.097
IC12B2	Sevattur	tonalite with sulf	bdl	1.086	0.074	0.826	0.072

Tab. 8. HSE normalized by values found in primitive mantle (Becker et al., 2006).

Locality	Rock	V (ppm)	Cr (ppm)	Co (ppm)	Ni (ppm)	Cu (ppm)	Zn (ppm)	Ga (ppm)	Pb (ppm)	Cd (ppm)	W (ppm)
Samalpatti	carbonatite	18	7.0	3.85	4.00	6.21	17.7	4.26	6.8	0.09	0.16
Samalpatti	carbonatite	bdl	4.00	2.16	bdl	4.42	13.9	2.62	5.1	0.12	0.24
Samalpatti	Ca-rich silicocarbonatite	28.0	14.2	5.14	8.4	14.7	11.7	4.87	5.9	0.13	0.78
Samalpatti	Ca-rich silicocarbonatite	13.0	13.0	3.50	8.14	15.40	31.5	4.38	11.3	0.13	0.12
Samalpatti	Mg-Cr-rich silicocarbonatite	71	1071	33.5	176	3.15	73.4	3.64	9.6	0.10	0.09
Samalpatti	Mg-Cr-rich silicocarbonatite	48.0	1285	30	172	4.36	23.9	2.37	10.3	bdl	0.11
Samalpatti	Mg-Cr-rich silicocarbonatite	63.0	1670	31.0	173	4.65	65.4	3.21	14.8	0.08	0.67
Samalpatti	Mg-Cr-rich silicocarbonatite	64.0	924	33.6	175	2.76	28.0	2.73	8.7	0.80	0.12
Samalpatti	Mg-Cr-rich silicocarbonatite	38.0	1803	33.4	207	5.86	13.6	1.69	22.6	0.04	0.09
Samalpatti	Mg-Cr-rich silicocarbonatite	74.0	1025	36.3	165	1.95	150	3.89	26.5	0.10	0.09
Samalpatti	calc-silicate marble	41.0	35	6.59	15.8	8.96	30.5	9.44	6.1	bdl	0.29
Samalpatti	pyroxenite	218.0	2.73	3.09	2.6	7.5	3.8	1.48	12.6	bdl	0.20
Samalpatti	pyroxenite	429.0	75.7	58.4	94	10.40	146	19.5	1.6	0.08	0.33
Samalpatti	pyroxenite	75.0	1471	42.3	149	3.92	32.4	3.74	1.3	0.07	0.19
Samalpatti	monzogabro	1064.0	5.61	53.6	8.4	1535	126	15.3	23.5	0.09	0.46
Samalpatti	monzogabro	bl	16.9	1.20	3.83	2.84	5.74	15.6	18.8	0.03	0.07
Samalpatti	syenite	73.0	2.35	0.66	0.15	4.34	14.7	15.4	3.0	0.12	0.08
Samalpatti	syenite	102.0	2.36	2.36	0.3	5.97	16.1	15.8	6.0	0.09	0.27
Sevattur	carbonatite	bdl	bdl	1.28	19	8.46	3.09	11.60	48.2	0.42	0.19
Sevattur	carbonatite	90.0	9.0	15.7	26.0	77.4	27.0	19.1	23.0	0.37	0.22
Sevattur	mt-carbonatite	78.0	3.00	16.9	14.00	17.6	16.6	12.30	68.8	0.41	0.21
Sevattur	carbonatite	bdl	bdl	1.4	22	0.87	0.23	9.77	19.4	bdl	0.10
Sevattur	phosphate+phl	50.0	6.0	17.0	29.9	51.6	54.2	22.7	23.7	0.26	0.44
Sevattur	magnetite	3483.0	545.0	41.3	21	44.3	269	6.70	5.4	0.12	0.21
Sevattur	monzogabro	114.0	109.0	18.4	54.4	32.3	69.8	17.2	28.7	0.17	1.39
Sevattur	qtz monzogabro	38.0	9.9	2.65	3.8	20.9	35.8	18.9	25.3	0.05	0.14
Sevattur	tonalite with sulf	144.0	23.1	3.9	10.2	7.6	14.0	3.4	2.3	0.06	0.32

Tab. 9. Concentrations of selected chalcophile and siderophile elements

6.2   Re-Os isotopic systematics

The Samalpatti carbonatites show radiogenic Re-Os isotopic compositions resulting from high Re/Os ratios. Sample IC05A has an increased $^{187}Re/^{188}Os$ ratio of 10.6 and $^{187}Os/^{188}Os$ of 0.387 while the second sample (IC05F1) has lower $^{187}Re/^{188}Os$ ratio 2.7, but much higher $^{187}Os/^{188}Os$ 1.36. Both these values are above average ratios for primitive mantle (e.g., Meisel et al., 2001) and tend to be closer to enriched mantle or even continental crust (Peucker-Ehrenbrink and Jahn, 2001). The Sevattur carbonatites exhibit an extreme variation in their $^{187}Os/^{188}Os$ ratios from value 0.1873 similar to mantle-derived melts from elsewhere (Day et al., 2016 and references therein) to extremely radiogenic value of 10.3 found in magnetite-rich carbonatite IC11A. Such value is connected with particularly high $^{187}Re/^{188}Os$ ratio (282) and therefore, time ingrowth of ^{187}Os over 800 Ma. Other two Sevattur carbonatites has $^{187}Os/^{188}Os$ of ~0.43.
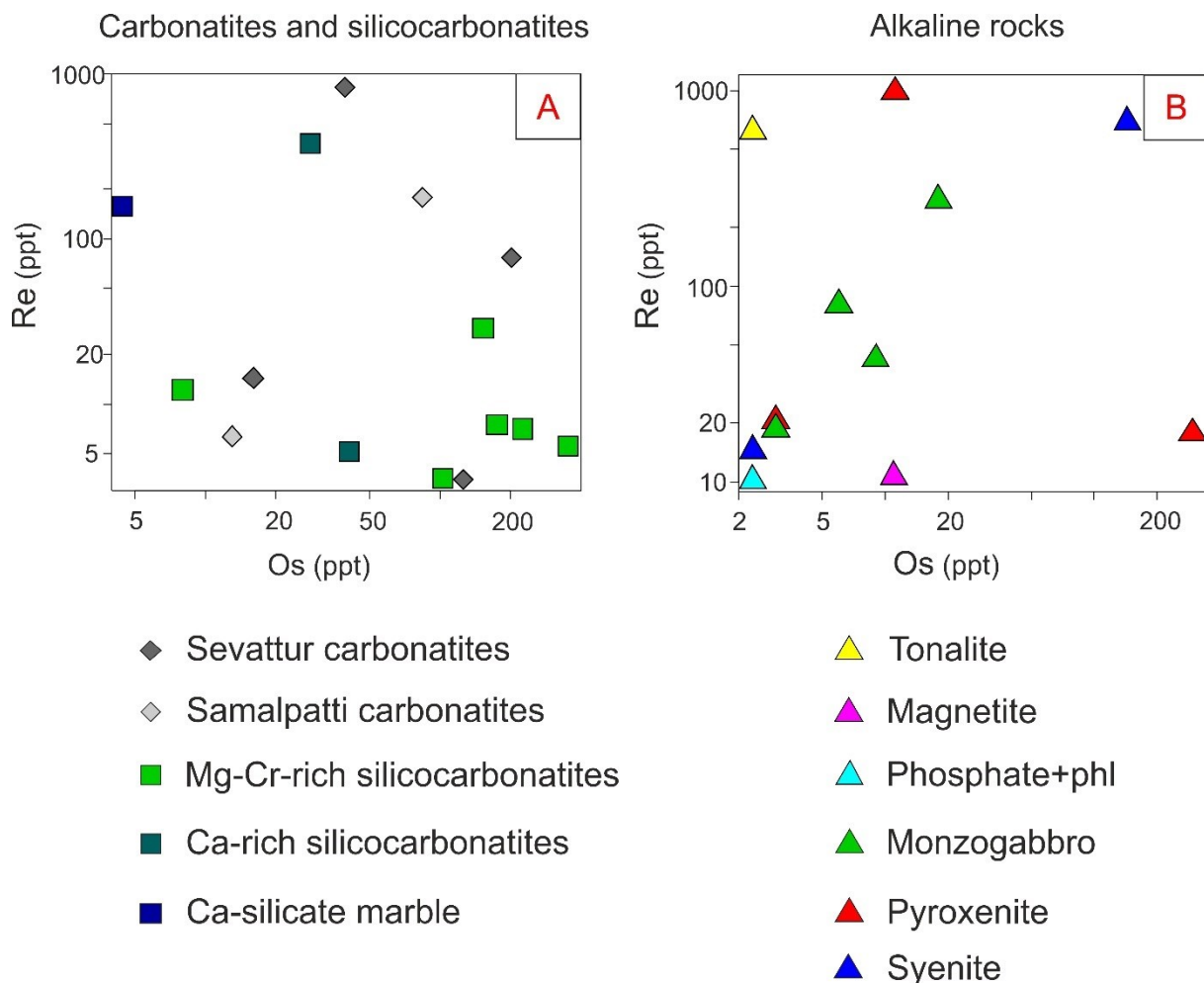
Fig. 24. Re/Os ratios for A) carbonatites and silicocarbonatites in Samalpatti and Sevattur region (radiogenic IC11A and IC18A excluded), B) alkaline rocks from Samalpatti and Sevattur (radiogenic IC05C excluded)

Two samples of Ca-rich silicocarbonatites yield highly variable $^{187}Os/^{188}Os$ of 0.420 and 5.9 without connection to their Re/Os ratios. In other words, sample IC18B with high Re of 0.378 has the lower $^{187}Os/^{188}Os$. On contrary, the Mg-Cr-rich carbonatites show mostly mantle-like Re-Os signatures with Os isotopic compositions in the range between 0.1453 to 0.5735 and low $^{187}Re/^{188}Os$ ratios < 1 (except sample IC03D with 7.7). Calc-silicate marble has $^{187}Os/^{188}Os$ ratio of 0.590 and $^{187}Re/^{187}Os$ is equal to 201.

With the exception of two samples (pyroxenite IC07D and syenite IC23B) from Samalpatti showing only mildly radiogenic Re-Os isotopic compositions, the alkaline silicate rocks from both complexes show largely variable, radiogenic $^{187}Os/^{188}Os$ from 1.0 to 4.5 typical for continental crustal materials. Magnetite separate yield radiogenic values 1.30 and 5.5 for $^{187}Os/^{188}Os$ and $^{187}Re/^{188}Os$, respectively.
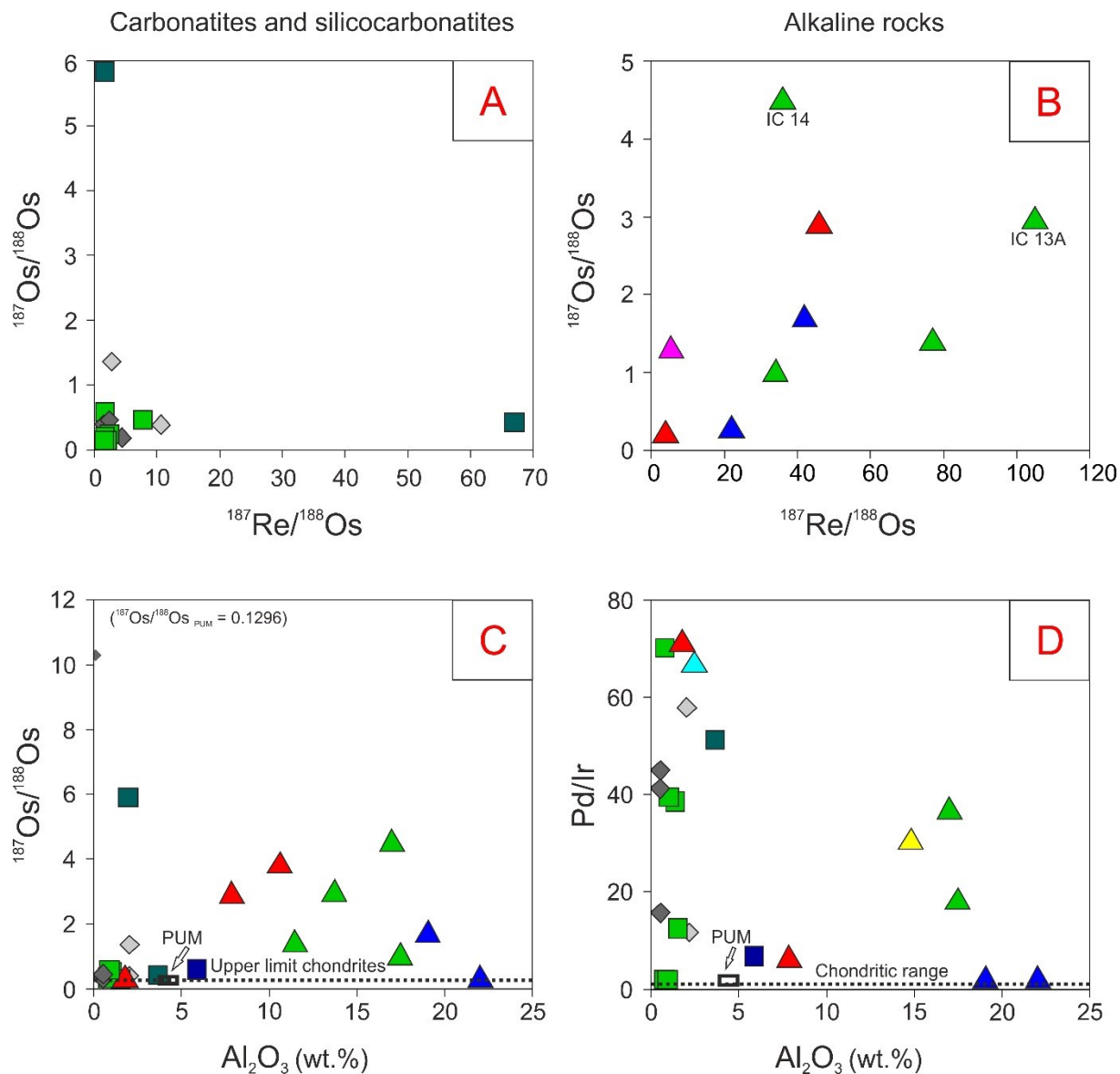
Fig. 25. Ratios of $^{187}Re/^{188}Os$ and $^{187}Os/^{188}Os$ in different rock systematics and $^{187}Os/^{188}Os$ with Al_2O_3 and Pd/Ir with Al_2O_3.

7 DISCUSSION

7.1 Siderophile and chalcophile element concentrations in carbonatites and insights to their mantle sources from the Re-Os isotopic systematics

Until now, only a few data exist on the HSE contents of mantle-derived carbonatitic magmas with no data being ever reported for Re–Os. These include PGE data from REE-rich and common carbonatites of Paleocene (65–45 Ma) age from China (Xu et al., 2003; Xu et al., 2008) and poorly characterized data from phoscorite-carbonatite complexes (Fontana, 2006) with PGE mineralization from Brazil (123–70 Ma) and South Africa (~2.0 Ga). These three studies reported large range of contents from ppt to ppm (e.g., 3200 ppb for Pt, 1330 ppb for Pd and 13500 ppb for Ir) levels, therefore, more than six order of magnitude differences. Such differences can result from the early separation of sulphide-rich melts (Xu et al., 2008) leading to the strong HSE depletion, transport of HSE through the volatile-rich melts/fluids causing moderate HSE enrichment (Cheng et al., 2003) or large concentration of HSE at even economic grade caused by a combination of mafic melt differentiation and post-magmatic evolution (Fontana, 2006).

The carbonatites from Samalpatti and Sevattur complexes are characterize by very low HSE abundances well-bellow primitive mantle values (except IC11A; 0.974 ppb) with the largest depletions found for Ir and Ru. When compared to MORB, the analysed carbonatites are enriched in Pt and one sample (IC05A) slightly in Os. On the other hand, HSE contents in OIB and komatiites are higher than those found in carbonatites (cf. Day et al. 2016 and references therein). The only one exception represents the sample IC11A having the highest content of Re (0.974 ppb) paralleled also by its higher content of Pb (69 ppm) and the most radiogenic $^{187}Os/^{188}Os$ composition of 10.3. When compared with Xu et al., 2008, who analysed carbonatites in central China, carbonatites from Tamil Nadu are mostly enriched in I-PGE. This assumption is valid for intrusive carbonatites, extrusive have higher concentration. Concentration of Pt is generally similar, but few samples from China are depleted and 4 samples are enriched. In case of Pd, the situation is similar.

The preliminary suggestion that very high Re content found in sample IC11A is connected with large magnetite contents was underscored by very low Re (0.011 ppb) found in separated magnetite fraction (Table 7) and the reason remain unknown. In general, very low HSE concentrations found for Tamil Nadu carbonatites are in agreement with their very low sulphur contents and HSE are considered to be bonded to sulphur (Brenan et al., 2016). Contents of S in carbonatites from Samalpatti and Sevattur typically do not exceed more than 0.024 wt. % with only one sample (IC05F1) reaching the concentration of 0.120 wt.% and absence of positive correlation with Ba suggest that S is rather bound to sulphides, not sulphates such as barite. As there is no correlation between S and HSE contents, it seems that HSE are rather hosted in some other mineral phases and/or they are concentrated in heterogeneously dispersed sulphides/HSE-bearing phases. The preliminary search for sulphides revealed that most samples are virtually devoid of any sulphide, with only minor amounts of pyrite found in sample IC05F1. To conclude, the most plausible explanation for the very low HSE contents found in analysed carbonatites from Tamil Nadu is a separation of S-rich melt extracting most of the HSE from the primary carbonatitic melt during the transport and/or melt fractionation. As there are virtually no differences in HSE concentrations between Samalpatti and Sevattur carbonatites in spite of their contrasting petrogenesis (see Ackerman et al., 2017) based mostly on lithophile element systematics, such process can be possibly generally valid for all carbonatitic magmas.

There are no significant differences in HSE patterns between Samalpatti and Sevattur. In overall, the primitive-mantle normalized HSE patterns do not correspond to that of primitive mantle and mantle-derived mafic melts (e.g., basalts) showing a continuous increase of contents from Os to Re and I-PGE/P-PGE fractionations showing Os_N/Ir_N to Pd_N/Re_N values < 1. Between Os and Ru for Samalpatti and Sevattur carbonatites, this condition was significantly met only for one sample (IC05F1, Ir_N/Ru_N = 0.37). For P-PGE values, most of the samples exhibit Pd enrichment over Pt and therefore, resemble the fractionation observed for basalts (with the exception of sample IC10A from Sevattur with Pd_N/Pt_N of 0.7). The most interesting feature comes from Os enrichment over Ir, which is absent in mafic mantle-derived melts. Our data indicate that this trend is systematic (found for all analysed carbonatites) and may suggest that carbonatitic magmas are capable to concentrate Os.

The Re–Os isotopic composition can, for the first time, provide some first-order information on the nature of carbonatitic melt sources with respect to their $^{187}Re/^{188}Os$ and $^{187}Os/^{188}Os$. For most carbonatites, it is possible to calculate initial (800 Ma) $^{187}Os/^{188}Os$ values spanning in the range from slightly unradiogenic (IC10A; 0.1285) through slightly radiogenic (IC05F1; 0.2451) to highly radiogenic (0.4–6.5). Such extreme range of values can be interpreted in two ways. First, this might be caused by large heterogeneity of melt source with a large, but variable incorporation of recycled crustal materials (e.g., eclogite, pyroxenites) with highly radiogenic $^{187}Os/^{188}Os$ composition (cf. van Acken et al., 2010) as can be inferred from positive γOs values (up to +5247). Alternatively, carbonatitic magmas can be contaminated by crustal materials during their transport to the Earth`s surface. However, a second scenario is very unlikely as carbonatitic magmas are believed to be transported very quickly and they are mostly not capable to inherit large proportions of crust due to their low melt temperatures.

Sevattur carbonatite IC10J contain almost 7 wt. % of P_2O_5 and the highest contents of Cu from all carbonatites (77 ppm). This particular sample contain a significantly abundant apatite (~20 vol. %), which may explain increased abundance of Cu. This explanation could be supported by strongly positive correlation between P_2O_5 and Cu (r = 0.98) (Fig. 26). However, the only one partitioning coefficient ever reported for apatite (Paster et al., 1974) and Cu imply incompatible behaviour of this element in apatite. Second sample enriched in P_2O_5 is IC11A. Both samples are also slightly enriched in FeO_{tot} (2.95 and 3.39 wt. %) and this elevated iron values (probably due to magnetite) can be also partly responsible for increased Cu contents. These two samples are further slightly enriched also in Co, V and Cr and IC11A have a highest γOs (+5247), so increased chalcophile elements might be of crustal origin. Contents of MgO at both localities are approximately the same (± 3 wt. %) but they differ in content of alkaline earth metal (AEM). Sevattur carbonatites are enriched in some AEM (Sr > 5000 ppm; Ba > 2000 ppm) and these values are higher than values for upper continental crust (Rudnick and Gao, 2014).
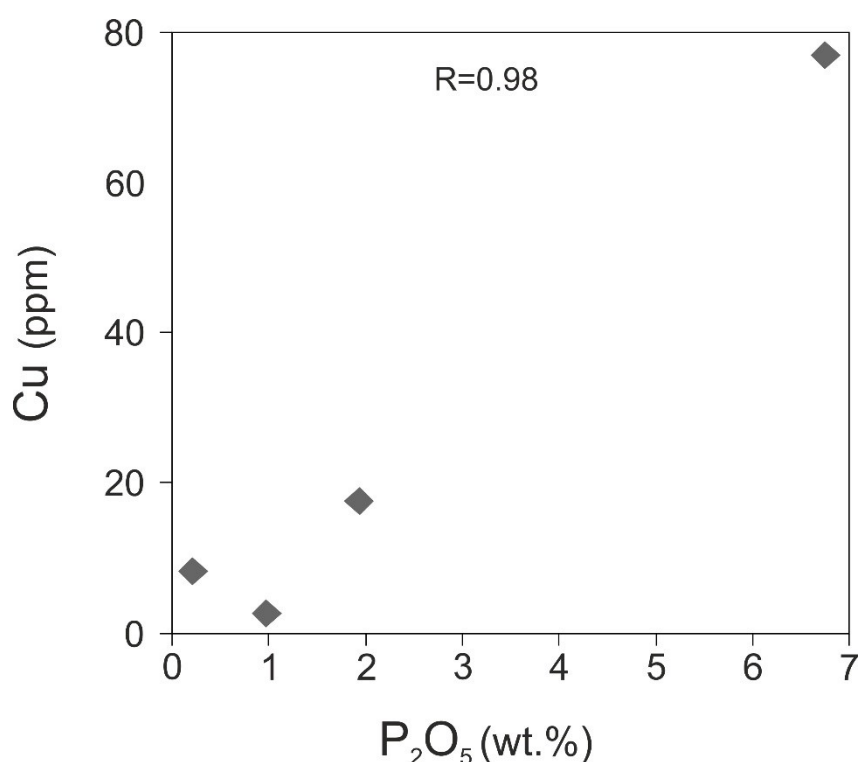

Fig.26. Cu/P_2O_5 ratio and their positive correlation of Sevattur carbonatites.

7.2 Constraints on the origin of silicocarbonatites from Samalpatti

The silicocarbonatites from Samalpatti have a strikingly much higher HSE contents and primitive- mantle normalized patterns than those found in carbonatites.

The Mg-Cr-rich carbonatites exhibit similar, elevated HSE concentrations in strong contrast to their very low S contents (< 0.026 wt. %) and negative correlation found between S and HSE (Fig. 27B). With the exception of one sample (IC06E), contents of Os are higher than in MORB, while other I-PGE have higher or similar concentration. When compared to OIB and komatiites, the Mg-Cr-silicocarbonatites yield lower I-PGE values. Amounts of Re does not those reported for continental crust (0.2 ppb in crust, < 0.029 ppb in Mg-Cr-rich silicocarbonatites). In contrast, Pt is abnormally enriched and several times exceeds content in MORB and OIB or even those reported for komatiites. Half samples reach or exceed concentration of Pd in MORB and OIB. The patterns for Mg-Cr-rich silicocarbonatites are more or less flat in I-PGE segment, then rise with Pt to values which are much higher than concentration in primitive upper mantle (up to 38 ppb) and converging down to Re with negative slope from Pt to Re. Only IC06E sample exhibits rather flat HSE distribution, which is typical for peridotites and negative or positive tilt at the end can be a result of some post-process like metamorphism or late alteration (Luguet et al., 2007). The high I-PGE contents found in the Mg-Cr-rich silicocarbonatites and absence of I-PGE fractionation request some direct incorporation of mantle-derived material in agreement with an increased concentration of Cr (up to 1800 ppm) and Ni (up to 200 ppm) emphasized also by positive correlation between Os and Ni (Fig. 27A).
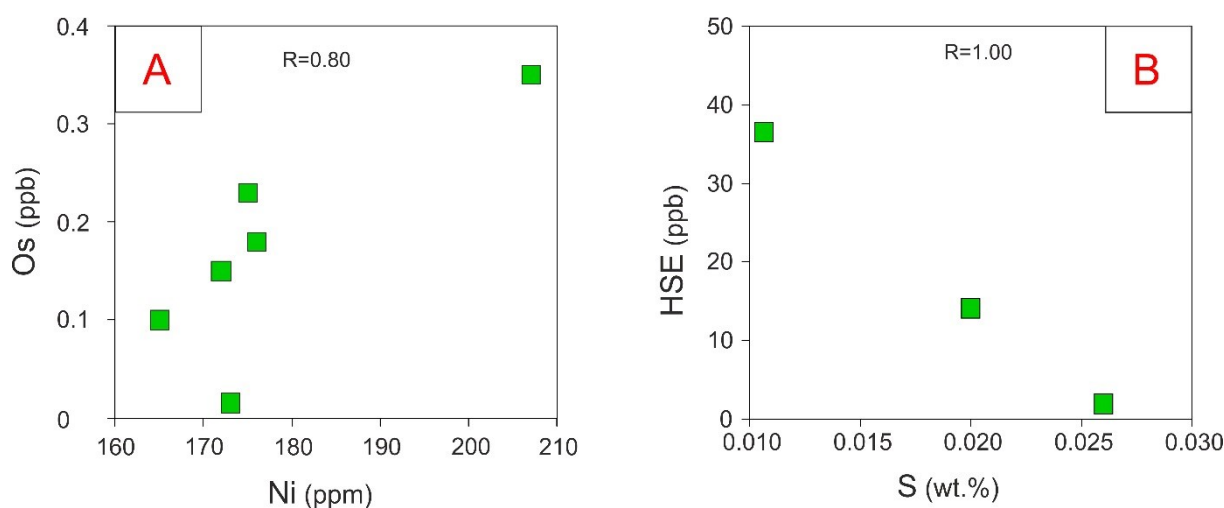
Fig. 27. A) Os/Ni ratios of Samalpatti Mg-Cr-silicocarbonatites, B) HSE/S ratios of Samalpatti Mg-Cr-silicocarbonatites

The Mg-Cr-rich carbonatites exhibit mostly only slightly radiogenic initial (800 Ma) $^{187}Os/^{188}Os$ compositions typically in the range between 0.144 and 0.180 and These slightly radiogenic values might lead to the conclusion that the Cr-Mg-rich silicocarbonatites are derived from upper mantle and in the past, have been contaminated with crustal material. This scenario might be also supported by values of $\delta^{13}C$ and $\delta^{18}O$ (±–4‰ and ± +10‰), which fit into the field of primary mantle-derived melts in $\delta^{13}C/\delta^{18}O$ diagram. However, as it was already pointed out by Ackerman et al. (2017), there are few discrepancies. The Mg-Cr-rich silicocarbonatites do not appear as individual bodies but occur as centimetre to decimetre-sized enclaves enclosed in pyroxenites with sharp contact at hand specimen scale (Ackerman et al., 2017) and mineral arrangement corresponds more to hydrous metasomatism by Na-rich carbonatitic melts at upper mantle conditions (Ackerman et al., 2017; Ali and Arai, 2013). Therefore, the origin of Mg-Cr-rich silicocarbonatites have probably closely related to fenitization of pyroxenite host rock and results from a mixing between primary, mantle derived alkali and CO_2-rich melts and crustal pyroxenites. Such hypothesis is also consistent with variable γ Os ranging from +19 to +370 and radiogenic initial $^{187}Os/^{188}Os$ compositions found for two samples (IC03D with 0.35 and IC06E with

0.571). This range suggest admixture of crustal material. The cause of Pt enrichment found in Mg-Cr-rich carbonatites remain unknown. Nevertheless, very high values found can be potentially connected with some Pt-bearing mineral phase. Platinum and palladium typically founds compounds with S (e.g. Cooperite [(Pt,Pd,Ni)S]), Sn (e.g., Paolovite; [Pd_2Sn]), As (e.g., Palladoarsenide; [Pd_2As]) or Se (e.g., Miesiite; [$Pd_{11}Te_2Se_2$]) but unfortunately these elements were not measured in our samples (webmineral.com).

The Ca-rich silicocarbonatites and calc-silicate marble have much lower I-PGE and Pt values when compared to Mg-Cr-types (Table 7). However, the Ca-rich silicocarbonatites have a same positive anomaly on Pt as Mg-Cr-silicocarbonatites, but with lower intensity. In case of P-PGE, both the calc-silicate marble and Ca-rich silicocarbonatite have an opposite pattern as Mg-Cr-rich silicocarbonatites, except IC18B, which have a negative slope (Re; 0.378 ppb). If compared to MORB, the Ca-rich silicocarbonatites have similar or lower concentrations of I-PGE and Os and Ir contents are rather similar to concentrations reported for continental crust (e.g., Rudnick and Gao, 2014). Elements from P-PGE group are more enriched in the Ca-rich silicocarbonatites than in MORB (except Pd in IC18B and Re in IC18C). The OIB and komatiites are richer in all HSE comparing to Ca-rich silicocarbonatites from Tamil Nadu except one sample reaching higher content of Re (0.378 ppb IC18B) reflecting most likely its higher pyrite content and one yielding higher Pd (IC18C; 2.6 ppb). The initial (800 Ma) $^{187}Os/^{188}Os$ value for the Ca-rich silicocarbonatites can be calculated only for one sample (IC18C with 5.9) indicating large perturbations of Re–Os systematics in these rocks. If this one value is real, it may infer large proportion of crustal material at least in this one sample. The calc-silicate marble yields negative initial $^{187}Os/^{188}Os$ value, which is consistent with late-stage pyrite mineralization found during thin section inspection.

7.3 Siderophile and chalcophile element concentrations and Re-Os systematics of alkaline rocks from Samalpatti

The alkaline rocks from Samalpatti (pyroxenite, monzogabbro, syenite) show wide range of HSE concentrations with sometimes clear relationship to their sulphur contents, especially in terms of Re.

When compared to MORB, OIB or komatiites, the pyroxenites have lower contents of I-PGE except sample IC07D, which have Ru content of 0.21 ppb. In comparison, concentrations of Pt in pyroxenites are similar to concentrations in MORB or even higher. Two samples have higher content of Pd than MORB and in case of Re, only one sample show higher values. Within the pyroxenites, two different HSE patterns can be recognized: (a) primitive HSE distribution at very low contents (sample IC06D), even much lower than those reported for continental crust (Rudnick and Gao, 2014) and (b) a zig-zag patterns from Os to Re with selective enrichments in Pd-Pt (IC05C) and Os-Pt (IC07D). The Pd-Pt and also Re enrichment in the IC05C sample is clearly related to high content of S (0.945 wt. %), which is expressed in a common abundance of pyrite in this sample. The largely negative initial (800 Ma) $^{187}Os/^{188}Os$ calculated for this sample indicate strong perturbation of the Re-Os systematics in this sample and may indicate that pyrite mineralization producing large Re enrichments is rather connected with some late-stage processes postdating the formation of this sample. Nevertheless, collectively with sample IC06D, the Re-Os isotopic compositions of these two samples argue for their derivation from crustal lithologies. On contrary, the IC07D pyroxenite exhibits only slightly radiogenic initial $^{187}Os/^{188}Os$ and γOs value of +41 in agreement with its high Os (0.32 ppb) and Ni-Cr contents (149 and 1471 ppm, respectively). Such signatures can be best explained by the reaction with mantle-derived melt and this particular sample therefore can represent the product of the reaction which also produces the Mg-Cr-rich silicocarbonatites described above.

The two analysed monzogabbros and syenite IC09 have rather similar, very low HSE contents far below MORB, OIB and komatiites, but also below estimates for continental crust. They produce I-PGE flat patterns that rise in P-PGE contents. These three samples exhibit largely radiogenic $^{187}Os/^{188}Os$ compositions paralleled by unrealistically low calculated initial values. All these signatures pointed out for their derivation from continental crust and perturbed Re–Os isotopic system, perhaps due to several hydrothermal overprinting. One exception represents syenite IC23B with elevated Re–Os and S contents, which reach in contents similar to OIB. Present-day 187Os/188Os value of this sample yield

0.27, which may attest a partial source for this sample within enriched mantle, rather than continental crust.

The alkaline rocks from Samalpatti show a pronounced positive correlation between Ir and SiO_2 as can be seen on Fig. 28, but the reason for such behaviour remain unclear as Ir is the only one element among HSE showing such relationship. Monzogabbro (IC06A) has enormous volume of Cu (1535 ppm), Ba (15338 ppm) and V (1064 ppm). This is probably related to the presence of chalcopyrite mineralization within this rock.
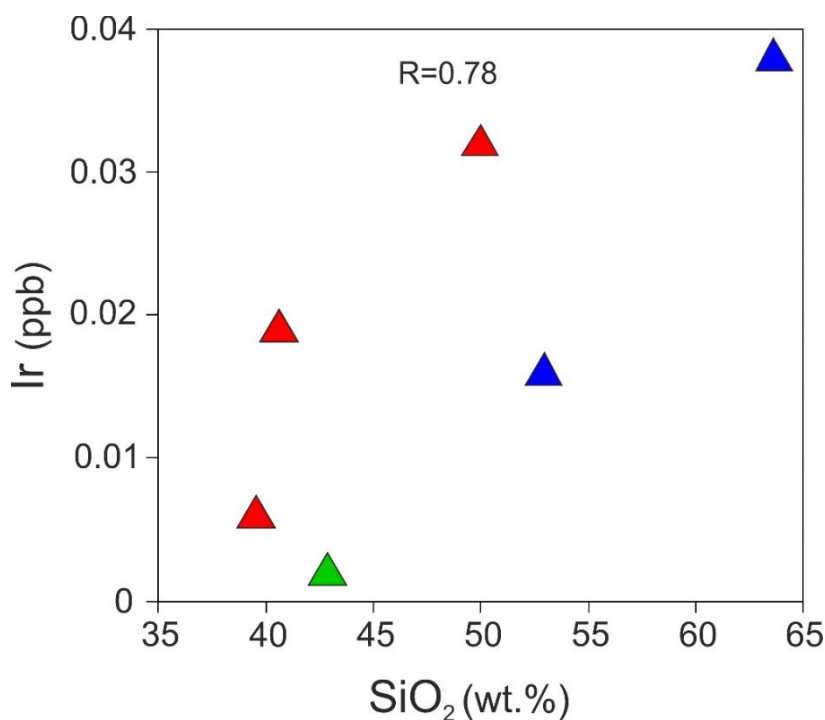
Fig. 28 Ir vs. SiO_2 contents in Samalpatti alkaline rocks (IC07E bellow detection limit).

7.4 Siderophile and chalcophile element concentrations and Re-Os systematics of alkaline rocks and minerals from Sevattur

The Sevattur alkaline rocks and minerals separated from carbonatite (magnetite IC16A) or with a close connection to carbonatite (phosphate+phlogopite IC10D) share some similarities with respect to their HSE contents and Re-Os isotopic ratios. They yield very low HSE contents, typically lower than all mafic, mantle-derived melts such as MORB, OIB or komatiites, but even lower than those found in continental crust. Their HSE patterns are almost identical with primitive I-PGE distributions followed by mildly increase in P-PGE and Re with common small Pt positive anomaly. The highest variation was found in Re contents, which are not directly related to sulphur concentrations. The initial (800 Ma) $^{187}Os/^{188}Os$ ratios of Sevattur alkaline rocks and carbonatite-related minerals range from 1.224 to 4.014, which clearly indicate predominant crustal origin of these rocks/minerals. This also in agreement with the low contents of chalcophile and other siderophile elements corresponding to average values found in continental crust. Content of Cr reach up to 545 ppm in magnetite and is in other samples is content 6–109 ppm. In magnetite is possible to observe increased volume of Zn (269 ppm) and Nb (487 ppm). Divalent Zn^{2+} replace Fe^{2+} in magnetite whereas Nb can be divalent and trivalent.

8   CONCLUSION

High precision analyses of highly siderophile elements and Re–Os isotopic compositions on 6 samples of carbonatites, 8 samples of silicocarbonatites and 12 samples of associated alkaline rocks from Samalpatti and Sevattur, south India was carried out in order to bring a new data to neglected area of mantle-derived melt geochemistry. The carbonatites from Samalpatti and Sevattur are characterized by low HSE abundances, much lower than primitive mantle values, but even lower than other mantle-derived melts such as variable types of basalts. Low concentrations of HSE are in agreement with low content of sulphur and chalcophile and siderophile elements. There are no significant differences between carbonatites from Samalpatti and Sevattur. The specific Os enrichment found in all analysed carbonatites over Ir may suggest that they are able to selectively concentrate Os. Initial ratios of $^{187}Os/^{188}Os$ in carbonatites are not uniform and increase from slightly unradiogenic to highly radiogenic. This is probably caused by large heterogeneity of melt source with high contribution of crustal material, like eclogite. Some Sevattur carbonatites are enriched in P_2O_5 and FeO_{tot} and contain apatite and magnetite which probably increase concentration of Cu.

The silicocarbonatites have a much higher HSE concentrations and primitive-mantle normalized patterns than those found in carbonatites. The Mg-Cr-rich silicocarbonatites are characterized by abnormally high content of Pt which even exceed the values estimated for primitive mantle, MORB, OIB and even komatiites. Flat distribution of I-PGE, which is typical for pyroxenes, and curved distribution of P-PGE may be result of post-processes like metamorphism or late alteration. The high contents of I-PGE and absence of their fractionation request direct incorporation of mantle-derived material. The composition of Mg-Cr-rich silicocarbonatites more correspond to hydrous metasomatism by Na-rich carbonatitic melts at upper mantle conditions, even though these rocks are slightly radiogenic and $\delta^{13}C$ and $\delta^{18}O$ fit to the field of primary mantle-derived melts. Origin of Mg-Cr-rich silicocarbonatites is probably closely related to fenitization of pyroxenite host rock and result of mixing between primary mantle-derived alkali and CO_2-rich melts. The Ca-rich silicocarbonatites have a lower contents of I-PGE and Pt than Mg-Cr-rich silicocarbonatites but same positive anomaly on Pt. Initial $^{187}Os/^{188}Os$ ratios can be calculated only for one sample, which indicate large disorder in Re-Os systematics in these rocks.

The alkaline rocks from Samalpatti exhibit wide range of HSE contents with a close relationship to sulphur, especially in terms of Re. The Re-Os systematic of pyroxenites argue for their derivation from crustal lithologies, however one sample has a negative initial $^{187}Os/^{188}Os$, which indicate perturbation of the Re-Os systematics, probably caused by pyrite mineralization and subsequent Re enrichment. The composition of this peculiar sample might be explained by reaction of mantle-derived melt with this pyroxenite. Monzonites and syenite have similar low content of HSE, flat I-PGE patterns that rise in P-PGE contents. By their half radiogenic and half unrealistic low $^{187}Os/^{188}Os$ point to their derivation from continental crust. One exception is sample of syenite, whose origin fits more to enriched mantle, rather than continental crust.

The alkaline rocks from Sevattur yield similarly low HSE contents. Their HSE patterns are almost identical with primitive I-PGE distributions followed by moderate increase in P-PGE and Re. An apparent positive anomaly on Pt on the pattern can be recognized. The initial $^{187}Os/^{188}Os$ ratios clearly sorted out, that these samples are attributed to crustal origin.

9 REFERENCES

Ackerman, L., Magma, T., Rapprich, V., Upadhyay, D., Krátký, O., Čejková, B., Erban, V., Kochergina, V.Y., Hrska, T., 2017. Contrastng petrogenesis of spatially related carbonatites from Samalpatti and Sevattur, Tamil Nadu, India. Lithos 284-285, 257-275.

Ali, M., Arai, S., 2013. Cr-rich magnesiokatophorite as an indicator of mantle metasomatism by hydrous Na-rich carbonatite. J. Mineral. Petrol. Sci. 108, 215–226.

Arndt, N., Lesher, M., Barnes, S., 2008. Komatiite. Cambridge University Press.

Bailey, D.K., 1977. Lithosphere control of continental magmatism. J. Geol. Soc. 133, 103–106.

Bailey, D.K., Woolley, A.R., 2005. Repeated, synchronous magmatism within Africa: Timing, magnetic reversals, and global tectonics. Geol. Soc. Am. Spec. Pap. 388, 365–377.

Barnes, S.-J., Naldrett, A.J., Gorton, M.P., 1985. The origin of the fractionation of platinum-group elements in terrestrial magmas. Chem. Geol. 53, 303–323.

Becker, H., Horan, M.F., Walker, R.J., Gao, S., Lorand, J.P., Rudnick, R.L., 2006. Highly siderophile element composition of the Earth's primitive upper mantle: Constraints from new data on peridotite massifs and xenoliths. Geochim. Cosmochim. Acta 70, 4528–4550.

Birck, J.L., Roy Barman, M., Capmas, F., 1997. Re-Os isotopic measurements at the femtomole level in natural samples. Geostand. Newsl. 21, 19–27.

Bizimis, M., Salters, V.J.M., Dawson, J.B., 2003. The brevity of carbonatite sources in the mantle: Evidence from Hf isotopes. Contrib. to Mineral. Petrol. 145, 281–300.

Bockrath, C., 2004. Fractionation of the Platinum-Group Elements During Mantle Melting. Science 305, 1951–1953.

Brenan, J.M., Bennett, N.R., Zajacz, Z., 2016. Experimental Results on Fractionation of the Highly Siderophile Elements (HSE) at Variable Pressures and Temperatures during Planetary and Magmatic Differentiatioon, in: Reviews in Minealogy & Geochemistry. pp. 1–87.

Brooker, R.A., 1998. The effect of CO_2 saturation on immiscibility between silicate and carbonate liquids: An experimental study. J. Petrol. 39, 1905–1915.

Büchl, A., Brügmann, G., Batanova, V.G., Münker, C., Hofmann, A.W., 2002. Melt percolation monitored by Os isotopes and HSE abundances: A case study from the mantle section of the Troodos Ophiolite. Earth Planet. Sci. Lett. 204, 385–402.

Condie, K.C., Allen, P., Narayana, B.L., 1982. Geochemistry of the Archean low- to high-grade transition zone, Southern India. Contrib. to Mineral. Petrol. 81, 157–167.

Creaser, R.A., Papanastassiou, D.A., Wasserburg, G.J., 1991. Negative thermal ion mass spectrometry of osmium, rhenium and iridium. Geochim. Cosmochim. Acta 55, 397–401.

Cullers, R.L., Medaris, G., 1977. Rare earth elements in carbonatite and cogenetic alkaline rocks: Examples from Seabrook Lake and Callander Bay, Ontario. Contrib. to Mineral. Petrol. 65, 143–153.

Dasch, E.J., 1969. Strontium isotopes in weathering profiles, deep-sea sediments, and sedimentary rocks. Geochim. Cosmochim. Acta 33, 1521–1552.

Day, J.M.D., 2013. Hotspot volcanism and highly siderophile elements. Chem. Geol. 341, 50–74.

Day, J.M.D., Pearson, D.G., Hulbert, L.J., 2013. Highly siderophile element behaviour during flood basalt genesis and evidence for melts from intrusive chromitite formation in the Mackenzie large igneous province. Lithos 182–183, 242–258.

Day, J.M.D., Pearson, D.G., Macpherson, C.G., Lowry, D., Carracedo, J.C., 2010. Evidence for distinct proportions of subducted oceanic crust and lithosphere in HIMU-type mantle beneath El Hierro and La Palma, Canary Islands. Geochim. Cosmochim. Acta 74, 6565–6589.

Day, M.D.J., Brandon, D.A., Walker, J.R., 2015. Highly siderophile elements in Earth, Mars, the Moon, and Asteroids. Nature 81, 161–238.

Deines, P., 1989. Stable isotope variations in carbonatites, in: Bell, K. (Ed.), Carbonatites: Genesis and Evolution. Academic Division of Unwin Hyman Ltd, London, pp. 301–359.

Deines, P., 2002. The carbon isotope geochemistry of mantle xenoliths. Earth-Science Rev. 58, 247–278.

Duncan, R.A., Pyle, D.G., 1988. Rapid eruption of the Decan flood basalts at the Cretaceous/Tertiary boundary. Nature 333, 403–405.

Ernst, R.E., Bell, K., 2010. Large igneous provinces (LIPs) and carbonatites. Mineral. Petrol. 98, 55–76.

Ertel, W., O'Neill, H.S.C., Sylvester, P.J., Dingwell, D.B., Spettel, B., 2001. The solubility of rhenium in silicate melts: Implications for the geochemical properties of rhenium at high temperatures. Geochim. Cosmochim. Acta 65, 2161–2170.

Escrig, S., Schiano, P., Schilling, J.G., Allègre, C., 2005. Rhenium-osmium isotope systematics in MORB from the Southern Mid-Atlantic Ridge (40-50 S). Earth Planet. Sci. Lett. 235, 528–548.

Fontana, J., 2006. Phoscorite-carbonatite pipe complexes. Platin. Met. Rev. 50, 134–142.

Gaillard, F., Malki, M., Iacono-Marziano, G., Pichavant, M., Scaillet, B., 2008. Carbonatite melts and electrical conductivity in the asthenosphere. Science (80-.). 322, 1363–1365.

Gannoun, A., Burton, K.W., Day, J.M.D., Harvey, J., Schiano, P., Parkinson, I., 2016. Highly Siderophile Element and Os Isotope Systematics of Volcanic Rocks at Divergent and Convergent Plate Boundaries and in Intraplate Settings. Rev. Mineral. Geochemistry 81, 651–724.

Gannoun, A., Burton, K.W., Parkinson, I.J., Alard, O., Schiano, P., Thomas, L.E., 2007. The scale and origin of the osmium isotope variations in mid-ocean ridge basalts. Earth Planet. Sci. Lett. 259, 541–556.

Gannoun, A., Burton, K.W., Thomas, L.E., Parkinson, I.J., Calsteren, P., Schiano, P., 2004. Osmium Isotope Heterogeneity in the Constituent Phases of Mid-Ocean Ridge Basalts. Science (80-.). 303, 70–72.

Grousset, F.E., Biscaye, P.E., Zindler, A., Prospero, J., Chester, R., 1988. Neodymium isotopes as tracers in marine sediments and aerosols: North Atlantic. Earth Planet. Sci. Lett. 87, 367–378.

Groves, D.I., Vielreicher, N.M., 2001. The Phalabowra (Palabora) carbonatite-hosted magnetite-copper sulfide deposit, South Africa: An end-member of the iron-oxide copper-gold-rare earth element deposit group? Miner. Depos. 36, 189–194.

Guarino, V., Azzone, R.G., Brotzu, P., de Barros Gomes, C., Melluso, L., Morbidelli, L., Ruberti, E., Tassinari, C.C.G., Brilli, M., 2012. Magmatism and fenitization in the Cretaceous potassium-alkaline-carbonatitic complex of Ipanema S??o Paulo State, Brazil. Mineral. Petrol. 104, 43–61.

Halliday, A.N., 1999. Mantle geochemistry: Unmixing Hawaiian cocktails. Nature 399, 733–734.

Hammouda, T., Keshav, S., 2015. Melting in the mantle in the presence of carbon: Review of experiments and discussion on the origin of carbonatites. Chem. Geol. 418, 171–188.

Hammouda, T., Laporte, D., 2000. Ultrafast mantle impregnation by carbonatite melts. Geol. 28, 283–285.

Handler, M.R., Bennett, V.C., 1999. Behaviour of Platinum-group elements in the subcontinental mantle of eastern Australia during variable metasomatism and melt depletion. Geochim. Cosmochim. Acta 63, 3597–3618.

Honda, M., Suzuki, K., Tatsumi, Y., 2002. Re-Os isotope systematics of HIMU oceanic island basalts from Tubuai , Polynesia 1, 1993–1996.

Howie, R.A., 2002. Lemaitre, R.W. (Ed.), Streckeisen, A., Zanettin, B., Le Bas, M.J., Bonin, B., Bateman, P., Bellieni, G., Dudel, A.,Efremova, S., Keller, A.J., Lameyre, J., Sabine, P.A., Schmid, R., Sørensen, H. and Woolley, A.R. <em>Igneous Rocks: a Classification . Mineral. Mag. 66, 623 LP-624.

Huang, X., Li, H., Xue, X., Zhang, G., 2006. Development status and research progress in rare earth hydrometallurgy in China. USGS open-file Rep. 24, 129–133.

http://www.palabora.com, 12.2.2017

http://webmineral.com – Nickel-Strunz Classification, 8.5.2017

Chabot, N.L., Jones, J.H., 2003. The parameterization of solid metal-liquid metal partitioning of siderophile elements. Meteorit. Planet. Sci. 38, 1425–1436.

Cheng, X., Zhilong, H., Congqiang, L., Liang, Q., Wenbo, L., Tao, G., 2003. PGE geochemistry of carbonatites in Maoniuping REE deposit, Sichuan Province, China: Preliminary study. Geochem. J. 37, 391–399.

Janardhan, A.S., Newton, R.C., Hansen, E.C., 1982. The transformation of amphibolite facies gneiss to charnockite in southern Karnataka and northern Tamil Nadu, India. Contrib. to Mineral. Petrol. 79, 130–149.

Jonášová, S., Ackerman, L., Žák, K., Skála, R., Ďurišová, J., Deutsch, A., Magna, T., 2016. Geochemistry of impact glasses and target rocks from the Zhamanshin impact structure, Kazakhstan: Implications for mixing of target and impactor matter. Geochim. Cosmochim. Acta 190, 239–264.

Jones, A.P., Genge, M., Carmody, L., 2013. Carbonate Melts and Carbonatites. Rev. Mineral. Geochemistry 75, 289–322.

Jones, C.E., Halliday, A.N., Rea, D.K., Owen, R.M., 1994. sediment and the insignificance of detrital REE contributions to. Earth Planet. Sci. Lett. 127, 55–66.

Kavecsanski, D., Moor, K.R., Wall., F., Lusty, P.A.J., 2016. The Proterozoic mantle source to carbonatite-hosted critical metal deposits and the role of phlogopite in hosting, transporting and concentrating the critical metals. Goldschmidt, Yokohama.

Kjarsgaard, B., Hamilton, D., 1988. Liquid immiscibility and the origin of alkali-poor carbonatites. Miner. Mag 43–55.

Kramm, U., Maravic, H. V., Morteani, G., 1997. Neodymium and Sr isotopic constraints on the petrogenetic relationships between carbonatites and cancrinite syenites from the Lueshe Alkaline Complex, east Zaire. J. African Earth Sci. 25, 55–76.

Kumar, A., Charan, S.N., Gopalan, K., Macdougall, J.D., 1998. A long lived enriched mantle source for two proterozoic carbonatite complexes from Tamil Nadu, southern India. Geochim. Cosmochim. Acta 62, 515–523.

Lee, W., Wyllie, P.J., 1997. Liquid immiscibility between nephelinite and carbonatite from 1.0 to 2.5 GPa compared with mantle melt compositions. Contrib. to Mineral. Petrol. 127, 1–16.

Lodders, K., 2003. Solar System Abundances and Condensation Temperatures of the Elements. Astrophys. J. 591, 1220–1247.

Lottermoser, B.G., 1990. Rare-earth element mineralisation within the Mt. Weld carbonatite laterite, Western Australia. Lithos 24, 151–167.

Luguet, A., Lorand, J.P., Seyler, M., 2003. Sulfide petrology and highly siderophile element geochemistry of abyssal peridotites: A coupled study of samples from the Kane Fracture Zone (45W 23´20N, MARK area, Atlantic Ocean). Geochim. Cosmochim. Acta 67, 1553–1570.

Luguet, A., Shirey, S.B., Lorand, J.P., Horan, M.F., Carlson, R.W., 2007. Residual platinum-group minerals from highly depleted harzburgites of the Lherz massif (France) and their role in HSE fractionation of the mantle>. Geochim. Cosmochim. Acta 71, 3082–3097.

Mann, U., Frost, D.J., Rubie, D.C., Becker, H., Audétat, A., 2012. Partitioning of Ru, Rh, Pd, Re, Ir and Pt between liquid metal and silicate at high pressures and high temperatures - Implications for the origin of highly siderophile element concentrations in the Earth's mantle. Geochim. Cosmochim. Acta 84, 593–613.

Martin, C.E., 1991. Osmium isotopic characteristics of mantle-derived rocks. Geochim. Cosmochim. Acta 55, 1421–1434.

McDonough, W.F., Sun, S., 1995. The composition of Earth. Chem. Geol. 120, 223–253.

McLennan, S.M., Hemming, S., 1992. Samarium / neodymium elemental and isotopic systematics in sedimentary rocks. Geochim. Cosmochim. Acta 56, 887–898.

Meisel, T., Walker, R.J., Irving, A.J., Lorand, J.-P., 2001. Osmium isotopic composition of mantle xenoliths: A global perspective. Geochim. Cosmochim. Acta 65, 1311–1323.

Mihaljevič, M., Galušková, I., Strnad, L., Majer, V., 2013. Distribution of platinum group elements in urban soils, comparison of historically different large cities Prague and Ostrava, Czech Republic. J. Geochemical Explor. 124, 212–217.

Miyazaki, T., Kagami, H., Shuto, K., Morikiyo, T., Ram Mohan, V., Rajasekaran, K.C., 2000. Rb-Sr geochronology, Nd-Sr isotopes and whole rock geochemistry of Yelagiri and Sevattur syenites, Tamil Nadu, south India. Gondwana Res. 3, 39–53.

Moralev, V.M., Voronovski, S.N., Borodin, L.S., 1975. New findings about the age of carbonatites and syenites from southern India. USSR Acad. Sci. 222, 46–48.

Murthy, V.R., 1991. Early differentiation of the Earth and the problem of mantle siderophile elements: a new approach. Science 253, 303–306.

Mysen, B.O., 1983. The structure of silicate melt. Annu. Rev. Earth Planet. Sci. 75–79.

O´Neill, H.S.C., Palme, H., 1998. Composition of the silicate Earth: Implications for acreton and core formation, in: Jackson, I. (Ed.), The Earth´s Mantle: Composition, Structure and Evolution. Cambridge University Press, pp. 3–126.

O`Brien, H.E., Irving, A.J., Mccallum, S., Thirlwall, M.F., 1995. Strontium, neodymium, and lead isotopic evidence for the interaction of post-subduction asthenospheric potassic mafic magmas of the highwood mountains, montana, usa, with ancient wyoming craton lithospheric mantle. Geochim. Cosmochim. Acta 59, 4539–4556.

Pandit, M.K., Sial, A.N., Sukumaran, G.B., Pimentel, M.M., Ramasamy, A.K., Ferreira, V.P., 2002. Depleted and enriched mantle sources for Paleo- and Neoproterozoic\rcarbonatites of southern India: Sr, Nd, C-O isotopic and geochemical\rconstraints. Chem. Geol. 189, 69–89.

Paster, T.P., Schauwecker, D.S., Haskin, L.A., 1974. The behavior of some trace elements during solidification of the Skaergaard layered series. Geochim. Cosmochim. Acta 38, 1549–1577.

Pearson, D.G., Carlson, R.W., Shirey, S.B., Boyd, F.R., Nixon, P.H., 1995. Stabilisation of Archaean lithospheric mantle: A ReOs isotope study of peridotite xenoliths from the Kaapvaal craton. Earth Planet. Sci. Lett. 134, 341–357.

Pearson, D.G., Irvine, G.J., Ionov, D.A., Boyd, F.R., Dreibus, G.E., 2004. Re-Os isotope systematics and platinum group element fractionation during mantle melt extraction: A study of massif and xenolith peridotite suites. Chem. Geol. 208, 29–59.

Peucat, J.J., Mahabaleswar, B., Jayananda, M., 1993. Age of younger tonalitic magmatism and granulitic metamorphism in South India transition zone (Krishnagiri area); comparsion with older Peninsular gneisses from the Gorur-Hassan area. J. Metamorph. Geol. 11, 879–888.

Peucker-Ehrenbrink, B., Jahn, B., 2001. the Upper Continental Crust. Geochemistry, Geophys. Geosystems 2, 1–22.

Pichamuthu, C.S., 1975. Some ascpects of the Precambrian geology of India. Geol Min Met. Soc India 47, 25–43.

Puchtel, I.S., Brandon, A.D., Humayun, M., Walker, R.J., 2005. Evidence for the early differentiation of the core from Pt-Re-Os isotope systematics of 2.8-Ga komatiites. Earth Planet. Sci. Lett. 237, 118–134.

Puchtel, I.S., Humayun, M., 2005. Highly siderophile element geochemistry of 187Os-enriched 2.8 Ga Kostomuksha komatiites, Baltic Shield. Geochim. Cosmochim. Acta 69, 1607–1618.

Ray, J.S., Ramesh, R., 2006. Stable Carbon and Oxygen Isotopic Compositions of Indian Carbonatites. Int. Geol. Rev. 48, 17–45.

Reisberg, L., Lorand, J.-P., 1995. Longevity of sub-continental mantle lithosphere from osmium isotope systematics\nin orogenic peridotite massifs. Nature.

Righter, K., Drake, M.J., 1997. Metal-silicate equilibrium in a homogeneously accreting earth: new results for Re. Earth Planet. Sci. Lett. 146, 541–553.

Ringwood, A.E., 1966. The chemical composition and origin of the Earth. Advences earth Sci. 65.

Rowan, L.C., Mars, J.C., 2003. Lithologic mapping in the Mountain Pass, California area using Advanced Spaceborne Thermal Emission and Reflection Radiometer (ASTER) data. Remote Sens. Environ. 84, 350–366.

Rudnick, R.L., Gao, S., 2014. Composition of the Continental Crust, 2nd ed, Treatise on Geochemistry: Second Edition. Elsevier Ltd.

Shirey, S.B., Walker, R.J., 1998. Isotope System in Cosmochemistry and High-Temperature Geochemistry. Annu. Rev. Earth Planet. Sci. 26, 423–500.

Schiano, P., Brick, J.-L., Allegre, C.J., 1997. Osmium-strontium-neodymium-lead isotopic covariations in mid-ocean ridge basalt glasses and the heterogenity of the upper mantle. Earth Planet. Sci. Lett. 150, 363–379.

Schleicher, H., Kramm, U., Pernicka, E., Schidlowski, M., Schmidt, F., Viladkar, S.G., Todt, W., Subramanian, V., 1998. Enriched Subcontinental Upper Mantle beneath Southern India : Evidence from Pb , Nd , Sr , and C – O Isotopic Studies on Tamil Nadu Carbonatites. J. Petrol. 39, 1765–1785.

Schleicher, H., Todt, W., Viladkar, S.G., Schmidt, F., 1997. Pb/Pb age determinations on the Newania and Sevattur carbonatites of India: evidence for multi-stage histories. Chem. Geol. 140, 261–273.

Sillitoe, R.H., 2002. Some metallogenic features of gold and copper deposits related to alkaline rocks and consequences for exploration. Miner. Depos. 37, 4–13.

Skoog, D. a., West, D.M., Holler, F.J., Couch, S.R., 2005. Fundamentos de Química Analítica, Fundamentos de Química Analítica.

Srivastava, R.K., Hall, R.P., 1995. Tectonic setting of Indan Carbonatites, in: Chandra, R. (Ed.), Magmatism in Relation to Diverse Tectonic Settings. Rotterdam, pp. 135–154.

Srivastava, R.K., Mohan, A., Filho, C.F.F., 2005. Hot-fluid Driven Metasomatism of Samalpatti Carbonatites, South India: Evidence from Petrology, Mineral Chemistry, Trace Elements and Stable Isotope Compositions. Gondwana Res. 8, 77–85.

Subramanian, V., Viladkar, S.G., Upendran, R., 1978. Carbonatite alkali complex of Samalpatti, Dharmapuri district, Tamil Nadu. J. Geol. Soc. India 19, 206–216.

Suskhenswala, R.N., Viladkar, S.G., 1978. Carbonatites of India. Explor. Res. At. Miner. 1, 15–81.

Tatsumoto, M., 1966. Genetic Relations of Oceanic Basalts as Indicated by Lead Isotopes. Science 80-153, 1094 LP-1101.

Udas, G.R., Krishnamurthy, P., 1970. Carbonatites of Sevathur and Jokipatti, Madras State, India. Proc. Indian Natl. Sci. Acad. 36.

van Acken, D., Becker, H., Walker, R.J., McDonough, W.F., Wombacher, F., Ash, R.D., Piccoli, P.M., 2010. Formation of pyroxenite layers in the Totalp ultramafic massif (Swiss Alps) - Insights from highly siderophile elements and Os isotopes. Geochim. Cosmochim. Acta 74, 661–683.

Veizer, J., Bell, K., Jansen, S.L., 1992. Temporal distribution of carbonatites. Geology 20, 1147–1149.

Veksler, I. V., Nielsen, T.F.D., Sokolov, S. V., 1998. Mineralogy of Crystallized Melt Inclusions from Gardiner and Kovdor Ultramafic Alkaline Complexes: Implications for Carbonatite Genesis. J. Petrol. 39, 2015–2031.

Viladkar, S.G., Bismayer, U., 2014. U-rich pyrochlore from sevathur carbonatites, Tamil Nadu. J. Geol. Soc. India 83, 175–182.

Viladkar, S.G., Subramanian, V., 1995. Mineralogy and geochemistry of the Carbonatites of the Sevathur and Samalpatti Complexes, Tamil Nadu.

Völkening, J., Walczyk, T., G. Heumann, K., 1991. Osmium isotope ratio determinations by negative thermal ionization mass spectrometry. Int. J. Mass Spectrom. Ion Process. 105, 147–159.

Walker, R.J., Storey, M., Kerr, A.C., Tarney, J., Arndt, T., 1999. Os isotopic heterogeneities in a mantle plume : Evidence from Gorgona Island and Curacao 63, 713–728.

Wallace, M.E., Green, D.H., 1988. An experimental determination of primary carbonatite magma composition. Nature.

Waren, P.H., Wasson, J.T., 1977. Pristine nonmare rocks and the nature of lunar crust, in: Proc Lunar Planet Sci 8th. pp. 2215–2235.

Wedepohl, K.H., 1995. The composition of the continental crust. Geochim. Cosmochim. Acta 59, 1217–1232.

Woolley, A.R., 1989. The spatial and temporal distribution of carbonatites, in: Bell, K. (Ed.), Carbonatites: Genesis and Evolution. Academic Division of Unwin Hyman Ltd, London, pp. 15–37.

Woolley, A.R., Kempe, D.R.C., 1989. Carbonatites: nomenclature, average chemical compositions, and element distribution, in: Bell, K. (Ed.), Carbonatites: Genesis and Evolution. Academic Division of Unwin Hyman Ltd, London, pp. 1–14.

Woolley, a. R., Bailey, D.K., 2012. The crucial role of lithospheric structure in the generation and release of carbonatites: geological evidence. Mineral. Mag. 76, 259–270.

Wyllie, P.J., Huang, W., 1976. at Mantle Pressures with Geophysical and Petrological Applications 107, 79–107.

Wyllie, P.J., Lee, W., 1998. Model system controls on conditions for formation of magnesiocarbonatite and calciocarbonatite magmas from the mantle. J. Petrol. 39, 1885–1893.

Xu, C., Qi, L., Huang, Z., Chen, Y., Yu, X., Wang, L., Li, E., 2008. Abundances and significance of platinum group elements in carbonatites from China. Lithos 105, 201–207.

Xu, C., Wang, L., Song, W., Wu, M., 2010. Carbonatites in China: A review for genesis and mineralization. Geosci. Front. 1, 105–114.

Yaxley, G.M., Brey, G.P., 2004. Phase relations of carbonate-bearing eclogite assemblages from 2.5 to 5.5 GPa: Implications for petrogenesis of carbonatites. Contrib. to Mineral. Petrol. 146, 606–619.

Ying, J.F., Zhou, X.H., Zhang, H.F., 2003. Geochemical and isotopic investigation of the Laiwu-Zibo carbonatites from western Shandong Province, China and implication for enriched mantle source. Goldschmidt, Kurashiki.